UNIVERSITÀ DEGLI STUDI DI MILANO
Dipartimento di Biotecnologie Mediche e Medicina Traslazionale

SCUOLA DI DOTTORATO IN SCIENZE BIOMEDICHE CLINICHE E SPERIMENTALI
DOTTORATO DI RICERCA IN BIOTECNOLOGIE APPLICATE
ALLE SCIENZE MEDICHE
XXVI CICLO

SPHINGOLIPID SIGNALING AND DISEASE: THE KEY ROLE OF CERAMIDE TRAFFIC IN CELL FATE REGULATION

Docente guida: Prof.ssa Paola VIANI

Coordinatore del Dottorato: Prof. Massimo LOCATI

Tesi di Dottorato di:

Loredana Brioschi

Matr. R09282

Anno Accademico 2014/2015

CONTENTS

ABBREVIATIONS

Cer	Ceramide
ER	Endoplasmic reticulum
FAs	Fatty acids
FFAs	Fatty free acids
GBM	Glioblastoma multiforme
GlcCer	Glucosylceramide
GSL	Glycosphingolipids
LacCer	Lactosylceramide
PH	Pleckstrin Homology
SM	Sphingomyelin
Sph	Sphingosine
S1P	Sphingosine-1-phosphate
T2D	Type 2 diabetes

ABSTRACT

Cancer and diabetes are among the most common diseases in western societies. Sphingolipids, a class of lipids ubiquitously present in eukaryotic membranes, play a key role in the regulation of different signal transduction pathways involved in the modulation of many cellular functions [1, 2]. The past two decades have seen increased interest in the bioactive sphingolipids ceramide (Cer) and sphingosine-1-phosphate (S1P). Cer, a central molecule of sphingolipid metabolism, is involved in the control of many cell-stress responses, including growth arrest, senescence and cell death [3]. On the other hand, several studies have proposed a crucial role of S1P in cell growth and survival, cell migration, angiogenesis, and inflammation [3]. Thus, Cer and S1P can differentially regulate cell death and survival by controlling opposing signaling pathways [4]. So far, a large amount of studies has clarified the complexity of the interplay between S1P, Cer and sphingolipid metabolism and these implications in the etiology of several human diseases. Effectively, deregulation of sphingolipid metabolism is implicated in numerous diseases, and accumulating evidence has shown a clear indication that sphingolipids have important role in the pathogenesis of diabetes and cancer [5].

Very recently, it is emerging a pivotal role of Cer traffic from the Endoplasmic Reticulum (ER) to the Golgi apparatus in the regulation of sphingolipid metabolism. In fact, Cer transport is a highly regulated step in the sphingolipid biosynthesis. Two main mechanisms are involved in Cer transport from ER to the Golgi apparatus: a protein-mediated transport, operated by CERT [6, 7] and a CERT-independent vesicular transport. Moreover, several studies reported that ER is a critical intracellular organelle involved in the control of cell fate [8, 9]. In this light, Cer accumulation in the ER appears to be a key element in the promotion of cell death in different human diseases, as well as in glioblastoma and diabetes.

In light of these findings, in my Ph.D. course I wanted to evaluate in cellular models of glioblastoma (GBM) and type 2 diabetes (T2D) the role of Cer transport in the regulation of cell fate.

<u>Part 1</u>: Glucolipotoxicity impairs ceramide flow from the ER to the Golgi apparatus in INS-1 β-cells

T2D is the most common form of diabetes characterized by insulin resistance and β-cell dysfunction. The etiology of T2D is not well established but it is know that loss of insulin secretion is directly linked to a loss of function and death of pancreatic β-cells [10]. Glucolipotoxicity is a condition determined by the combined action of elevated glucose and

free fatty acids (FFAs) levels that exerts deleterious effects on pancreatic β-cell function and survival. Several mechanisms have been proposed for glucolipotoxicity-induced β-cell dysfunction, and, among them, ER stress and elevations of the proapoptotic sphingolipid Cer appear to play key roles. Moreover, Cer accumulation due to glucolipotoxicity can be associated to the induction of ER stress. As in other cells, in the INS-1 insulinoma cell line, two main mechanisms are involved in Cer transport from the ER to the Golgi apparatus: a CERT-mediated transport [6, 11], and a CERT-independent vesicular transport. Glucolipotoxic conditions, obtained with 0.4 mM palmitate and 30 mM glucose administration, strongly affected both of them by reducing CERT protein synthesis and activity, and the rate of Cer vesicular traffic, thus promoting Cer accumulation in the ER. [11, 12]. The two Cer transport mechanisms are effectively involved in the control of sphingolipid metabolism, participating in the regulation of Cer accumulation in the ER involved in pancreatic β-cell function and death during T2D.

<u>Part 2</u>: The stimulation of Cer traffic from the ER to the Golgi apparatus S1P-dependent as a survival factor in T98G glioma cells.

GBM is the most common malignant primary brain tumor in adults and one of the most lethal human cancers [13]. S1P and Cer have emerged as bio-effectors molecules, involved in both glioblastoma development and resistance [3, 14-17]. Several lines of evidence indicated that, different anticancer drugs, including etoposide, exert cytotoxic effects also promoting accumulation of Cer in the ER. Thus, the transport of Cer from ER to Golgi apparatus could be represent a key pathway for limiting Cer accumulation in the ER and escape from cell death. Moreover, we recently demonstrated that vesicular-mediated Cer transport is positively regulated by the pro-survival pathway phosphatidylinositol 3-phosphate kinase (PI3K)/Akt [18], known effectors of extracellular S1P.

In T98G glioma cells, S1P treatment was able to increase vesicular Cer transport from the ER to the Golgi apparatus by PI3K/Akt pathway activation, inducing Cer conversion to SM and glycosphingolipids (GSL). In these cells, the cytotoxic Cer accumulation in the ER promoted by the anticancer drug etoposide was strongly reduced after S1P administration. S1P, by enhancing Cer traffic, act as pro-oncogenic factor, favoring both the reduction of the pro-apoptotic Cer at the ER and the synthesis of complex sphingolipids. By this mechanism S1P also stimulates the generation of new membranes, functional to cell growth and consequently to the tumor survival and progression.

STATE OF THE ART

Shpingolipids

Sphingolipids represent a heterogeneous class of lipids that contains backbone of sphingoid bases and are essential constituents of eukaryotic cell membranes. For long time they have been considered merely as structural components, fundamental in the definition of the membrane bilayers. In the last 20 years, advances in biochemical and molecular research led to the identification of sphingolipids acting as intra- and extra-cellular messengers involved in the regulation of crucial aspects of cell biology such as cell growth, death, migration, senescence and inflammatory response [3].

Sphingolipids are amphipathic molecules, characterized by a hydrophilic (or polar head) and a hydrophobic (or tail) portion. Cer (Fig.1) represents the structural element common to all sphingolipids. It consists of a long-chain sphingoid base, linked via amide bond to a long-chain fatty acid, mainly palmitic (C_{16}) or stearic acid (C_{18}) Sphingosine (Sph), an amino-alcohol containing 18-20 carbon atoms (C-18 or C-20) and characterized by the presence of a double bond across C4-C5, is the most frequent sphingoid base constituting Cer in humans, followed, in very small proportions, by C-18/C-20 sphinganine (which lacks the double bond C4-C5). Both are in the *trans* D-*erythro* form.

Cer is the central building block of all sphingolipids, and represents the hydrophobic portion, or tail, of these molecules. Through its primary alcoholic residue, Cer can be conjugated to different hydrophilic groups, which represent the polar head of sphingolipids. Cer binding to phosphocholine or saccharidic structures leads to the generation of sphingomyelins (SM) and glycosphingolipids (GSL), respectively. In GSL, the oligosaccharide chain, linked to Cer through a β-glycosidic bond, may contain 15-20 saccharide units, among which, the most frequent are glucose, galactose, N-acetylglucosamine, N-acetylgalactosamine and different species of sialic acid. Furthermore, both the sphingoid base (sphingosine) and Cer may exist in the phosphorylated form in correspondence with the carbon in position 1 (C-1) [19, 20]. Sphingolipids are ubiquitous membrane components, being present in different organelle membranes and particularly abundant in the plasma membrane. Cer is present in small amounts within cell membranes, as it functions primarily as an intermediate of complex sphingolipid metabolism and acts as a cell signalling mediator [21].

In biological plasma membranes, SM and GSL represent the major sphingolipids, displaying an asymmetric or polarized distribution, and play important roles in the regulation of membrane fluidity and sub-domain structures.

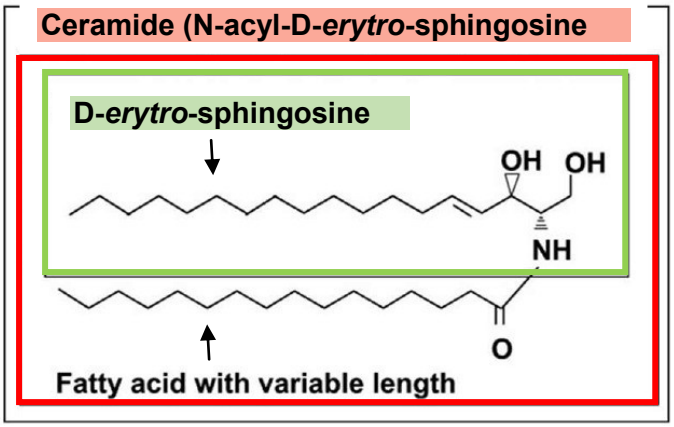

Figure 1: Ceramide chemical structure

In particular, bth SM and GSLs are mainly localized in the outer leaflet of the cell membrane. GLS show a distribution on the membrane specific for each cell type, which can vary with differentiation and neoplastic transformation [20].

Sphingolipids, thanks to their amphipathic properties, are able to diffuse laterally within the membrane and, together with cholesterol and specific proteins, may give rise to microdomains, specialized platforms able to compartmentalize cellular processes by serving as organizing centres for the assembly of signalling molecules [22].

Sphingolipid metabolism

The metabolic pathway of sphingolipids consists of a complex network of synthetic and degradative reactions. Sphingolipids can originate from both the "*de novo* synthesis" or from the degradation of complex sphingolipids (Fig. 2) [15].

The "*de novo*" biosynthesis of sphingolipids starts at the cytosolic leaflet of the ER and begins with the condensation of palmitoyl-CoA with L-serine. This reaction is catalyzed by the enzyme serine-palmitoyl transferase (SPT) and leads to the formation of 3-ketosphinganine, which is subsequently reduced to sphinganine by a NADPH-dependent oxidoreductase, the 3- ketosphinganine reductase. Sphinganine is the substrate of the (dihydro)-Cer synthase (CerS), which uses an acyl donor to bind sphinganine to a fatty acid, forming dihydroCer. In mammalian cells, six different isoforms of CerS have been recently identified and are encoded by six different genes, members of the LASS family (Longevity

Assurance Genes). Each of these genes specifically synthesise one of the several Cer species that differ in the fatty acid chain length. In particular, LASS1 is involved in the production of C_{18}Cer, LASS2 of C_{22}Cer, LASS3 of C_{18}/C_{24}Cer, LASS4 of C_{20}Cer, LASS5 and LASS6 of C_{16}Cer and C_{14}/C_{16}Cer respectively [23, 24]. The product of the reaction catalyzed by CerS, dihydroCer, is desaturated in position 4,5 of the sphingoid base by a NADPH-dependent oxydoreductase, the dihydroCer desaturase (DES), with the consequent formation of Cer [25]. All the enzymes involved in the *de novo* biosynthesis of Cer are localized in the ER membrane, acting on the cytosolic surface of the same, and the reaction products remain there anchored.

Cer is the common precursor for the synthesis of all complex sphingolipids. Through its hydroxyl group at the carbon in position 1, Cer can bind to additional functional groups, generating GSL, Cer 1-phosphate and SM.

GLS derive from the conjugation of the Cer primary alcoholic residue with one or more saccharide units, through β-glycosidic bond.

Galactosylceramide (GalCer) is synthesized from Cer and UDP-galactose by the galactosyltransferase, enzyme expressed at the luminal side of the ER membrane in Schwann cells and oligodendrocytes. GalCer, together with its sulphate derivative, sulfatide synthesized at the Golgi, is an important lipidic component of myelin (formed by Schwann cells in the peripheral nervous system and oligodendrocytes in the central nervous system), and confers rigidity and stability to the membranes, allowing a correct conduction of nerve impulses [26].

Glucosylceramide (GlcCer) is obtained from Cer and UDP-glucose, through a reaction catalyzed by GlcCer synthase (GCS), which is localized at the cytosolic leaflet of the Golgi apparatus [27]. Therefore, GlcCer biosynthesis requires an efficient transport mechanism of Cer from the cytoplasmic side of the ER to the cytoplasmic side of the cis-Golgi. Once synthesized, GlcCer can be routed directly to the plasma membrane (via a vesicular system), or it can be further modified by subsequent glycosylations, with the consequent production of more complex glycosphingolipids, such as gangliosides. This process is catalyzed by different glycosyl-transferases acting by associating to GlcCer individual saccharide units, following a precise sequential order [14]. The enzymes involved in these reactions are located and act in the luminal surface of the Golgi cisternae; thus a flippase mechanisme mediating the translocation of GlcCer from the cytoplasmic to the luminal side of the cis-Golgi has be active [28, 29]. GlcCer can be transported from the cis-Golgi cisterna to the trans Golgi network (TGN) through a non-vesicular mechanism that requires the FAPP2

protein. FAPP2 contains a PH domain, similar to FAPP1 at the N-terminus, that recognizes both PI4P and Arf1 localized at the TGN [7].

Cer can also undergo phosphorylation of the hydroxyl group of the carbon in position 1 by the Cer kinase (CERK), with the consequent formation of Cer 1-phosphate (C1P) [3]. The subcellular localization of this enzyme has not been definitely identified, but it seems to be at the level of the plasma membrane, the Golgi apparatus, and the cytoplasm [30].

SM represents approximately 10% of the lipids present in mammalian cells. SM synthesis is based on the transfer of phosphocholine from phosphatidylcholine to Cer, with the production of a diacylglycerol (DAG) molecule. This reaction is catalyzed by SM synthase (SMS). Several studies suggest the existence of two different enzymatic SMS isoforms: SMS1, localized in the luminal side of the cis/medial Golgi apparatus and SMS2, primarily localized to the plasma membrane [3, 31]. Experimental evidence has shown that about 90% of the de novo synthesis of SM occurs in the cis/medial Golgi, and only a small percentage occurs at the level of the plasma membrane. Therefore, most of SM biosynthesis, as well as that of GlcCer, requires a mechanism of Cer transport from the ER, where it is synthesized, to the Golgi apparatus. The localization of SMS2 at the plasma membrane suggests its role as a regulator of SM and Cer levels for signalling pathways and signal transduction [14].

Sphingolipids reach their final destination at the plasma membrane, mainly following the vesicular flow of exocytosis from the ER or the Golgi apparatus to the plasma membrane.

Membrane GSL are constitutively degraded by a process involving endocytosis and the endo-lysosomal district; the enzymatic steps of this degradation process include exoglycohydrolases requiring an acidic pH, guaranteed within the lysosomal or endosomal vesicles, in order to perform their catalytic activity. These enzymes catalyze the degradation of GSL, determining the sequential hydrolytic detachment of monosaccharides [32] from Cer.

SM degradation is catalyzed by sphingomyelinase (SMase), an enzyme able to hydrolyze the SM phosphodiester bond, with the consequent formation of Cer and phosphocholine. Three isoforms of this enzyme have been described and distinguished, according to their subcellular localization and the optimum pH, in acidic, neutral, and alkaline SMase. The acid SMase is located mainly in the lysosomal compartment. Another isoform of acidic SMase has been identified, due to a splice variant in the transcription of the encoding gene; this enzyme can be secreted or localized in the outer membrane leaflet [3, 33]. The neutral SMase has different subcellular locations including the inner leaflet of the plasma membrane, ER, Golgi, and even the nucleus [33].

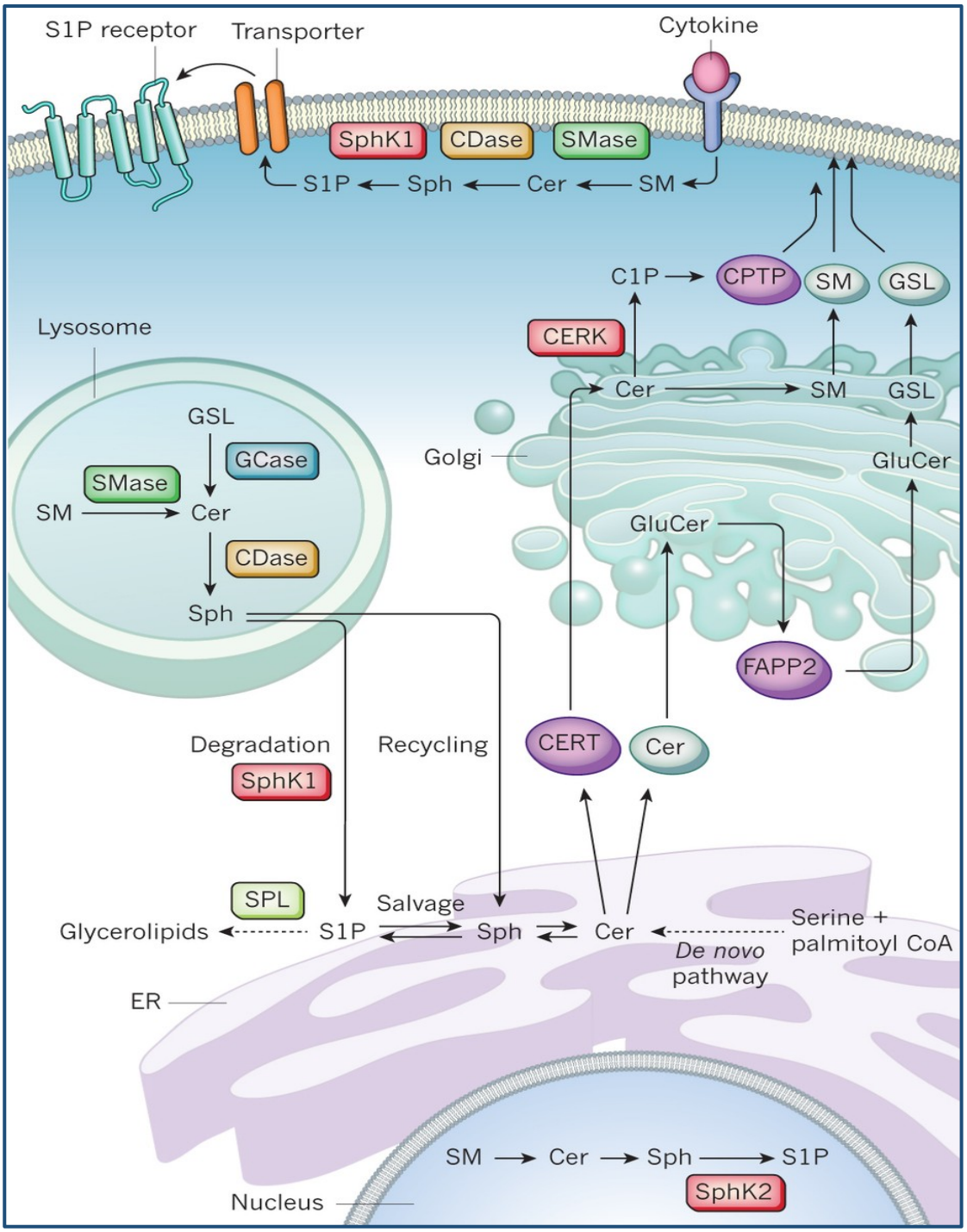

Figure 2: Subcellular compartmentalization of sphingolipid metabolism
Image from M.Maceyka and S. Spiegel Nature 510; 58–67 2014

The localization of alkaline SMase is more restricted, being mainly expressed in the intestinal tract, and in the bile where it participates to SM digestion [34].

Cer is degraded by ceramidases (CDases); three isoforms of CDases have been identified and classified by their pH optima as acidic, neutral and alkaline CDases. These CDases are located at the plasma membrane, lysosome, and ER/Golgi complex, respectively [35]. These

enzymes hydrolytically cleave Cer in fatty acid and sphingosine (Sph) [14]. Notably, Sph origin is exclusively catabolic, since it only derives from sphingolipids degradation [36].
Cer-derived Sph can be recycled or undergo phosphorylation in position C1 with the generation of S1P (Fig.3) by sphingosine kinases (as described below). S1P can be metabolized through the irreversible cleavage in position C2-C3, to hexadecenal and phosphoethanolamine in a reaction catalyzed by the S1P lyase enzyme, located on the ER cytosolic side [37]. This reaction, and the SPT catalyzed one, are the reactions of the entire sphingolipid metabolism which occur in only one direction, the enzymes catalysing the opposite reaction being absent. S1P can also be dephosphorylated back to Sph through a reaction catalyzed by either lipid phosphate, or S1P specific phosphatases [38-40].

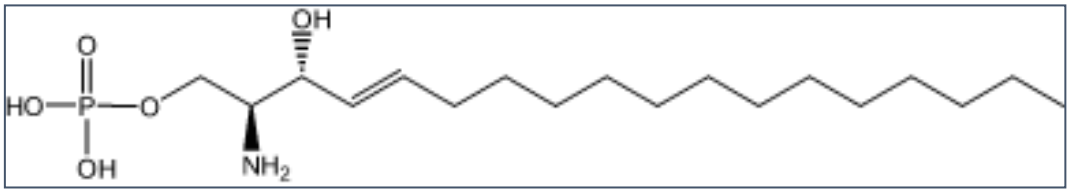

Figure 3: Sphingosine-1-phosphate (S1P) chemical structure

Concerning to recycling pathway, the products obtained from sphingolipids degradation such as saccharide residues, fatty acids and, particularly, Sph can be reused for the synthesis of complex sphingolipids. In this process, Sph produced from SM and GSL catabolism reaches the ER where it is N-acylated to Cer. Cer can then be used for the biosynthesis of complex sphingolipids, as described in *de novo* biosynthesis (Fig.2). This pathway is called "salvage pathway" [3].
The Sph recycling process is an energy advantage to cells and, in different cell types, such as cells of glial origin, may constitute the principal pathway of sphingolipids synthesis [41].

ER to Golgi Ceramide transport pathways

To date, two transport mechanisms are known to operate in the cell to transfer Cer from ER to the Golgi apparatus for the synthesis of complex sphingolipids: a CERT-dependent, and a vesicular CERT-independent pathway.

CERT-dependent Ceramide transport

CERT was originally isolated as a protein that restores SM synthesis in a SM-defcient CHO mutant cell line, LY-A [6]. CERT is a 68-kDa cytosolic protein that is identical to GPBPΔ26, a splice variant of Goodpasture antigen-binding protein (GPBP) that lacks 26

amino acids in the serine rich region. CERT and GPBP (also termed $CERT_L$) both have a Cer transfer activity between membranes in a non-vesicular manner (Fig.4). CERT transports Cer in an ATP-dependent and non-vesicular manner, specifically for the SM biosynthesis CERT contains different domains and motifs: the C-terminal steroidogenic acute regulatory protein (StAR)-related lipid transfer (START) domain (~230 amino acids); two phenylalanines (FF) in an acidic tract (FFAT) motif at the N-terminal side of the START domain; a serine repeat (SR) motif and the N-terminal PH domain (~100 amino acids). The structure of the START domain reveals a long amphiphilic cavity in which one Cer molecule is located. At the far end of the cavity, the amide and hydroxyl groups of Cer form hydrogen bonds with specific amino acid residues that are involved in stereospecific Cer recognition. Moreover, the wall of the hydrophobic cavity limits the size and shape for ceramides [42] working as a molecular measuring device similar to the bacterial membrane acyltransferase, PagP [43]. The START domain extracts Cer from donor membranes favoring ceramides with a chain length of 14–20 carbon atoms than ceramides with longer acyl chains (i.e. C22–C24) [[44].

The N-terminus of CERT contains a pleckstrin homology (PH) domain that predominantly recognizes phosphatidylinositol 4-phosphate (PI4P) produced by phosphatidylinositol 4-kinase III beta (PtdIns-4K IIIβ) that co-localize with PtdIns-4KIIIβ in *cis*/medial-Golgi compartments. The PH domain of CERT is required for its efficient association with the Golgi via PI4P[6]. Moreover, a coiled-coil motif is found in the middle region of CERT, between the PH and START domains, containing the consensus sequence EFFDAXE, namely the FFAT motifs [45]. The FFAT motifs interact with the ER-resident type II membrane proteins, VAP-A and VAP-B (vesicle-associated membrane protein- associated proteins). VAPs recruit CERT to the cytosolic surface of ER membranes, and it is this interaction which is crucial for the association with the ER membrane [44]. Cer binding to CERT may result in conformational changes leading to alternating exposure and concealment of PH and FFAT domains, resulting in unidirectional Cer transport between the ER and Golgi apparatus [46]. CERT can exists in hyperphosphorylated and hypophosphorylated forms. Mass spectrometry analysis confirms that 7‑9 serines/threonines can be phosphorylated in the SR region. Two kinases are involved in the phosphorylation of the SR motif: the first kinase is protein kinase D (PKD), which phosphorylates serine 132, and the second kinase is an isoform of casein kinase 1 (CK1 γ 2) [7]. In normally growing cells, CERT exists mainly as the hyperphosphorylated forms. CERT phosphorylations

inhibit both START domain-mediated Cer transfer activity and PH domain-mediated PI4P-binding activity thus PKD and CKI γ 2 function as negative regulators of CERT.

The hyperphosphorylated CERT is dephosphorylated by protein phosphatase 2Cε (PP2Cε), a transmembrane protein of the ER. PP2Cε interacts with VAP-A and its activity on CERT is dependent on the expression of VAP-A. Saito S. at al. demonstrated that the dephosphorylation enhances both the localization of CERT to the Golgi and the interaction of CERT with VAP-A, indicating that PP2C ε activates Cer CERT-dependent transport from the ER to the Golgi [7].

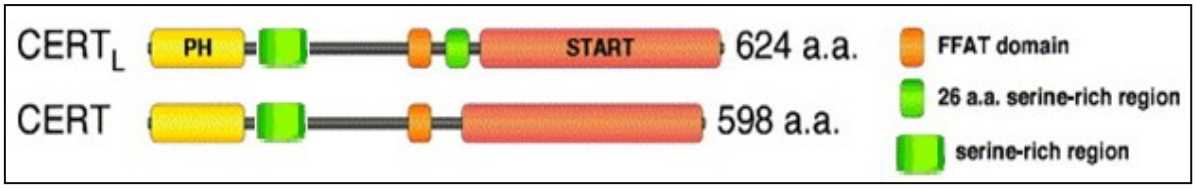

Figure 4: CERT$_L$ and CERT structures

Modified image from: R.J. Perry, N. D. Ridgway Biochimica et Biophysica Acta 1734 (2005) 220 – 234.

Vesicular CERT- independent Ceramide transport

Cer can be also transported to the Golgi apparatus from ER-derived vesicles. Vesicular transport represents a crucial mechanism by which Cer travels as membrane component of small carrier vesicles that origin from a donor compartment and fuse with specific target membranes. The vesicular transport of Cer is thought to operate by molecular machineries similar to those of proteins [22], although the molecular mechanism for the recruitment of Cer into COPII-coated vesicles is unknown. Cer vesicular transport appears crucial for production of SM and/or GlcCer. In fact, biosynthesis of SM is, at least in part, dependent on the vesicular transport and CERT downregulation inhibits SM biosynthesis, but not that of GlcCer in different cells [47].

Intriguingly, PI3K/Akt has been shown to regulate the ER-Golgi vesicular transport of Cer and consequently Cer levels in C6 glioma cells [18], implying this traffic in Cer-mediated signaling too.

Ceramide and Sphingosine 1-phosphate as bioactive messengers

Cer is a central hub in sphingolipid metabolism. It acts as an intracellular second messenger by regulating different intracellular effectors involved in many different processes such as cell growth, differentiation, senescence, necrosis, proliferation and apoptosis. Increased of

Cer levels can lead to cell growth arrest or cell death. Cer is able to activate the serine/threonine protein phosphatases PP1 and PP2A. These phosphatases act on several substrates such as retinoblastoma protein (pRB), Bcl-2, c-JUN, PKCα, SR proteins and Akt which are all implicated in cell pathways regulating proliferation and apoptosis. Cer-mediated activation of PP1 seems to be involved in the cell cycle arrest in the G1 phase, due to the dephosphorylation of pRB [16, 48]. Furthermore, PP1 induces the dephosphorylation of SR proteins, a family of serine/arginine-domain proteins known modulators of mRNA splicing, thus inducing the alternative splicing of the genes encoding Bcl-X and caspase-9, generating pro-apoptotic splice variants [49, 50]. Mitochondrial membrane potential can also be altered by Cer, probably through the PP2A-mediated dephosphorylation of Bcl-2, causing its inactivation and thus favouring the apoptotic process [51]. Cer also activates Cathepsin D protease which in turn recruits and activates, via proteolytic breakdown, the pro-apoptotic protein BID resulting in the induction of apoptosis [16].

Another important Cer target is PKC-ζ. Increased levels of Cer induce the activation of this protein, by phosphorylation. The activated PKC-ζ, in turn phosphorylates the hnRNP A1 factor, involved in the mechanisms of alternative splicing. This factor might be involved in the alternative splicing of genes involved in apoptosis [52].

Cer can also exert an antiproliferative role through the inhibition of MAPK pathway, promoting the dephosphorylation of ERK1/2 (extracellular signal regulated protein kinase 1 and 2), serine/threonine kinases belonging to the family of MAP kinase (MAPK) [53]. These proteins, if dephosphorylated, are inactive and thus not able to migrate into the nucleus to promote the expression of genes involved in cell proliferation [54, 55]. ERK1/2 inhibition induced by Cer can be associated with the ability of this mediator to activate, in systems "cell free", the serine/threonine protein phosphatase PP2A [56-58].

Many stimuli activating acid SMase at the plasma membrane induce the formation of Cer-enriched domain that trap and cluster signalling proteins [59]. In these domains, the initial signal can be amplified via concentration and oligomerization of proteins that transmit signals across the plasma membrane. Such clustering has been shown for proteins associated with apoptotic signalling. Fas receptors, Fas-associated death domain-containing protein (FADD) and caspase-8 have been shown to cluster within Cer-enriched domain [60]. Furthermore, Cer can induce apoptosis by forming membrane channels in mitocondria, which are large enough to cytochrome c release [61].

Cer levels can be regulated by different mechanisms, such as modulation of Cer metabolic enzymes and/or Cer transport mechanisms, thus producing other sphingolipids that may

have different cellular effects. Reduction of intracellular Cer levels is therefore one mechanism that can mediate cell survival.

S1P, the other relevant sphingolipid messenger, plays a role in proliferation, cell growth, cell survival, cell migration, inflammation, angiogenesis, vasculogenesis and resistance to apoptotic cell death. S1P is formed from sphingosine and ATP in a reaction catayzed by the enzyme sphingosine kinase (SphK). So far, two isoenzymes, known as SphK1 and SphK2, have been identified in mammals. SphK1 and SphK2 display different subcellular localization, tissue distribution and temporal expression pattern during development [62] SphK1 is largely cytoplasmic and can acutely associate with the plasma membranes, phagosomes, and endosomal vesicles, whereas SphK2 even if present in the cytoplasm is predominately in the nucleus [63].

S1P can interact, in an autocrine and/or paracrine manner, with five specific transmembrane receptors ($S1P_{1-5}$) coupled to different G-proteins and displaying tissue-specific expression patterns [64]. Through its receptor S1P can activate several signal transduction pathways, and thus elicit a variety of cell-specific responses controlling cell behaviour [65]. The activation of these G proteins coupled receptors results in the modulation of different signalling pathway such as ERK, c-Jun N-terminal kinase (JNK), the small GTPases of the Rho family (Rho and Rac), phospholipase C (PLC), adenylate cyclase and PI3K/Akt signalling [65-67]. Through its receptors, S1P is able to regulate different cellular processes, such as cell proliferation, motility, invasion, cytoskeletal rearrangement, angiogenesis, vascular maturation and lymphocyte trafficking and actions.

Part 1: Glucolipotoxicity impairs Ceramide flow from the ER to the Golgi apparatus in INS-1 cells

INTRODUCTION

Diabetes is a complex disease characterized by a chronic abnormal elevation of plasma glucose concentrations. It is one of the major causes of death worldwide and the World Health Organization (WHO) proposes this disease to become the seventh leading cause of death by 2030.

Diabetes may be classified into two groups based on its pathophysiology. Type 1 diabetes is caused by a lack of insulin due to the destruction of insulin-producing beta cells in the pancreas by the immune system. Often, type 1 diabetes is diagnosed when most of β-cells have already been damaged, so afflicted people need daily insulin treatment to survive. Type 1 diabetes typically occurs in children and young adults, though it can appear at any age [10].

Type 2 diabetes

T2D, the most common form of diabetes, is a multi-factorial disease characterized by insulin resistance and β-cell dysfunction. In this pathological state, peripheral target tissues (skeletal muscle, liver, and adipose) are unable to respond effectively to normal circulating concentrations of insulin. Thus, insulin resistance is generally reversed by enhanced secretion of insulin from the β-cells, and T2D only develops in those individuals when β-cells do not produce enough insulin.[68] The etiology of T2D is not well established but it is know that loss of insulin secretion is directly linked to a loss of function and death of pancreatic β-cells [10]. The development of this pathology results from genetic susceptibility, social and environmental factors. T2D develops most often in middle-aged and older people. Moreover, accumulating evidence suggests that T2D is often associated with alteration in lipid metabolism, high levels of circulating lipids and is strongly associated with obesity. Free fatty acids (FFAs) are important physiological nutrients for β-cell, and they are readily degraded by β-oxidation acting as supplemental fuel able to potentiate insulin secretion in response to glucose However, chronically elevated levels of circulating FFAs have been proposed to induce peripheral insulin resistance and impairment of β-cell insulin secretion, a phenomenon that has been called “lipotoxicity” [69]. Pietiläinen and colleagues, in a study on weight-discordant twins, demonstrated that obese individuals showed signs of insulin resistance in adipose tissue, if compared with their lean twins [70] . This alteration was due to significant differences in adipose tissue fatty acid composition; in particular, a reduction of stearic, linoleic, and α-linolenic acids, and increased amount of palmitoleic and arachidonic acids in obese twins.[69] However, the molecular mechanisms

underlying the pathogenesis of lipotoxicity in pancreatic β-cells has not been elucidated. A growing amount of studies demonstrates that the excessive adipose tissue increase has further consequences at the cellular and subcellular levels of β-cells; in particular, at the ER that is commonly affected in obese subjects. Chronic exposure of β-cells to high FFAs and glucose levels, also termed glucolipotoxicity, results in β-cell dysfunction and loss by ER stress and oxidative stress resulting in apoptosis [71] (Fig.1).

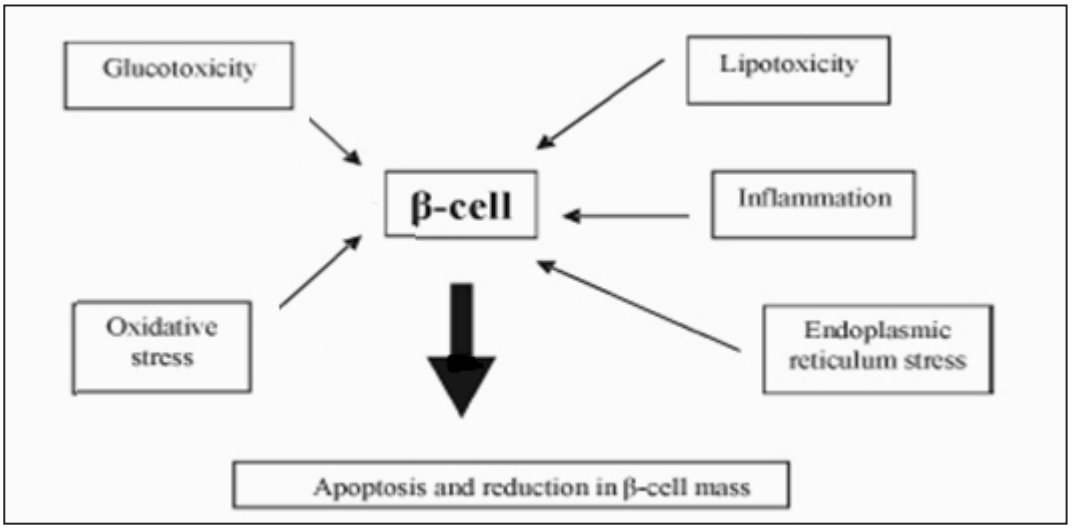

Figure 1: Mechanisms of β-cells failure in Type 2 diabetes
Modified image from Rev. Bras. Hematol. Hemoter. vol.32 2010

ER stress in Type 2 diabetes

ER is a organelle responsible for the synthesis, post-translational modification and folding of peptides, synthesis of lipids, and control of the intracellular calcium homeostasis. Accumulating evidence suggests that ER stress is correlated to T2D. During diabetes, the high insulin demand induces a markedly increase of pro-insulin synthesis and folding in the ER of β-cells to counteract hyperglycemia. Under this condition, ER function progressively worsened and this led to an adaptive defense known as the "unfolded protein response" (UPR), a mechanism to restore the ER homeostasis. Moreover, elevated levels of ER stress markers were observed in pancreatic islet of diabetic human subjects [5]. When severe or prolonged ER stress occurs, the URP switches in to β-cells death. FFA overload beyond the esterification capacity of β-cells in the ER is associated with ER stress response, thus triggering β-cell death or dysfunction [5]. Impaired ER-to-Golgi trafficking itself can contribute directly to the reduction of insulin production by compromising the maturation of

pro-insulin in post-Golgi compartments. ER stress has been recognized to induce inflammation and there are direct links between ER stress/UPR and both local and systemic inflammation. ER stress is associated with the production of pro-inflammatory cytokines, mainly IL-1β. IRE1α is a key factor involved in the transcription of inflammatory genes, and its interaction with TNF receptor–associated factor 2 (TRAF2) promotes NF-κB and JNK pathways. Moreover, IRE1α/TRAF2 can also activate AP1 transcription factor, which promotes the expression of inflammatory cytokines [72]. JNK may also be involved in the FFAs-induced pancreatic β-cell dysfunction. The key role of the NF-kB pathway in the induction of inflammatory responses in T2D, has been highlighted in several studies [5]. Fatty acids (FAs), in particular saturated FAs induce the expression of NF-κB through Toll-like receptor 4 (TLR4) signaling. An improvement in insulin sensitivity was observed in animal model of FFA-induced insulin resistance when the gene encoding for TLR4 was mutated [5]. Recent studies, discovered a role of Src in JNK activation and the upregulation of two proteins, DP5 and PUMA, involved in palmitate-induced β-cell apoptosis [73]. A role for caspase-2 induction in ER stress-induced cell death has also been reported. ER stress may also lead to β-cell dysfunction by degradation of insulin mRNA through IRE1a activation [5]. ER stress and induction of UPR can also result in mithocondrial dysfunction and ROS generation. Moreover, when conditions of glucotoxicity and lipotoxicity are combined (glucolipotoxic conditions), β-cell stress responses can be amplified, potentiating effects of elevated glucose and FFAs [5] (Fig.2).

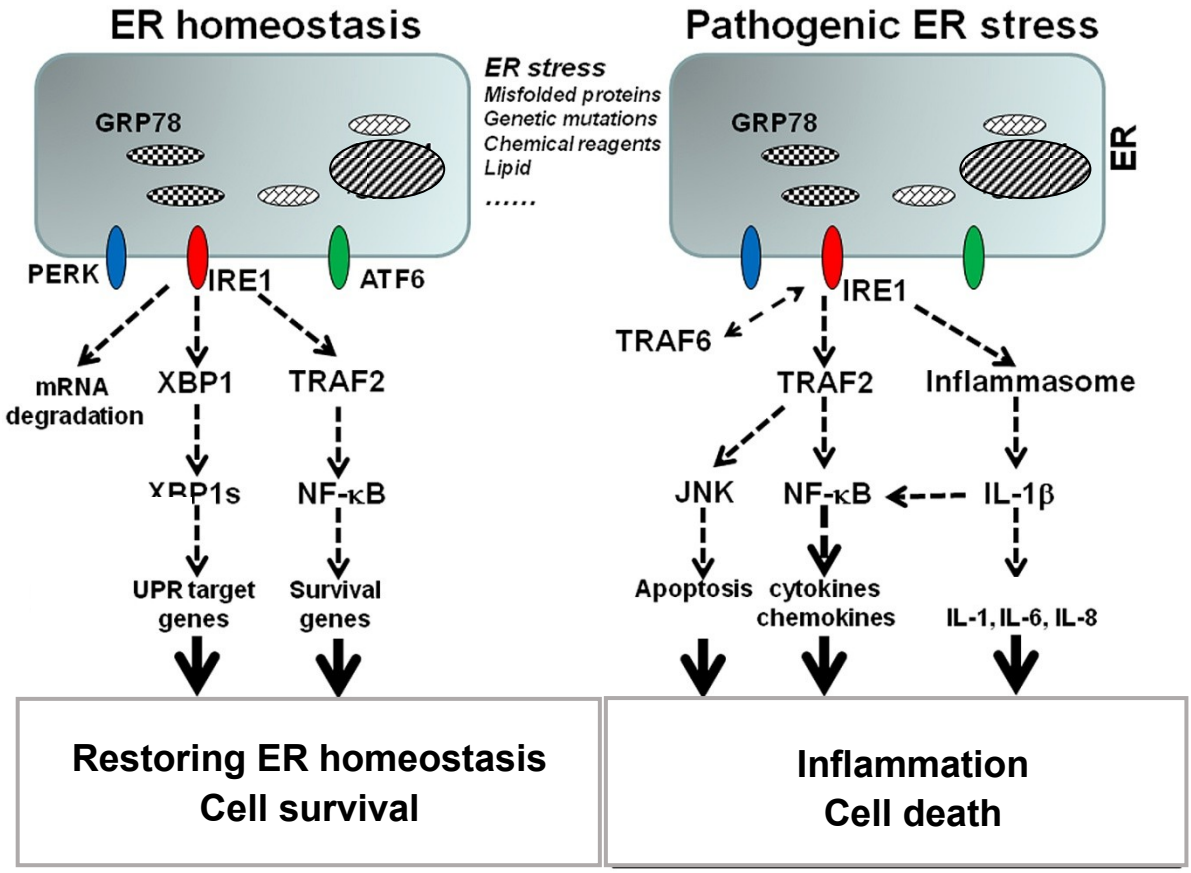

Figure 2: The model of ER stress-associated inflammation and cell death
Modified image from: Front. Genet., 25 July 2014 [74]

Ceramide in Type 2 diabetes

Recent advances in the study of sphingolipid metabolism, have underlined the relevant roles that sphingolipids play in pancreatic β-cells. Sphingolipid metabolites such as Cer, GSL, S1P and gangliosides modulate many β-cell signaling pathways and processes involved in β-cell diabetic disease such as apoptosis, β-cell cytokine secretion, ER-to-Golgi vesicular trafficking, islet autoimmunity and insulin gene expression [75].

In particular, Cer, has been implicated as an important effector in the FAs-induced apoptosis of pancreatic β-cells [76]. Fatty acids, particularly saturated FAs have been shown to promote ER stress to induce β-cell apoptosis [77]. The toxic effect of saturated FAs may be related to the formation of Cer. Infact, different observations from several studies demonstrate that Cer is involved in ER stress-induced β-cell apoptosis. Both Cer synthesis via the *de novo* pathway and via SM hydrolysis have been reported to cause ER stress-induced β-cell apoptosis [5]. A study of Lei et al demonstrated that induction of β-cell apoptosis in response to strong ER stress is associated to Cer accumulation due to the activation of neutral SMase. Inhibition of neutral SMase protected β-cell from ER stress

induced apoptosis, demonstrating the role of Cer in ER stress-induced cell death. Cer increase in ER stress also activates intrinsic mitochondrial pathway of apoptosis in β-cells by altering the mitochondrial membrane permeability and release of cytochrome c [78]. ER stress and induction of UPR can also result in ROS generation, and the role of ROS, both as upstream and downstream, to Cer activation is well known [5].

Ceramide and mechanisms of β-cell apoptosis

Several studies indicate that extensive apoptosis of pancreatic β-cell is a relevant event in the pathogenesis of diabetes. The involvement of Cer in this process is also well established [5]. A large number of evidence suggests that Cer-induced pancreatic β-cell apoptosis is mediated by extrinsic death receptors, ER stress, mitochondrial dysfunction with cytocrome c release and ROS production [5].

Cytokines and saturated FAs promote the activation of extrinsic pathway leading apoptosis of pancreatic β-cell. Binding of different cytokines such as tumor necrosis factor-alpha (TNF- α), Interleukin-1 beta (IL-1β) and Interferon-gamma (IFN-γ) to their specific receptors results in the activation of the estrinsic pathway that activate typically caspase-8, which in turn activates downstream effector caspases (i.e. caspase-3) [79] (Fig.3).

Pancreatic β-cells when exposed to cytokines show an increase in Fas expression; moreover, pancreatic β-cells that lacks caspase-8 has shown protection against both Fas and Cer-induced cell death [80]. Liadis et al. demonstrated that caspase-3 knockout mice were protected from diabetes [81], underlying the role of caspase cascade in β-cell apoptosis.

A group of proteins belonging to the B-cell lymphoma-2 (Bcl-2) family regulates the intrinsic mitochondrial pathway. The apoptotic action of Cer is mediated by the recruitment and activation of pro-apoptotic Bax at the mitochondria. Different studies, have demonstrated that induction of Cer formation from SM, determines the translocation and activation of Bax at the mitochondria with cytochrome c release [5]. In agreement with this, depletion of Bax or overexpression of Bcl-2, prevented Cer-induced apoptosis [5].

The intrinsic mitochondrial pathway is also involved in the FAs-induced β-cell apoptosis (Fig. 3). It has been reported that treatment of β-cells to saturated FAs results in enhanced mitochondrial membrane permeability and cytochrome c release [82]. Furthermore, reduction in Bcl-2 expression and Bax up-regulation was also observed when β-cells were exposed to FAs [5]. Cer also inhibits Akt activation, and thereby, promotes the mitochondrial membrane permeability, and cytochrome c release by preventing the Akt induced inactivation of pro-apoptotic Bcl-2 members [83].

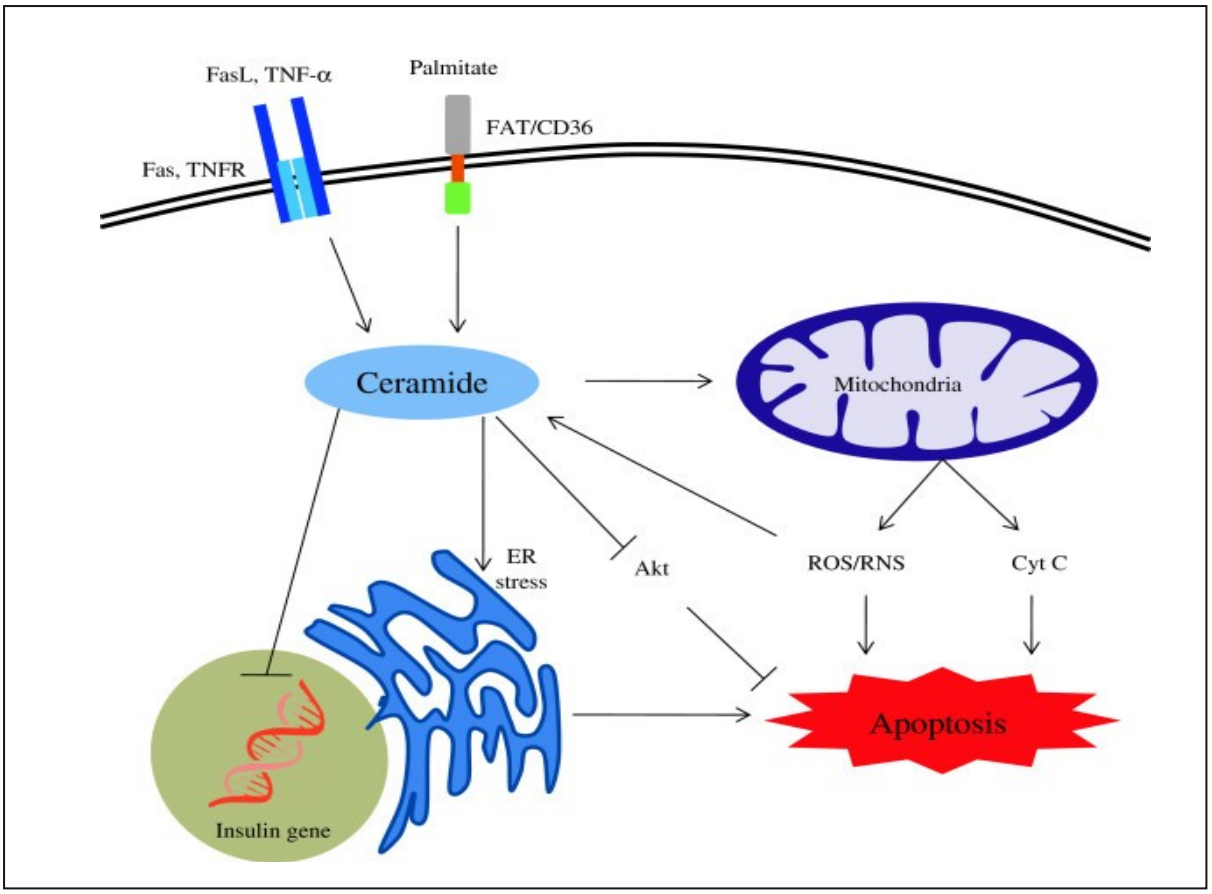

Figure 3: Schematic representation of mechanism of beta-cell apoptosis caused by ceramide

Image from Galadari S. et al. Lipids in Health and Disease 2013 12:98 [5]

Role of ceramide in insulin resistance

Increasing evidence demonstrates that Cer plays significant role in insulin resistance.

Studies using cultures of skeletal muscles and adipocytes treated with Cer provided the first evidence of Cer implication in insulin resistance. These experiments have demonstrated that long treatment with palmitate of cultured myotubes, L6 skeletal muscle cells, 3 T3 adipocytes and cardiac myocytes [5] increases Cer accumulation and promotes Akt inhibition. Further studies using different approaches to block the enzymes of Cer biosynthesis, have demonstrated the role of Cer in saturated FA-induced insulin resistance [84] [85]. In agreement with this, reduction of Cer level, prevented the palmitate-induced Cer accumulation and improved insulin signalling [86].

Animal models studies using mice fed with high-fat diet show an increased expression of Cer synthase [87] Furthermore, in animal models, infusion of lipid emulsion increases muscle Cer content and decrease peripheral insulin sensitivity. These effects were blocked by inhibitors of *de novo* Cer biosynthesis enzyme SPT, indicating the role of Cer [88]. Recently, a study that compared the effect of saturated FAs and unsaturated FAs on insulin

sensitivity in rats, has demonstrated that both of these treatments decrease glucose uptake and Akt activation, but ceramide increase occurs only with saturated FAs oil infusion Analysis of several studies using lipid with different composition in unsaturated and saturated FAs, indicates that Cer plays a role only in insulin resistance induced by saturated fats. In another study, lipid infusion in humans is found to increase skeletal muscle Cer and decrease insulin sensitivity [89].

Ceramide and insulin synthesis

Several studies reveal that Cer is involved also in the reduction of insulin synthesis by decreasing insulin mRNA levels in pancreatic β cells. Saturated FAs also have been shown to increase Cer and impair insulin gene expression. This effect was reversed by inhibitors of *de novo* Cer synthesis [5]. Furthermore, treatments that increase endogenous Cer are able to reduce insulin mRNA levels [90, 91]. Two mechanisms of inhibition of insulin gene transcription by Cer have been proposed. First, Cer activates JNK which inhibits insulin gene transcription both via c-jun-dependent, and oxidative stress-dependent pathways [5]. Second, Cer directly activates PKCζ which phosphorylates and inactivates Pancreatic and duodenal homeobox gene-1 (*PDX-1*), a transcription factor which regulates insulin gene expression [5]. Moreover, Cer has also been shown to decrease transcription of the *Glut-4* gene (Fig.4). In conclusion, these results suggest that Cer modulates signaling pathways involved in the transcriptional regulation of the insulin gene.

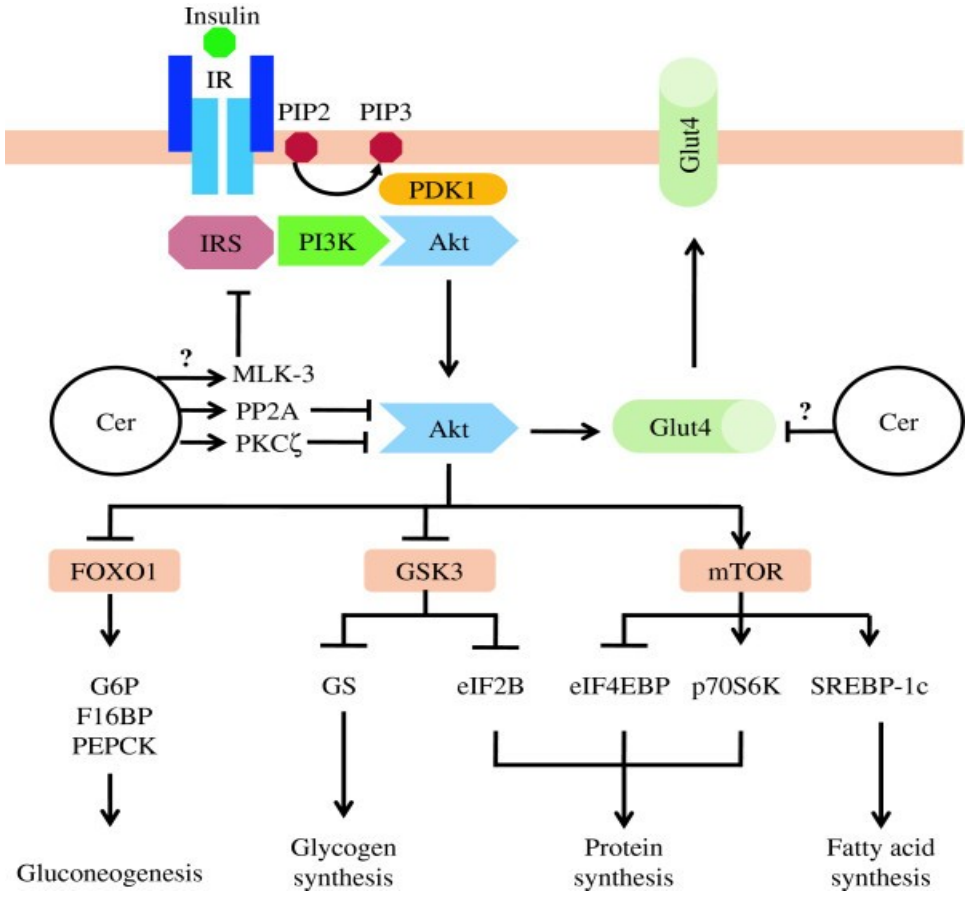

Fig. 4: Major pathways in insulin receptor signaling and mechanism of ceramide in insulin resistance. Activation of insulin receptor leads to Akt activation. Once activated, Akt reduce blood glucose level by inducing glucose uptake, glycogen synthesis, protein synthesis and fatty acid synthesis. Akt also act by inhibiting gluconeogenesis. Some of the metabolic effects of insulin may also be mediated via other signaling branches than those depicted. Ceramide causes insulin resistance by PP2A and PKCζ mediated inhibition of Akt and MLK-3 mediated inhibition of IRS. Ceramide may also decrease *Glut-4* gene transcription. Cer, Ceramide.
Image from Galadari S. et al. Lipids in Health and Disease 2013 12:98[5]

AIM

Glucolipotoxicity is the condition in which the combined action of elevated glucose and FFAs levels synergizes in exerting deleterious effects on pancreatic β-cell function and survival [69, 92, 93]. Several evidence suggests that this condition is a key component in T2D, contributing to β-cell dysfunction and death (reviewed in [94]). Among different FFAs, palmitate represents one of the major species particularly potent in reducing β-cell viability of β-cells from primary rodent, as well as in human islets [77, 95, 96]. Several mechanisms have been proposed for glucolipotoxicity-induced β-cell dysfunction and failure, and, among them, ER stress and elevations of the proapoptotic sphingolipid Cer appear to play key roles. Moreover, these two processes appear to be strictly connected [97-99] and Cer accumulation due to glucolipotoxicity can be associated to the induction of ER stress.

Cer synthesized in the ER is transferred to the Golgi apparatus, where it is subsequently converted to SM, GlcCer and more complex GSL [100]. As mentioned above, two pathways are known to transport Cer from the ER to the Golgi apparatus: a protein-mediated transport, by the soluble Cer transfer protein CERT (for SM formation) [6, 11, 22, 42], and a CERT-independent vesicular traffic (for the biosynthesis of SM or GlcCer) [11, 12, 22]. The two ways of Cer transport coexist separately contributing to the regulation of Cer metabolism and levels in cells. Increased levels of Cer in ER may be due to enhanced Cer biosynthesis and/or decreased Cer utilization. Several data suggest that the accumulation of Cer in the ER compartment of β-cells is crucial in determining β-cell fate. The aim of this study was to gain insights into the molecular mechanisms of glucolipotoxicity to better understand the relationship between Cer accumulation and ER stress, particularly focusing on Cer metabolism and transport mechanisms from the ER to the Golgi, involved in glucolipotoxicity of INS-1 cells.

MATERIALS AND METHODS

Materials

All reagents were of analytical grade unless otherwise stated. The culture medium RPMI 1640 was purchased from Lonza (Basel, Switzerland). L-glutamine, sodium pyruvate solution, penicillin/streptomycin, dimethyl sulfoxide (DMSO), palmitate, glucose, Hepes, bovine serum albumin fraction V (BSA), fatty acid free-BSA, 3-[4,5-dimethylthiazol-2-yl]2,5-diphenyl tetrazolium bromide (MTT), leupeptin, aprotinin, wortmannin (Wm), Thapsigargin (Tg), Kodak Biomax film, HPLC grade water, tetrahydrofuran (THF), methanol, LC-MS grade water, formic acid and ammonium formate were purchased from Sigma-Aldrich (St. Louis, MO, USA). Fetal calf serum (FCS) was from Euroclone (Pero, Milano, Italy). LY294002 was from Cayman Chemical (Ann Arbor, MI, USA). Lipofectamine 2000 and the Stealth RNAi were from Invitrogen (Carlsbad, CA, USA). D-erythro-[3-^{3}H]sphingosine (Sph) (19.7 Ci/mmol), was from PerkinElmer Life Science (Boston, MA, USA). Pepstatin was from Roche Applied Sciences (Mannheim, Germany). High performance thin layer chromatography (HPTLC) silica gel plates were from Merck (Darmstadt, Germany). The Golgi marker Texas red wheat germ agglutinin (WGA), 6-((N-(7-nitrobenz-2-oxa-1,3-diazol-4-yl) amino) hexanoyl) sphingosine (NBD-C_6Cer) and N-(4,4,-difluoro-5-,7-dimethyl-bora-3a,4a-diaza-sindacene- 3-pentanoyl)sphingosine (BODIPY-C_5Cer) were from Life Technologies (Italy). The antibodies recognizing Phospho-Akt (Ser473) were from Cell Signaling Technology, Inc. (Danvers, MA, USA); polyclonal antibodies against Cer transfer protein (CERT) from Bethyl Laboratories (Montgomery, TX, USA). Primary mouse monoclonal anti-phospho-serine, goat anti-GRP78 and rabbit anti-GAPDH antibodies, and secondary HRP-conjugated anti-rabbit or anti-goat antibodies were from Santa Cruz Biotechnology (Santa Cruz, CA, USA). Secondary anti-mouse HRP-conjugated antibody, SuperSignal WestPico Chemioluminescent Substrate and SuperSignal WestFemto Maximum Sensitivity Substrate were from Thermo Scientific (Rockford, IL, USA). Ceramide/Sphingoid Internal Standard Mixture I from Avanti Polar Lipids (Alabaster, Alabama, USA) was used for quantitative analysis. The plasmid of CERT tagged with green fluorescent protein (CERT-GFP) was kindly provided by Dr. Maria Antonietta De Matteis, Telethon Institute of Genetics and Medicine, Napoli (Italy).

Cell culture

Rat insulinoma INS-1 cells, provided by Merck–Serono, were grown in RPMI 1640 medium buffered with 10 mM Hepes containing 10% (v/v) FCS, 2 mM L-glutamine, 1 mM sodium pyruvate, 50 μM 2-mercaptoethanol and 100 units/ml penicillin/streptomycin at 37 °C in an atmosphere of 5% CO_2 and 95% humidified air. Before each experiment, INS-1cells were plated at 2×10^5 cell/cm^2 ,cultured for 24 h in RPMI 1640 plus 10% FCS and then cultured in the presence of 5 mM or 30 mM glucose with or without 0.4 mM palmitate for 12 h; Cells incubation with 30 mM glucose and 0.4 mM palmitate mimics glucolipotoxicity conditions. When indicated, the cells were preincubated with 20μM LY294002, or 10 nM Wm or 0.1 nM Tg for 30 min. Palmitate was resuspended in ethanol and dissolved in PBS containing 5% (w/v) BSA free fatty acid (FFA) to obtain a 4 mM stock solution. The palmitate/BSA FFA stock solutions were diluted in RPMI 1640 medium supplemented with 1% FCS to obtain a 0.4 mM final concentration [101].

Analysis of cell viability

Cell viability was measured by MTT assay. MTT (3-[4,5-dimethylthiazol-2-yl]-2,5-diphenyltetrazolium bromide; thiazolyl blue) is a water soluble tetrazolium salt. Dissolved MTT is converted to an insoluble purple formazan by cleavage of the tetrazolium ring by dehydrogenase enzymes. This water insoluble formazan can be solubilized using solvents and the dissolved material is measured spectrophotometrically yielding absorbance as a function of concentration of converted dye. INS-1 cells were plated and cultured in the presence of 5 mM or 30 mM glucose with or without 0.4 mM palmitate for 12 h, as previously described, or for 24 hours. At the end of the treatments, the medium was replaced by MTT dissolved in fresh medium (0.8 mg/ml) for 4 hours. The formazan crystals were then solubilized in isopropanol/formic acid (95:5 v/v) for 10 minutes and the absorbance (570 nm) was measured using a microplate reader (Wallack Multilabel Counter, Perkin Elmer, Boston, MA, USA) [101].

RNA interference

INS-1 cells were transfected with siRNA duplexes for rat CERT (Gene accession number XM 345143.1) using LipofectAMINE 2000according to the manufacturer's protocol. S87, S522 and control non-targeting siRNAs (scrambled sequences of S87 and S522 oligonucleotides) described in [11] were used. We used Stealth RNAi, the chemically modified synthetic RNAi duplexes that virtually eliminate the induction of non-specific cellular stress response, and that improve the specific, effective knockdown of gene

expression. INS-1 cells plated at $2x10^5$ cell/cm^2 were maintained for 24 h in RPMI 1640 plus 10% FCS and then transfected in the same medium with a 1:1 (by mol) mix of S87 + S522 (si-CERT) or the non-targeting corresponding sequences (si-CT) . The final concentration of siRNA–lipofectamine duplex mixture was 100 nM. All the experiments were performed 72 h after transfection [101].

Plasmid Transfection

INS-1 cells were plated at 2×10^5 cell/cm^2 on a glass coverslip and grown in RPMI 1640 supplemented with 10% FCS until they were 50–70% confluent. Then cells were transfected with expression plasmid encoding the protein CERT tagged with GFP (CERT-GFP) or pcDNA3.1 empty vector using the Lipofectamine 2000 reagent according to the manufacturer's directions [101].

[^{3}H]Sphingosine metabolism

INS-1 cells and INS-1 cells siCT and siCERT plated at 2×10^5 cell/cm^2 were cultured in the presence of 5 mM or 30 mM glucose with or without 0.4 mM palmitate for 12 h. Then cells were pulsed with [^{3}H]Sph (0.3μCi/ml) for 1 h at 37°C. Stock solutions of [^{3}H]Sph were prepared in absolute ethanol and added to fresh medium. In all cases, the final concentration of ethanol never exceeded 0.1% (v/v). At the end of pulse, cells were washed twice with phosphate-buffered saline (PBS) at 4°C, harvested and submitted to lipid extraction and partitioning as previously described [102]. The methanolized organic phase and the aqueous phase were analyzed by HPTLC using chloroform/methanol/water (55:20:3 by vol) and chloroform/methanol/0.2% $CaCl_2$ (55:45:10 by vol) as solvent system respectively. Digital autoradiography of HPTLC plates was performed with Beta-Imager 2000 (Biospace, France) and the radioactivity associated with individual lipids was measured using the software provided with the instrument [101]. The [^{3}H]-labeled sphingolipids were recognized and identified as previously described [102].

Liquid chromatography-tandem mass spectrometry (LC-MS/MS) protocol for lipid extraction and quantitation

Cellular lipids were extracted from INS-1 cells according to Shaner *et al.* [103] with modifications. Briefly, freeze-dried INS-1 cells (2 million) were transferred to a 5 ml glass tube, spiked with 10 µl of internal standard (12.5 µM Ceramide/Sphingoid Internal Mix I), and extracted with 2 ml of chloroform:methanol (1:2, v/v) following brief sonication and

constant agitation in a 50°C water bath for 2 h. After cooling to room temperature, 200 µl of 1M KOH in methanol were added and incubated for 2 h at 37ºC. After cooling, 15 µl of glacial acetic acid were added to neutralize the extract. Following centrifugation, the supernatant was transferred to a new glass tube and the extraction was repeated with a further 2 ml of chloroform:methanol (1:2, v/v). The resulting supernatants were pooled and dried under a stream of N_2. The lipids were resuspended in 200 µl of mobile phase (mobile phase A: mobile phase B, 1:1, v/v). After centrifugation, aliquots were used for LC-MS analysis. Inorganic phosphate (Pi) content of extracts were determined according to van Veldhoven and Mannaerts [104]. Peak areas were used for quantitation by comparison with the peak areas of internal standards.

Chromatographic separation of lipids was performed with an HPLC system consisting of a binary pump, auto sampler, column oven (1200 RRLC, Agilent Technologies, http://www.chem.agilent.com). The lipid molecules were separated using a GeminiNX C_{18} analytical column (2.0 mm I.D. x 100 mm, particle size 3 µm, Phenomenex, http://www.phenomenex.com). Column oven and auto sampler temperatures were maintained at 45°C and 4°C, respectively. The mobile phase consists of solvent A (15 mM ammonium formate (pH 4.0):MeOH:THF, 5:2:3) and solvent B (15 mM ammonium formate (pH 4.0):MeOH:THF, 1:2:7). Elution was performed at a flow rate of 0.30 ml min^{-1} in a binary gradient mode. The initial composition of mobile phase was 65:35 (A:B), linearly changed to 70:30 (A:B) over 12 min, and maintained this composition over 22 min, changed to initial composition 65:35 (A:B) over 1 min, followed by 7 min of column re-equilibration. Column eluant was directed to waste for the initial 1 min.

The HPLC system was coupled online to an Agilent 6460 triple quadrupole mass spectrometer (Agilent Technologies) equipped with a Jet Stream ion source. Data were recorded in positive ionization mode using electrospray ionization with nitrogen as the nebulizing gas. The gas temperature and flow rate was 350°C and 10 l min^{-1}, and the sheath gas temperature and flow rate was 360°C and 12 l min^{-1}, respectively. The ESI needle voltage was adjusted to 4000V in positive mode and optimum fragmentor voltages and collision energies were assigned by analysis of reference compounds (SM (d18:0/12:0); Cer (d18:1/12:0); GlcCer (d18:1/12:0); S1P (d18:1-P)) in selected ion and product ion scanning mode to determine multiple-reaction monitoring (MRM) conditions and mass spectrometric structural studies. MRM detection was applied using nitrogen as the collision gas [101].

Analysis of the Intracellular Distribution of Fluorescent Ceramides

INS-1 cells were plated and grown on a glass coverslip and cultured as previously described. At the end of the treatments, the cells were loaded with 2.5 μM BODIPY-C_5-Cer or NBD-C_6-Cer (as 1:1 complex with fatty acid free BSA) in RPMI 1640 at 4 °C for 30 min [11]. After loading, the cells were incubated 30 min at 37 °C in RPMI 1640 containing 5 mM or 30 mM glucose in the presence or absence of 0.4 mM palmitate and fixed with 0.5% glutaraldehyde solution in PBS for 10 min at 4 °C. The specimens were immediately observed and analyzed with a fluorescence microscope (Olympus BX-50) equipped with a fast high resolution charge-coupled device camera (Colorview 12) and an image analytical software (Analysis from Soft Imaging System GmbH) [101].

Analysis of intracellular localization of CERT-GFP by Cconfocal microscopy

INS-1 cells plated at 2×10^5 cell/cm^2 were grown on a glass coverslip and maintained 24 h in RPMI 1640 plus 10% FCS. The cells were then transfected with the plasmid, CERT-GFP using lipofectamine 2000 according to manufacturer's instructions. 24 h after transfection, cells were treated with 5 mM or 30 mM glucose ± 0.4 mM palmitate for 12 h and fixed with 0.5% glutaraldehyde solution in PBS for 10 min at 4 °C. The cells were then permeabilized with 0.2% Triton X-100 for 30 min at room temperature and stained with WGA-texas red. The specimens were analyzed with a confocal microscope (Leica SP5) [101].

Immunoblotting

Phosho-Akt and GRP78 immunoblotting were performed on INS-1 cells lysed with lysis buffer (20mM Tris-HCl pH 7.4, 150 mM NaCl, 1% NP-40, 10 mM sodium fluoride, 1mM EDTA, 10mM $Na_4P_2O_7$, 1mM Na_3VO_4, and the protease inhibitor cocktail). Solubilized proteins were centrifuged at 14000xg at 4 °C for 10 min. Supernatants were subjected to 10% SDS polyacrylamide gel electrophoresis and transferred to nitrocellulose membranes. Membranes were blocked for 1 h at room temperature in Tris-buffered saline (10 mM Tris-HCl, pH 7.4, 140 mM NaCl) containing 0.1% Tween-20 (TBS-T) and 5% skim milk, and then incubated with primary antibodies against phosho-Akt overnight at 4°C or against GRP78 1 h at room temperature. Membranes were washed in TBS-T, and bound antibodies visualized with horseradish peroxidase-coupled secondary antibodies (Santa Cruz Biotechnology) and chemiluminescent substrate. The relative intensities of bands were quantified by densitometry.

CERT immunoblotting were performed using wild type or si-CT and si-CERT transfected cells lysed with CERT buffer (10mM Tris-HCl pH 7.4, 0.25mM sucrose, 0.5mM

phenylmethylsulfonyl fluoride, 10µg/ml aprotinin, 5µg/mL leupeptin, 5µg/mL pepstatin), processed and analyzed as previously described [11]. The membranes were stripped 30 minutes at 50°C in 2% SDS, 100mM DTT, 0.5M Tris-HCl pH 6.8, washed in TBS-T and incubated 1 hour in Tris-buffered saline (10 mM Tris-HCl, pH 7.4, 140 mM NaCl) containing 0.1% Tween-20 (TBS-T) and 5% BSA and then incubated with the primary antibody against phospho-serine 2 h at room temperature. Membranes were washed in TBS-T and bound antibodies visualized with horseradish peroxidase-coupled secondary antibodies (Santa Cruz Biotechnology) and chemiluminescent substrate [101].

RNA isolation, reverse transcription and Real-Time PCR

INS-1 cells were plated and grown on a glass coverslip and cultured as previously described. At the end of the treatments, total RNA was isolated from INS-1 cells with the RNeasy mini kit and treated with the RNase-free DNAse I. One microgram of RNA was reverse transcribed using the iScript cDNA synthesis kit according to manufacturer's instructions. Real-Time PCR was performed using the iQ5 Real-Time PCR detection system (Biorad Laboratories, Hercules, CA, USA). Specific SYBR green expression assays (SYBR green super mix) for CERT and TBP (TATA-box-binding protein) were carried out. Simultaneous amplification of the target sequences was carried out as follows: 3 minutes at 95 °C, 50 cycles 95°C 10 sec, 59 °C 40 sec and 60 °C 30 sec and 1 cycle of 60 °C 3 minutes. Results were analyzed using the iQ5 optical system software (Biorad Laboratories, Hercules, CA, USA). Relative gene expression was determined using the $2^{-\Delta\Delta Ct}$ method [105]. Data were normalized to TBP expression (used as endogenous control) and INS-1 G5 cells were used as calibrator [101].

Sphingomyelin synthase activity

INS-1 cells were plated and treated as described above. At the end of the treatments, the cells were loaded with 2.5 µM NBD-C_6-Cer (as 1:1 complex with fatty acid free BSA) in RPMI 1640 at 4 °C for 30 min. After loading, the cells were incubated 15 or 30 min at 37 °C in RPMI 1640 with 5mM glucose or 30 mM glucose ± 0.4 mM palmitate. At the end of the incubation, cells were immediately put at 4°C to stop the enzymatic reaction; lipids were extracted with chloroform -methanol [106] and separated by thin-layer chromatography (TLC) using chloroform/methanol/0.1M KCl (1:2:0.8 [vol/vol/vol]) as the developing solvent. Fluorescence-labeled sphingomyelin was quantified with a luminescence spectrometer (LS50B PerkinElmer) [101].

Other methods

Total protein amount was assayed with the Comassie Blue based Pierce reagent, using BSA fraction V as standard. Radioactivity was measured by liquid scintillation counting.

Statistical analysis

Statistical significance of differences was determined by one-way ANOVA.

RESULTS

Effect of palmitate and glucose on cell viability and ER stress in INS-1 cells

We first evaluated the effect of palmitate and glucose on cell survival and ER stress in INS-1 cells. To this end, we treated cells for 12 hours with both 0.4 mM palmitate (P4) and 30 mM glucose (G30) alone and in coadministration (G30P4); our results demonstrated that not all treatments affected cell viability. (Fig. 1 left panel). After 24 hours of treatment with palmitate or 30 mM glucose we did not observe any toxic effects; G30 treatment determined an increase of INS-1 cell as demonstrated in a previously paper [107]. On the contrary, in INS-1 cells, G30P4 treatment for 24 hours decreased cell viability by 53% (Fig. 1a right panel).

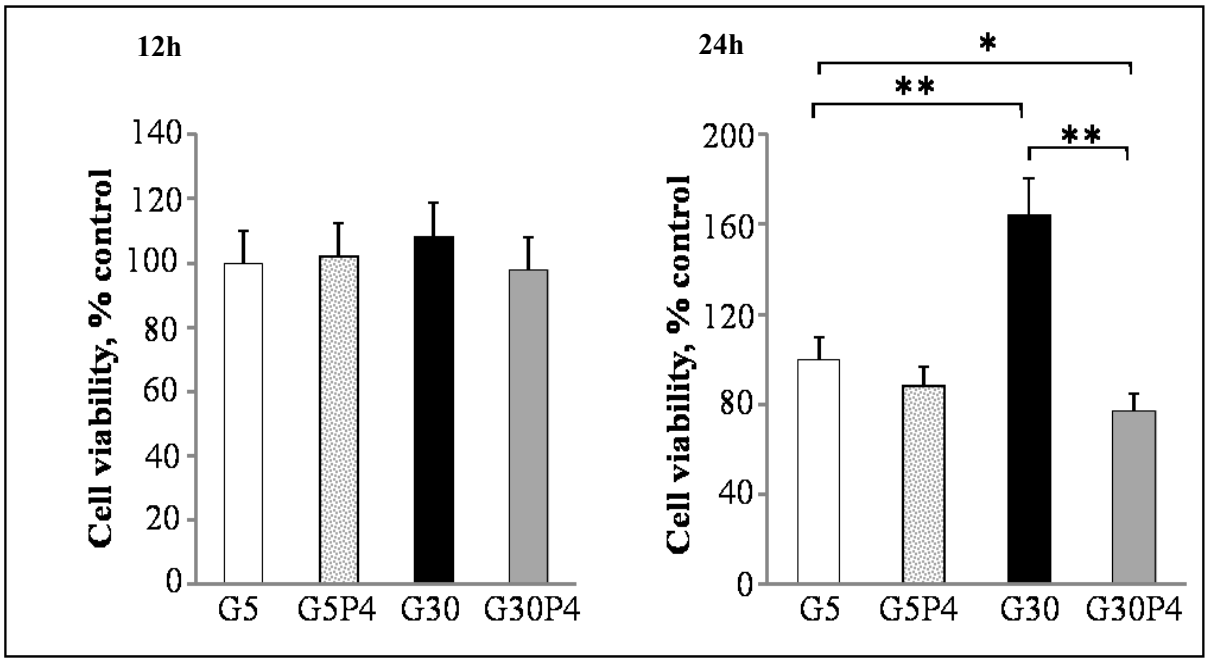

Figure 1: **Palmitate and glucose regulate cell viability in INS-1 cells.** Cells were treated for 12 h (left panel) or 24 h (right panel) with 0.4 mM palmitate (P4) or without palmitate in the presence of 5mM or 30mM glucose. Cell viability was assessed by MTT assay. Results are expressed as percentage of cell viability with respect to 5 mM glucose-treated cells (100%). Data are the mean ± S.D. of three independent experiments. *, $p< 0.05$; ** $p< 0.01$.

Moreover, evaluation of GRP78 expression, an ER stress indicator, by Western blot, showed that 12 hours treatment with G30P4 induced about 60% increase in GRP78 levels compared to G5, G5P4, G30 conditions in INS-1 cells (Fig.2). These data suggested that glucolipotoxic conditions induced ER stress. We treated INS-1 cells with 0.1 μM thapsigargin (Tg) in the presence of 5 mM glucose to have a positive control with an increased amount of GRP78 (Fig.2) [101].

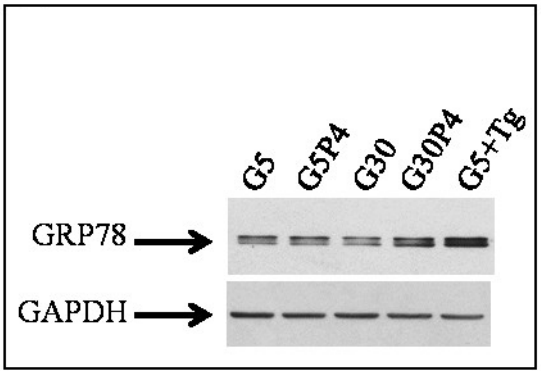

Figure 2: **Palmitate and glucose regulate GRP78 expression in INS-1 cells**. INS-1 cells were treated with 5 mM or with 30 mM glucose in the presence or not of 0.4 mM palmitate and harvested in lysis buffer for immunoblot analysis as described in experimental procedures. INS-1 cells were pretreated 30 min with or without 0.1 μM thapsigargin (Tg). Equal amounts of protein from homogenates were analyzed by immunoblotting with an anti-GRP78 antibody and an anti-GAPDH antibody.

Effect of palmitate and glucose on [^{3}H]Sph metabolism in INS-1 cells

We wanted to evaluate the effect of G30P4 treatment on Cer utilization for the biosynthesis of SM and GSLs in INS-1 cells. We used tritiated sphingosine as a metabolic precursor. In fact, [^{3}H]Sph is rapidly bring inside the cells, efficiently N-acylated to Cer, which is transformed to SM and GlcCer and then to complex GSL. We executed short pulse experiments in order to observe the use of newly synthesized Cer for the biosynthesis of SM and GlcCer [12]. In all conditions studied, tritiated Sph was mainly processed into N-acylated compounds: Cer, SM and, in lower amounts, GSL (Fig.3); the levels of [^{3}H]N-acylated sphingolipids is similar in all treatments. In the presence of P4 the distribution of radioactivity between the different tritiated metabolites were significantly modified with respect to G5 treatment. In INS-1 cells P4 treatment induced [^{3}H]Cer accumulation which was associated to a decrease of [^{3}H]SM levels (Fig.3). G30 treatment also decrease [^{3}H]Cer conversion to [^{3}H]SM. Moreover, G30 treatment strongly increase the reduced utilization of Cer for SM biosynthesis induced by palmitate, and significantly reduced GSL biosynthesis (Fig.3). The percent increase of [^{3}H]Cer was 23% and 14%, respectively in G5P4 and G30 treated cells; in G30P4 treated cells [^{3}H]Cer was 54% higher (Fig.3) than in G5 treated cells. On the contrary, the reduction of [^{3}H]SM was 32% and 23% in P4 or G30 treated cells and 64% in G30P4 treatment, demonstrating that glucolipotoxic condition has a greater effect than the sum of the individual treatments (palmitate or 30 mM glucose). Taken together, these results strongly support that in pancreatic β–cells, glucolipotoxicity can control the utilization of Cer for the biosynthesis of complex sphingolipids in the Golgi apparatus [101].

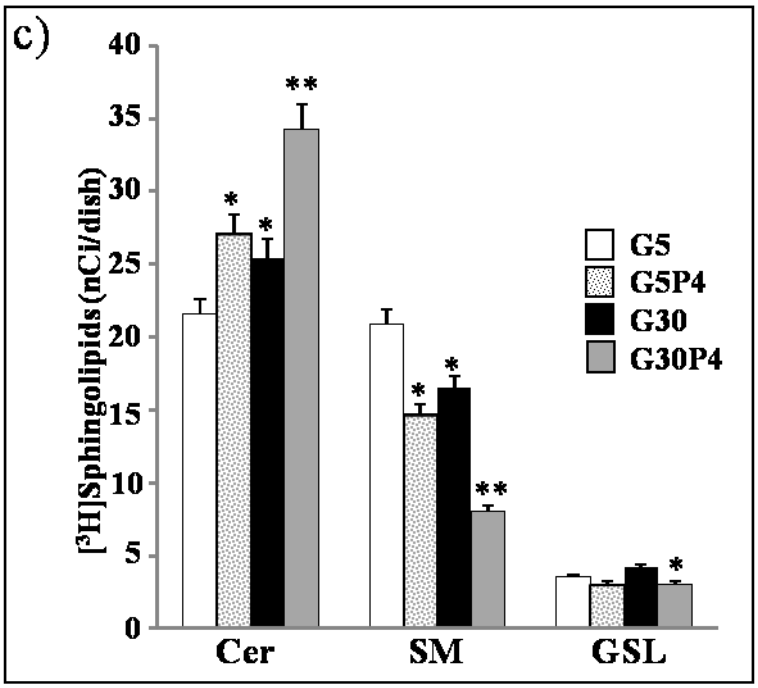

Figure 3: Palmitate and glucose regulate the use of Cer for the biosynthesis of complex sphingolipids in INS-1 cells. Cells were treated for 12 h with or without palmitate in the presence of 5mM or 30mM glucose and then pulsed with 0.3 μCi/ml [C3-^{3}H]Sphingosine for 1 h. At the end of pulse, cells were harvested and submitted to lipid extraction and partitioning. The methanolized organic phase and the aqueous phase were analyzed by HPTLC and digital autoradiography of HPTLC (see experimental procedures). G5, 5 mM glucose; G5P4, 5 mM glucose+0.4 mM palmitate; G30, 30 mM glucose; G30P4, 30 mM glucose+0.4 mM palmitate. Data are the mean ± S.D. of at least three independent experiments. *p<0.05, **p <0.01

Effect of palmitate and glucose on Cer, SM and GlcCer molecular species

Next, we evaluated the levels of Cer, SM and GlcCer and their molecular species by LC/MS/MS in INS-1 cells treated with palmitate. Our results showed that G5P4 as well as G30 treatments did not significantly modify Cer, SM and GlcCer mass levels in INS-1 cells (Fig.4); Conversely, G30P4 condition promoted an increase of Cer mass levels with a associated decrease in the mass levels of SM but not that of GlcCer. Our data show that glucolipotoxic conditions induce an increase in saturated ceramides, mostly in C18:0-Cer and C22:0-Cer (Fig. 4). Moreover, this condition manly reduces the levels of saturated SM, specifically C18:0-SM and C24:0-SM (Fig.4).

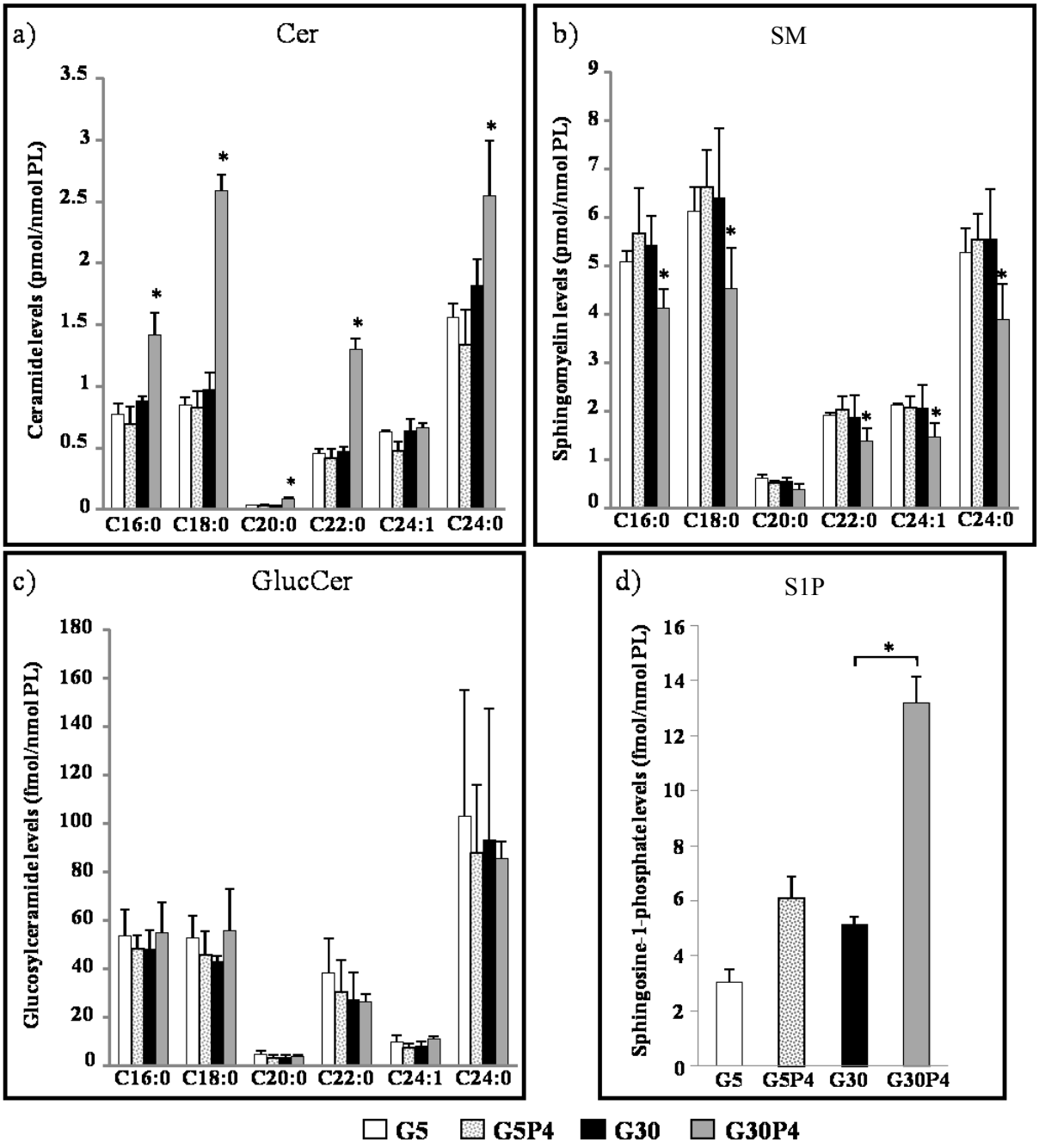

Figure 4: Chain-length specificity of ceramide, sphingomyelin and glucosylceramide in response to palmitate and high concentrations of glucose in INS-1 cells. Cells were incubated with 0.4 mM palmitate in the presence of 5 mM (G5) or 30 mM (G30) glucose for 12 h. Levels of N-acyl chain lengths of Cer (a), SM (b)and GlcCer (c) were determined by LC–MS/MS. Levels of S1P in INS-1 cells were also determined by LC-MS/MS measurement (d). Results are expressed as pmol/nmol of phospholipids (PL) for Cer and SM and as fmol/nmol PL for GlcCer and S1P and are means ± S.D. for three independent experiments. *p <0.05 vs G5 except for S1P *p <0.05 vs G30.

On the contrary, glucolipotoxicity condition did not alter significantly the levels of the different GlcCer molecular species (Fig.4). We also evaluated the levels of S1P in INS-1 cells treated with palmitate. Our data showed that G5P4 treatment did not increase significantly S1P levels in INS-1 cells. However, after a 12 hours of G30P4 treatment S1P

levels were considerably increased (Fig.4), in agreement with data obtained by Verét et al. [108].

Altogether, these data suggest that glucolipotoxicity increased Cer levels and decreased SM levels in pancreatic β-cells, but did not appear significantly affect the amounts of GlcCer [101].

Effect of palmitate and glucose on Sphingomyelin Synthases activity

We wanted to evaluate if the decrease observed in SM levels induced by glucolipotoxicity could be due to the inhibition of SMS activity. To this end, we used the NBD-C_6-Cer, a fluorescently labeled Cer that is a good substrate for SM synthases. G5P4 or G30P4 treatments demonstrated that the activity of SMS in INS-1 cells was not altered (data not shown), suggesting that the enzymes activities involved in the biosynthesis of SM were not affected by glucolipotoxic conditions in INS-1 cells [101].

Effect of palmitate and glucose on intracellular distribution of BODIPY-C_5Cer and NBD-C_6Cer

We then evaluated if the glucolipotoxicity can affect the Cer transport from the ER to Golgi apparatus (where SM and GSL biosynthesis occurs). To follow the movement of endogenous Cer from the ER to the Golgi apparatus we studied BODIPY-C_5-Cer redistribution in cells [106]. In INS-1 cells, G5 and G30 treatments showed most of the fluorescence localized in the perinuclear region (Fig.5a), representative of the Golgi apparatus. In INS-1 cells, G5P4 treatment induces fluorescence accumulation in the perinuclear region in a lesser extent compared to control cell, suggesting a deficit in Cer traffic (Fig. 5a).

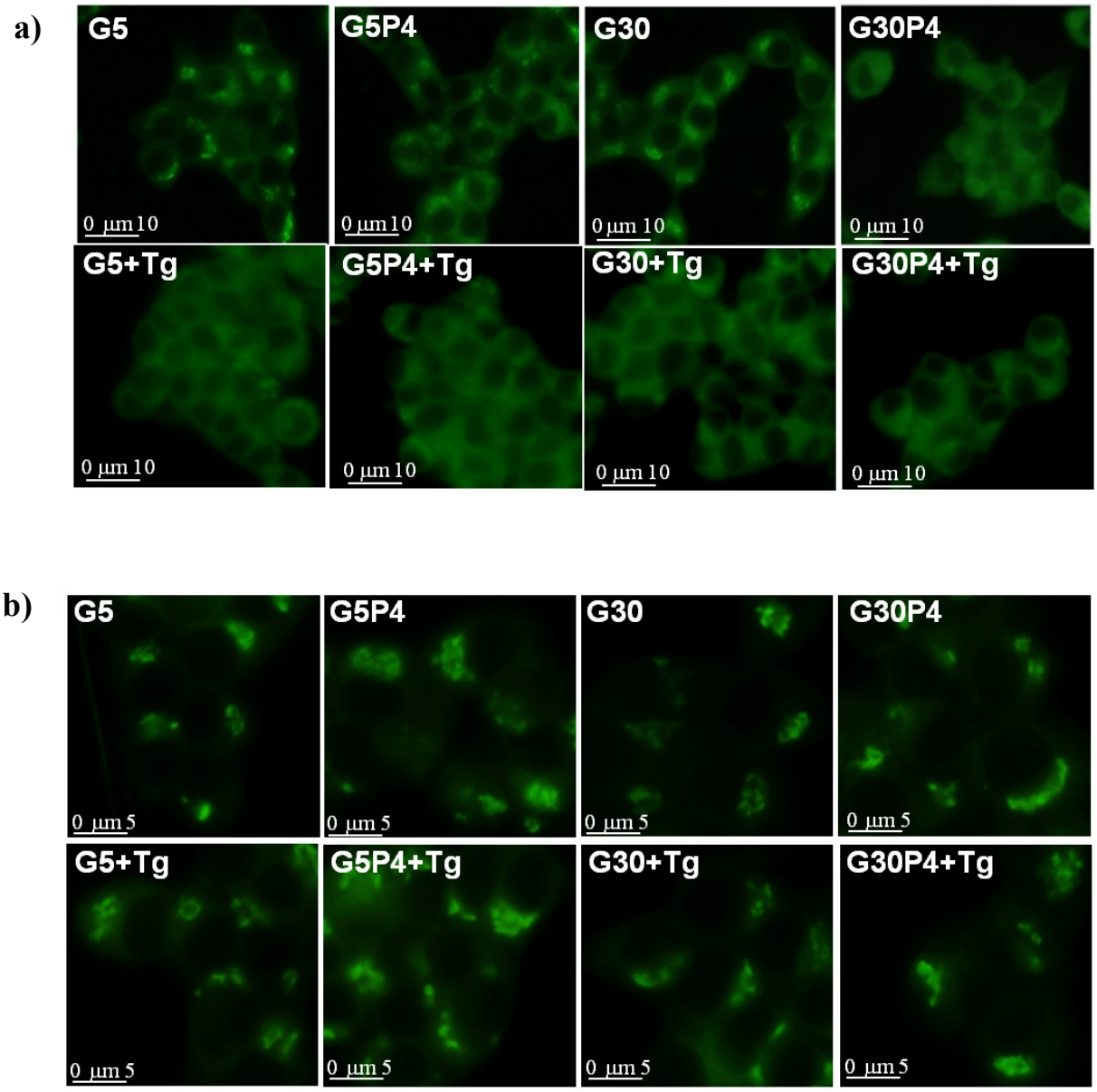

Figure 5: Palmitate and glucose impairs ceramide flow from the ER to the Golgi apparatus in INS-1 cells. INS-1 cells grown on a glass coverslip were pretreated 30 min with or without 0.1 µM thapsigargin. At the end of the pretreatment, the cells were treated with or without palmitate in the presence of 5 mM or 30 mM glucose for 12 h and then incubated with a) 2.5 µM BODIPY-C_5Cer or b) 2.5 µM NBD-C_6Cer as BSA complex 1:1 (m/m) in DMEM for 30 min at 4 °C; labeled cells were incubated at 37 °C for 30 min and analyzed. All images were processed and printed identically.

Glucolipotoxic condition (G30P4) determines a strong reduction of fluorescence accumulation in the Golgi apparatus (Fig.5a), supporting an impairment of Cer flow from the ER to the Golgi apparatus. In INS-1 cells, Tg, which is an ER stress activator in β-cells (Fig.2) [98], has the same effect of G30P4 treatment, strongly reducing the fluorescence staining at the Golgi apparatus (Fig.5a). The effect of Tg was not modified in the presence of glucose or palmitate. In contrast, in INS-1cells labeled with NBD-C_6Cer, which rapidly stain the Golgi apparatus [106], 5 mM and 30 mM glucose in the presence or not of 0.4 mM palmitate with or without Tg did not modify the accumulation of NBD fluorescence in the perinuclear Golgi region (Fig. 5b). Altogether, these results suggest that glucolipotoxicity induces an impairment of Cer flow from the ER to the Golgi apparatus in pancreatic β-cells [101].

Effect of palmitate and glucose on CERT expression and phosphorylation

Recent findings suggest that in INS-1 cells, long-term treatment (48 h) with palmitate inhibit CERT-mediated Cer transport modifying the repression of pro-insulin gene expression [109]. On these premises, we evaluated if a shorter treatment (12 h) of INS-1 cells with palmitate and glucose can modify the levels and the activation status of the protein CERT. Western blot analysis demonstrated that both 0.4 mM palmitate or 30 mM glucose alone did not significantly alter the expression of the CERT protein (Fig.6) whereas cotreatment with 0.4 mM palmitate and 30 mM glucose induced a 65% reduction in the total amount of CERT in INS-1 cells (Fig.6). Moreover, in order to evaluate the amount of phosphorylated CERT, we used an antibody against phospho-serine according to Guo [109]. We found that palmitate or 30 mM glucose alone did not modify significantly the amount of phospho-CERT. Interestingly, coadministration of 0.4 mM palmitate and 30 mM glucose doubled the levels of phospho-CERT in INS-1 cells (Fig.6).

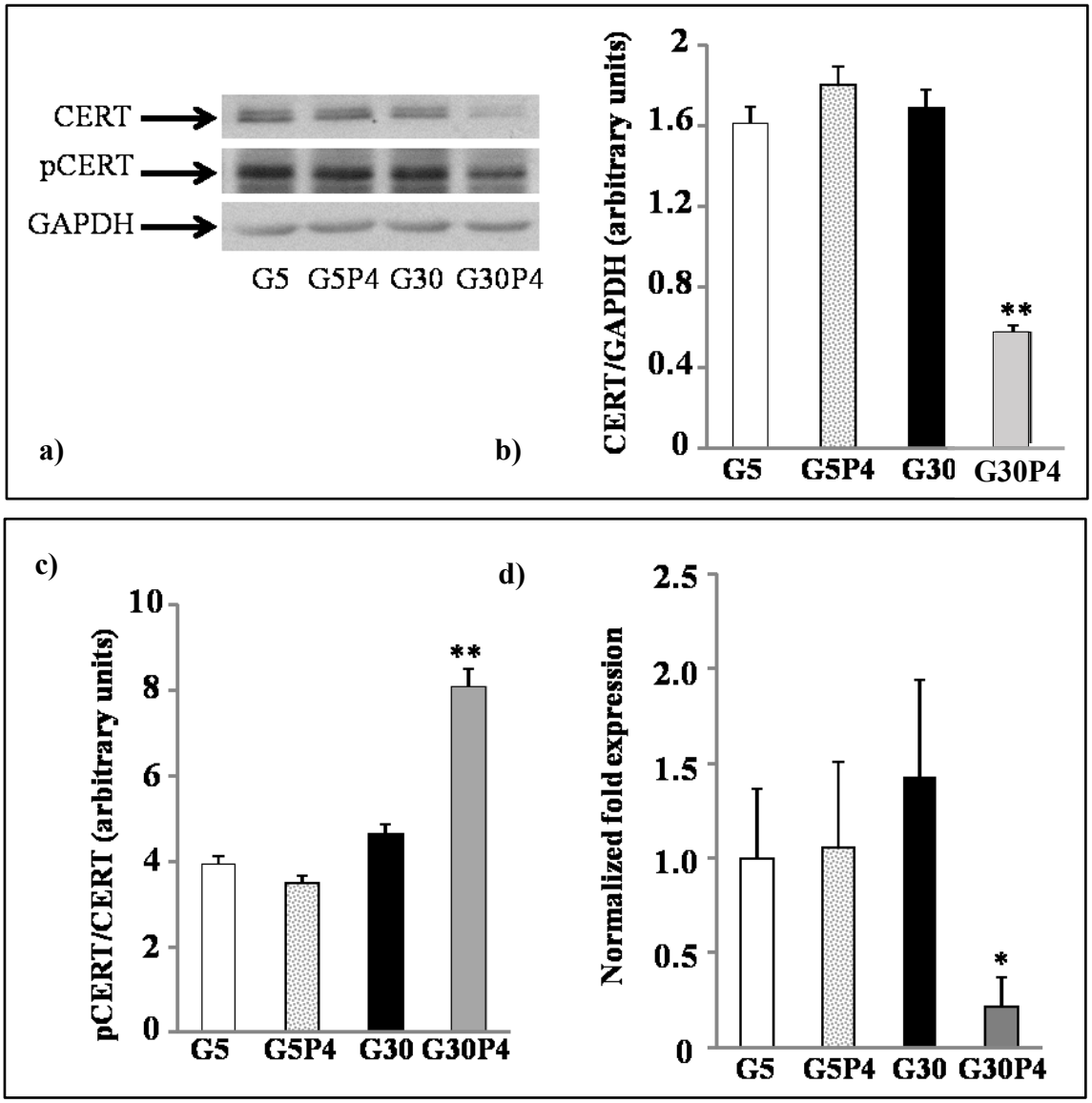

Figure 6: Palmitate and glucose regulate CERT expression and activation in INS-1 cells. a) INS-1 cells were harvested in lysis buffer as described in material and methods. Equal amounts of protein from homogenates were analyzed by immunoblotting with an anti-CERT antibody, an anti-phosphoserine and an anti-GAPDH antibody; b) the amount of CERT expressed was determined by densitometric quantitation and normalized for GAPDH **p <0.01 for G30+palmitate compared with G30; c) the amount of pCERT expressed was determined by densitometric quantitation and normalized for CERT **p <0.01 for G30+palmitate compared with G30; d) Relative expression of CERT assessed by Real-Time PCR. Results are expressed as fold-change relative to G5 *p < 0.05 G30+palmitate cells vs G30. Values are mean ± SD of three independent experiments.

In order to assess if palmitate regulates CERT expression at the transcriptional level, CERT expression was evaluated by Real-Time PCR assay in INS-1 cells. The results obtained (Fig. 6d) show that palmitate in the presence of 30 mM glucose induced a reduction of 80% of CERT expression, thus demonstrating that glucolipotoxicity regulates CERT expression [101].

Effect of palmitate and glucose on CERT subcellular localization

The phosphorylated form of CERT should have the docking site for the Golgi apparatus covered by the START domain. In this conformation, CERT should not be able to colocalize with the Golgi apparatus [110]. To this end, we evaluated the ability of CERT to localize at the Golgi apparatus in INS-1 cells. We analysed the co-localization of over-expressed CERT-GFP with the Golgi marker WGA in INS-1 cells. The images obtained (Fig.7a) showed that in INS-1 cells treated with 5 mM glucose in the presence or the absence of 0.4 mM palmitate, or treated with 30 mM glucose, CERT and WGA co-localized. In contrast, co-treatment with 30 mM glucose and 0.4 mM palmitate significantly reduced co-localization between CERT and WGA in INS-1 cells (Fig.7a) according to the Pearson's colocalization coefficients (Fig.7b). Moreover, when INS-1 cells were treated with 5 mM glucose in the presence or absence of 0.4 mM palmitate, or treated with 30 mM glucose alone, CERT and WGA colocalize in more than 90% of the cells analysed (Fig.7c). On the contrary, in cells treated with 30 mM glucose in the presence of 0.4 mM palmitate the colocalization of CERT and WGA was detectable in only 8% of the cells (Fig.7c). Altogether, our results (Fig.6 and 7) demonstrated that glucolipotoxicity impair CERT-mediated Cer transport by reducing both CERT levels and CERT activity through its phosphorylation, a condition that reduces the capacity of CERT to bind Cer and prevent its localization to the Golgi apparatus [101].

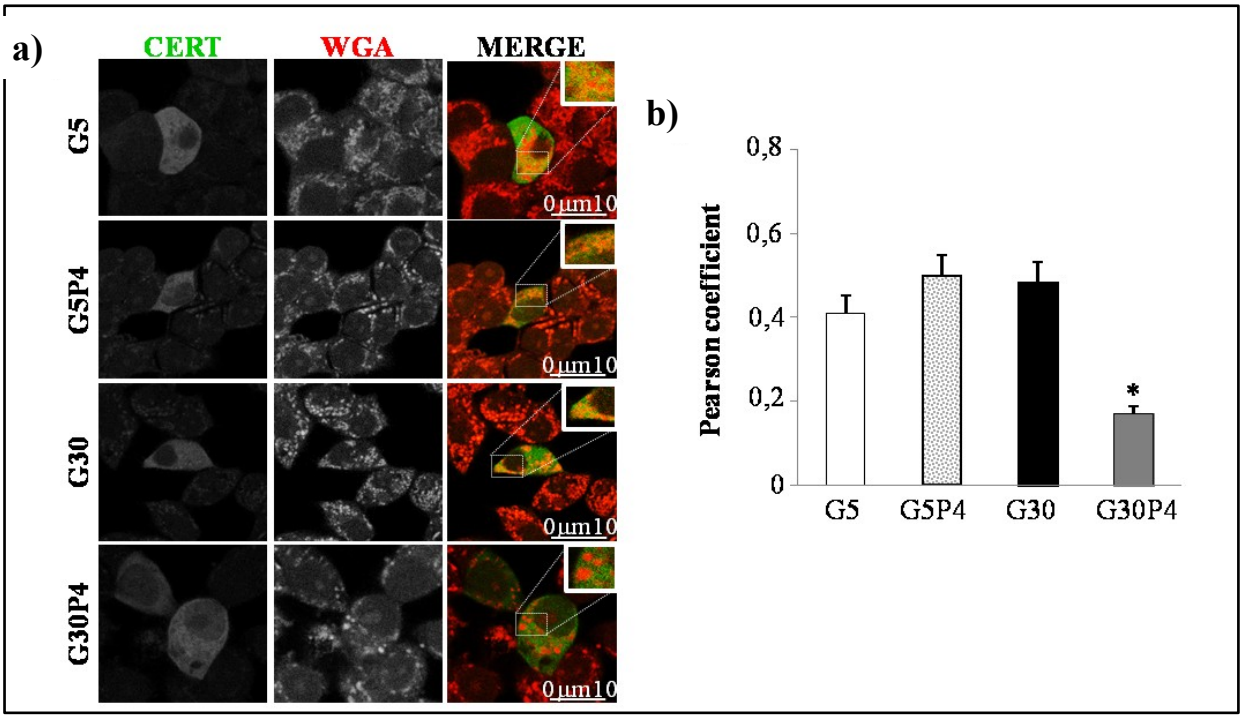

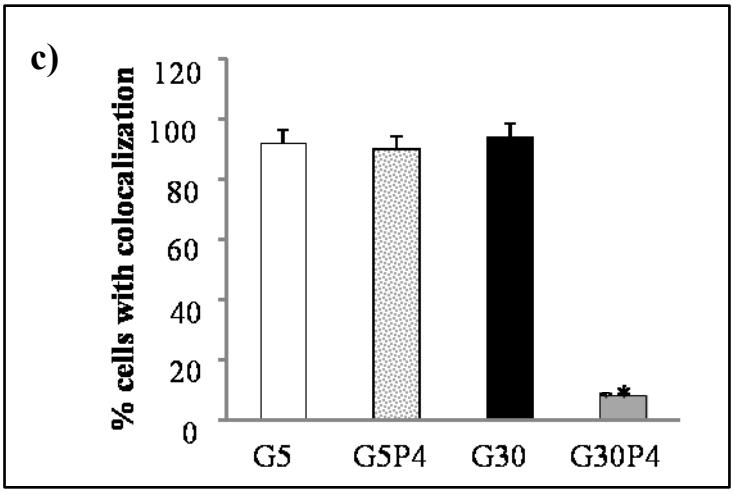

Figure 7: Palmitate and glucose prevent colocalization of CERT and Golgi apparatus in INS-1 cells. INS-1 cells grown on a glass coverslip were transfected with the plasmid CERT-GFP as described in experimental procedures. 24 h later, the cells were treated with or without palmitate in the presence of 5 mM or 30 mM glucose for 12 h. Cells were then fixed and immunostained with WGA texas red-conjugated, a specific marker for the Golgi apparatus. a) Representative confocal microscopy images are shown; all images were processed identically. b) The colocalization between CERT and WGA has been quantified through the software Image J and reported as Pearson colocalization coefficient c) The percentage of cells with colocalization of CERT and WGA was determined. The data are means ± the SD. *$p<0.005$

Effect of palmitate and glucose on [^{3}H]Sph metabolism in INS-1 cells silenced for CERT

Based on the results obtained, we next evaluated if CERT depletion could mimic the defect in Cer utilization induced by glucolipotoxicity. To this purpose, we studied the effect of palmitate with high glucose (30 mM) on [^{3}H]Sph metabolism in control and CERT-down-regulated INS-1 cells. The condition of CERT silencing determines a ≥90% reduction in CERT expression when cells were transfected with a mixture of S87 and S522 (1:1 ratio), as shown in the immunoblot in fig.8a.

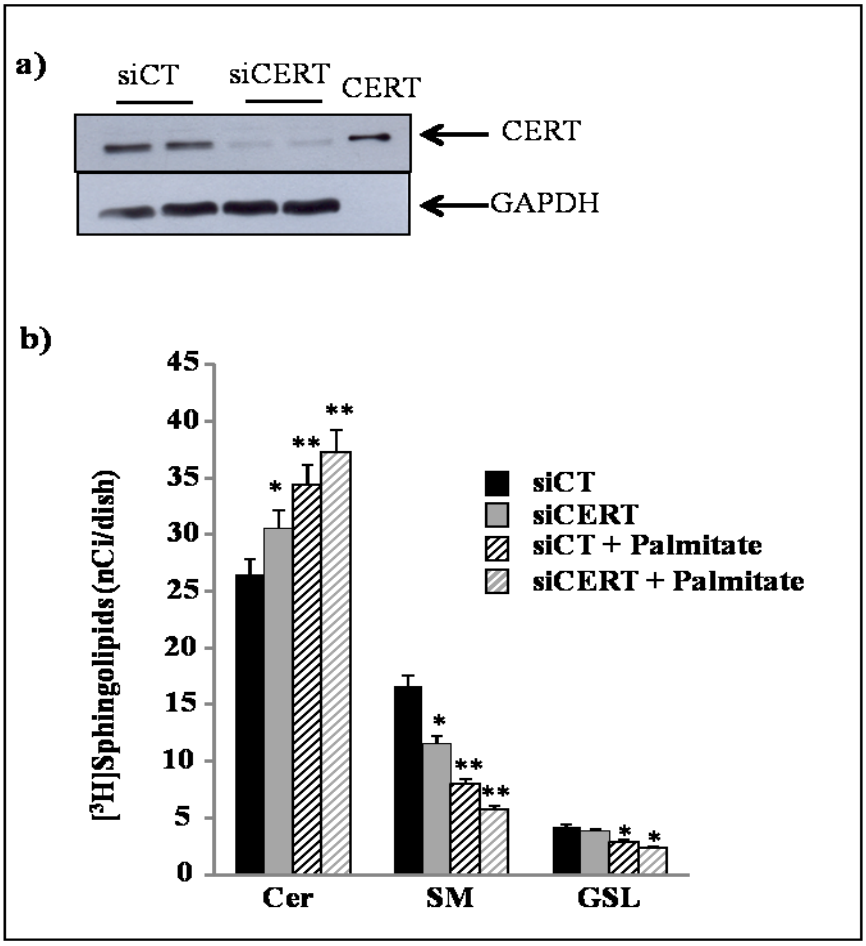

Figure 8: Palmitate and glucose affect vesicular-mediated Cer transport. **a)** Cells were transfected with siRNA for CERT (siCERT) and the corresponding non-targeting corresponding sequences as control (siCT) and 72 h after transfection harvested in lysis buffer. The same amount from homogenate fractions and recombinant CERT (CERT) were analyzed by immunoblotting with polyclonal antibody anti-CERT and monoclonal anti-GAPDH. **b)** INS-1 cells downregulated for CERT were treated for 12 h with or without palmitate in the presence of 30 mM glucose. Then the cells were pulsed with 0.3 μCi/ml [C3-^{3}H]Sphingosine for 1 h and processed and analyzed as described in the legend of fig. 3. Data are mean ± S.D. of at least three independent experiments. *p<0.05; **p <0.1.

As expected, down regulation of CERT promoted a significant but not complete reduction of [^{3}H]Cer conversion to [^{3}H]SM without modifying the amount of synthesized [^{3}H]GSL (Fig. 8b). Palmitate together with 30 mM glucose decreased [^{3}H]Cer utilization for the synthesis of [^{3}H]SM and [^{3}H]GSL in control cells (siCT) but also in siCERT ones (Fig. 8b). In particular, our results demonstrated that glucolipotoxicity induced a 52% decrease of [^{3}H]SM in siCT cells and 65% in siCERT cells compared to cells treated with 30 mM glucose in the absence of palmitate. These results suggest that glucolipotoxicity, in addition to its effect on CERT-mediated Cer transport, can also affect vesicular-mediated Cer transport in pancreatic β-cells [101].

Effect of PI3K/Akt on [^{3}H]Sph metabolism in INS-1 cells treated with palmitate and glucose

We previously demonstrated [18] that the PI3K/Akt pathway regulates the Cer vesicular traffic in glioma cells, so we determined if this occurs in INS-1 cells. Based on the literature, we first evaluated if a 12 h treatment with palmitate and high glucose levels was able to regulate the PI3K/Akt pathway in INS-1 cells. Western blot analysis with a specific antibody for Akt phosphorylated at Ser473, demonstrated that 30 mM glucose did not modify pAkt levels, but 0.4 mM palmitate alone decreased pAkt levels and 0.4 mM palmitate together with 30 mM glucose induced a marked decrease of pAkt levels in INS-1 (Fig. 9).

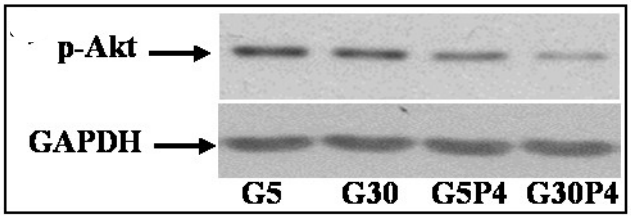

Figure 9: **Palmitate and glucose inhibit PI3K/Akt pathway**. INS-1 cells were treated with 5 mM or with 30 mM glucose in the presence or not of 0.4 mM palmitate and harvested for immunoblot analysis of phospho-Akt and GAPDH levels as described in experimental procedures.

To investigate the effect of PI3K/Akt on Cer metabolism in INS-1 cells, we utilized LY294002, an inhibitor of PI3K. We initially set up working concentrations to specifically inhibit PI3K/Akt. To this purpose, we evaluated the ability of LY294002 and Wm to inhibit the PI3K/Akt pathway. Immunoblot analysis demonstrated that both 20 μM LY294002 and 10 nM Wm strongly reduced Akt activation (data not shown). INS-1 cells, treated with 5 mM or 30 mM glucose with or without palmitate, were pulsed with [^{3}H]Sph in the presence or absence of LY294002 or Wm and the PI3K inhibitors did not alter the [^{3}H]Sph uptake, determined as the radioactivity amount in the total lipid extract (data not shown). In all cases, [^{3}H]Sph was mainly metabolized to N-acylated compounds (Fig.10 a-d) and the extent of N-acylation (evaluated as the sum of tritiated Cer, SM and GSL) was always very similar in the control and treated cells. However, treatment with LY294002 or Wm strongly modified the radioactivity distribution among the different Sph metabolites both in the presence of 5 mM or 30 mM glucose (Fig.10 a and 10 b). In 5 mM glucose plus LY294002 or 5 mM glucose plus Wm treated INS-1 cells, the radioactivity associated to [^{3}H]Cer was respectively 21% and 17% higher than that in 5 mM treated cells, with a concomitant reduction of both [^{3}H]SM and [^{3}H]GSL levels. In particular, [^{3}H] SM was 39% and 32%

lower respectively in the presence of LY294002 and Wm, whereas [^{3}H]GSL were 29% and 27% lower, respectively in the presence of LY294002 and Wm compared to 5 mM treated cells (Fig.10a).

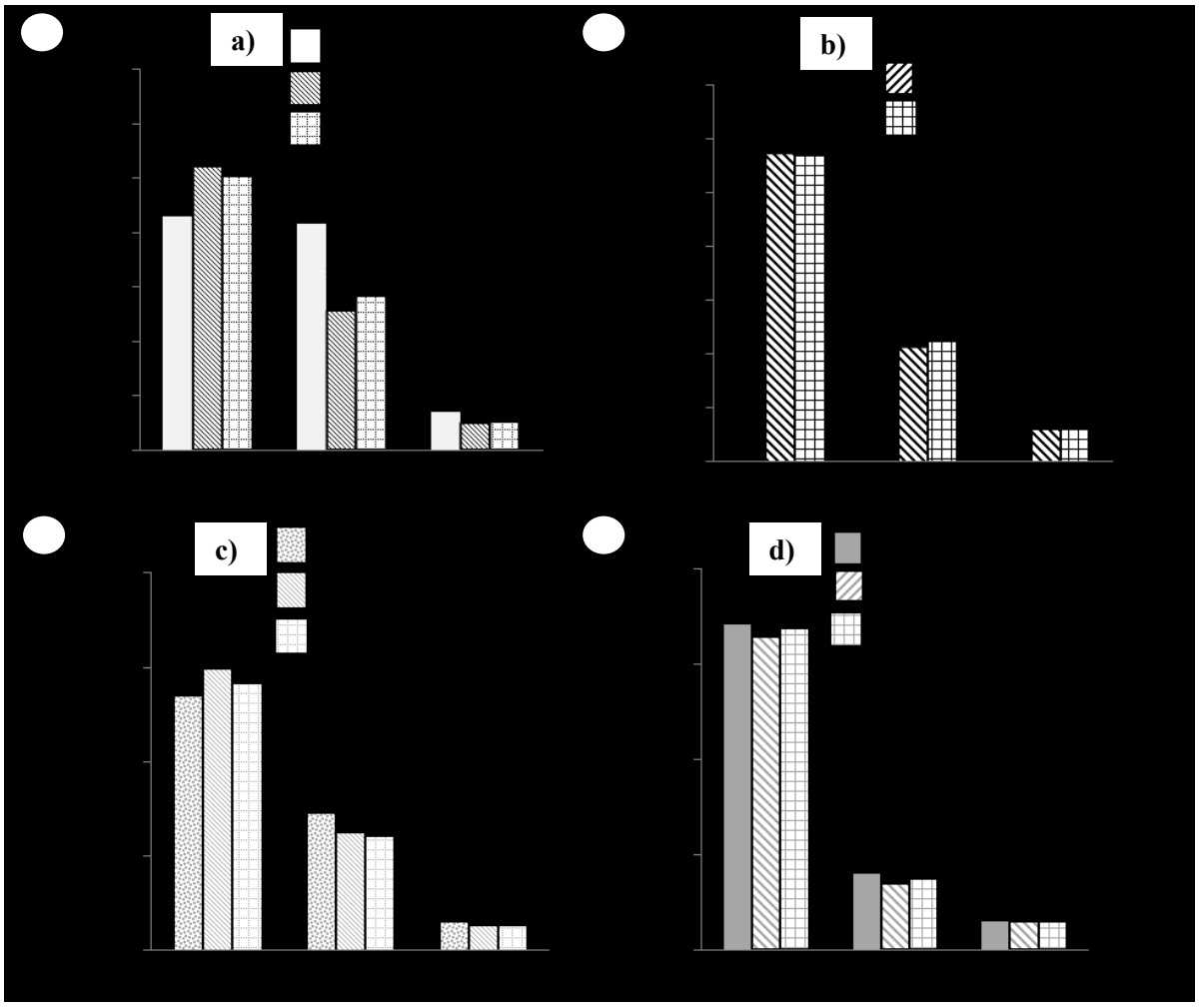

Figure 10: **Palmitate and glucose inhibit vesicular-mediated Cer traffic a**) INS-1 cells were treated for 12 h with 5 mM glucose in the presence or absence of LY294002 or of Wm; **b**) INS-1 cells were treated for 12 h with 30 mM glucose in the presence or absence of LY294002 or Wm; **c**) INS-1 cells were treated for 12 h with 5 mM glucose plus 0.4 mM palmitate in the presence or absence of LY294002 or Wm; **d**) treated for 12 h with 30 mM glucose plus 0.4 mM palmitate in the presence or absence of LY294002 or Wm. Then cells were pulsed 1 h with [^{3}H]Sph in the absence (*opened and dotted bars*) or presence of 20μM LY294002 (*striped bars*) or 10 nM Wm (*square bars*). At the end of pulse, cells were harvested and submitted to lipid extraction and analyzed as described in the legend of fig. 3. All values are the mean $\pm$ S.D. of at least three individual experiments. *p<0.05, **p <0.01.

Similarly, in cells treated with 30 mM glucose, LY294002 and Wm promoted about 30% reductions in synthesized [^{3}H]SM and 20% decrease in [^{3}H]GSL compared to 30 mM glucose treated cells (Fig.10 b). Taken together these results suggest that the PI3K/Akt pathway can regulate the metabolic utilization of Cer through the modulation of the

vesicular traffic of Cer, favouring the maintenance of low Cer levels in INS-1 cells even in conditions (high glucose) of reduced utilization of Cer for the biosynthesis of complex sphingolipids. In cells treated with 5 mM glucose+palmitate, LY294002 or Wm slightly reduced the amount of synthesized SM and GSL (Fig.10 c). In G30P4 treated cells (characterized by a reduced utilization of Cer for the biosynthesis of complex sphingolipids), LY294002 or Wm did not further reduce the amount of synthesized SM and GSL (Fig.10 d). Altogether, this data suggest that palmitate inhibits vesicular-mediated Cer traffic through downregulation of PI3K/Akt pathway. This effect is strongly potentiated in glucolipotoxic conditions, thereby contributing to the accumulation of Cer in pancreatic β-cells [101].

DISCUSSION

Based on different approaches using a tritiated precursor and fluorescent analogs of Cer, this study provides evidence that, in INS-1 cells, elevated glucose and fatty acid levels affect Cer traffic from the ER to the Golgi apparatus, promoting Cer accumulation in the ER. In particular, 12 hours of glucolipotoxic treatments reduce Cer utilization for the biosynthesis of SM, GlcCer and complex GSL. We demonstrated that, consequently, Cer levels increase whereas total SM but not GlcCer levels decrease. Interestingly, glucolipotoxicity modified only saturated SM species in β-cells, thus leading to the accumulation of saturated Cer species such as C18:0-Cer, which are known mediator of apoptosis in β-cells [107]. The reduction of SM biosynthesis was not due to a possible effect of glucolipotoxicity on SMS activity in the Golgi apparatus. In fact, under glucolipotoxic condition, using the SMS substrate NBD-C_6-Cer, which reaches the Golgi apparatus by easy diffusion through the cytosol, we established that INS-1 cells maintained the ability to properly synthesize SM. On the other hand, in the same experimental conditions, the analysis of intracellular distribution of BODIPY-C_5-Cer, which employs the same transport mechanisms of natural Cer [12, 106, 112], demonstrated a defect in the Cer intracellular traffic from the ER to the Golgi apparatus. These data support that in glucolipotoxic conditions, this mechanism can contribute to Cer accumulation at the ER. Moreover, several recent studies have demonstrated that palmitate–dependent accumulation of Cer at the ER is associated to ER stress induction and apoptosis of pancreatic β-cells [98, 106, 113, 114]. In agreement with these observations, our data demonstrated that 12 h of treatment with palmitate and high glucose concentrations induce ER stress in INS-1 cells, underling the crucial role of Cer accumulation in the ER as a mechanism to promote β-cells apoptosis, thus contributing to the development of type 2 diabetes [101]. As previously discussed, in INS-1 cells too, two main mechanisms operate to transport Cer from the ER to the Golgi apparatus: a CERT-dependent and a CERT-independent system; we demonstrated that glucolipotoxicity strongly affected both of them. In particular, we observed a significant decrease in the total amount of CERT protein as well as in the mRNA level [101]. In this respect, Granero et al. identified a human-specific TNFα-responsive promoter for CERT [116] involved in the transcriptional CERT regulation. Moreover, we demonstrated that, in glucolipotoxic conditions, the remaining CERT protein is in a highly phosphorylated status that impairs the correct recognition and localization to the Golgi apparatus of the CERT PH domain, strongly limiting CERT transfer activity [110]. Altogether, these data demonstrate that glucolipotoxicity impairs the CERT-mediated Cer traffic from the ER to the Golgi

apparatus, thus supporting that, under glucolipotoxic conditions, this mechanism contributes to the accumulation of Cer at the ER.

The vesicle-mediated CERT-independent Cer transport was also impaired under glucolipotoxic condition. In fact, in INS-1 cells silenced for CERT, glucolipotoxicity is still able to reduce the metabolic utilization of Cer for the synthesis of SM and GSL. In INS-1 cells, the PI3K/Akt pathway is involved in the positive regulation of Cer metabolism [101], as demonstrated also in glioma cells [18]. Glucolipotoxicity promotes a strong inhibition of Akt, consistent with previous studies showing that long-term exposure to glucolipotoxic conditions and/or high palmitate decreases Akt activation in pancreatic β-cells [117-119]. Also palmitate alone partially decreased pAkt levels and this was associated to the inhibition of Cer vesicular traffic.

Moreover, our results demonstrated that glucolipotoxicity increased total S1P levels in INS-1 cells. Giussani et al. [115] demonstrated that the decrease of S1P is associated to a Cer traffic impairment; in addition, in the second part of this thesis, we demonstrated that S1P promotes Cer vesicular transport from the ER to the Golgi apparatus. This lead us to hypothesize that increased S1P levels are not sufficient to counteract the effect of glucolipotoxicity on Cer traffic [101].

The PI3K inhibitors, LY294002 and Wortmannin, which are not effective in glucolipotoxic conditions, have a slight effect on Cer flow in cells treated with palmitate in the presence of 5 mM glucose, probably because palmitate alone partially inhibits pAkt. The results of our study support the idea that glucolipotoxicity inhibits the PI3K/Akt pathway in INS-1 cells, which in turn could inhibit Cer vesicular trafficking [101]. On the other hand, we demonstrated that 30 mM glucose decreases the biosynthesis of SM but does not modify pAkt levels and Cer traffic suggesting that in this case the effect on SM could be associated with increased N-SMase activity, consistent with previous papers [113, 120] wich demonstrate that high glucose levels increased N-SMase activity. Thus, in glucolipotoxic conditions we cannot exclude a contribution of this pathway to the decrease of SM levels.

Altogether, our data demonstrate that the two Cer transport mechanisms can separately contribute to the control of sphingolipid metabolism and Cer levels in INS-1 cells [101], thus participating in the regulation of Cer accumulation in the ER involved in pancreatic β-cell function and death during T2D [98, 114]. Moreover, these findings suggest that an impairment in ER to Golgi Cer traffic can act synergistically with enhanced *de novo* Cer biosynthesis [107, 121], leading to accumulation of Cer in the ER in response to glucolipotoxicity.

Further information on the mechanisms that regulate the accumulation of Cer at the ER will be important to develop new strategies to prevent T2D. Moreover, the capacity of the PI3K/Akt pathway to regulate sphingolipid metabolism may also be pathologically relevant in β−cells if we consider that the PI3K/Akt pathway plays a crucial role in the control of β-cell mass and function by modulating a dynamic balance of proliferation, cell size and apoptosis [122].

Part 2: The stimulation of Ceramide traffic from the ER to the Golgi apparatus S1P-dependent as a survival factor in T98G glioma cells

INTRODUCTION

Glioblastoma

GBM is the most common malignant primary brain tumor in adults and one of the most lethal human cancers. Furthermore, GBM is characterized by elevated resistant to radiation and cytotoxic chemotherapy [123], with a median survival ranging from nine to twelve months [124, 125] despite aggressive surgical resection and conventional therapy [126]. The surgical approach often cannot be applied without functional loss of large areas of central nervous tissue with severe neurological impairment [123]. GBMs are part of the spectrum of malignant gliomas, which are thought to arise from the intrinsic glial cells of the brain [127]. Gliomas include a group of highly heterogeneous cancers classified, according to cell line derivation and differentiation morphological evidence, in astrocytoma, oligodendroglioma, oligoastrocytoma, ependymoma and choroid plexus tumours [124]. Astrocytomas are the highest incidence gliomas (75% of all gliomas) [128], sorted by the World Health Organization (WHO) in different classes, distinguished by the presence of specific histological characteristics such as nuclear atypia, mitotic activity, endothelial proliferation and necrosis [129]. In particular, it is possible to distinguish four different classes of astrocytomas: pilocytic astrocytoma (grade I), diffuse or fibrillary astrocytoma (grade II), anaplastic astrocytoma (Grade III), and glioblastoma multiforme (grade IV). The tumours belonging to the class I and II are considered with low-grade malignancy, while those of III and IV class are considered to be high-grade malignant [129]. Glioblastoma multiforme or simply glioblastoma (GBM) (WHO grade IV) is the most frequent malignant primary brain tumour and it is one of the most aggressive cancer.

As defined by the term “multiforme”, GBM comprises morphologically heterogeneous neoplasms, in which the cellular composition can be highly variable. GBM is characterized by uncontrolled cell proliferation, diffuse infiltration, massive angiogenesis, high genomic instability, strong resistance to apoptosis and then to radio-chemotherapy, all distinguishing features representing useful prognostic factors for overall survival [126, 127, 130].

Two classes of GBM have been identified: primary GBM (or GBM de novo) and secondary GMB [124]. Primary GBM accounts for about 90% of GBM cases and it is diagnosed without evidence of a previous lower-grade tumour. Primary GBM generally occurs in elderly patients (60-70 years old) and it is characterized by a very short clinical history (less than 3 months). On the other hand, secondary GBM, representing the minority of GBM cases, derives from a lower-grade tumour that undergoes the process of tumour progression

to higher malignancy grades. Secondary GBM usually occurs in adults between fifty and sixty years, and the time of progression from lower to higher degree of malignancy ranges from months to decades [130, 131].

Altered signalling pathways in glioblastoma tumorigenesis

GBM has been selected to be profiled by the National Institutes of Health's Cancer Genome Atlas (TCGA) and now it is one of the most molecularly profiled of all human tumors. TCGA and those of other groups [132], have defined that molecular alterations of GBM area characterized by amplification of *EGFR*, *MET*, platelet-derived growth factor receptor A (*PDGFRA*), *MDM4*, *MDM2*, *CCND2*, and phosphatidylinositol-4,5-bisphosphate 3-kinase A (*PIK3CA*), among others, and deletion of cyclin-dependent kinase inhibitor 2A/B (*CDKN2A/B*), *CDKN2C*, *PTEN*, retinoblastoma protein 1 (*RB1*), and *NFKB1A*. Somatic mutations of *p53*, *PTEN*, neurofibromatosis type 1 (*NF1*), *RB1*, isocitrate dehydrogenase 1 (*IDH1*), and *IDH2* have also been detected with varying frequencies, as have *EGFR* extracellular domain mutations, including EGFR variant III (*EGFRvIII*). Also, an integrated analysis of the wealth of genetic lesions already identified has revealed that these genomic lesions cluster into three core pathways: (*a*) receptor tyrosine kinase/RAS/phosphatidylinositol 3 kinase (RTK/RAS/PI3K) signaling (altered in 88% of GBMs); (*b*) p53 signaling (altered in 87% of GBMs); and (*c*) Rb signaling (altered in 78% of GBMs) [132].

PI3K /Akt/PTEN pathway

Among the pathways altered in glioblastomas there is also the phosphatidylinositol 3-kinase (PI3K)/Akt (PKB)/PTEN (Phosphatase and tensin homolog) signalling. PI3K are a family of kinases that phosphorylate membrane lipids, in particular phosphoinositides and phosphatidylinositols, such as the phosphatidylinositol 4,5-bisphosphate (PtdIns (4,5) P_2) which is converted in phosphatidylinositol 3,4,5-triphosphate (PtdIns (3,4,5) P_3).

PI3K activation can occur through G proteins coupled receptors or growth factors tyrosine-kinases receptor. Upstream receptor tyrosine kinases (RTKs), such as EGFR, activate class IA PI3Ks. The binding of the p85 regulatory subunit of PI3K to phosphotyrosine residues on activated RTKs leads to a conformational change in p85, releasing the inhibition of the catalytic subunit p110 (a, b, and d isoforms) of PI3K. The PtdIns (3,4,5) P_3 binds to different cytosolic proteins, including Akt which undergoes a conformational change that facilitates

its activation through phosphorylation in correspondence of the two amino acid residues T308 and S473 by phosphoinositide-dependent kinases (PDK) 1 and 2, respectively (Fig.1).

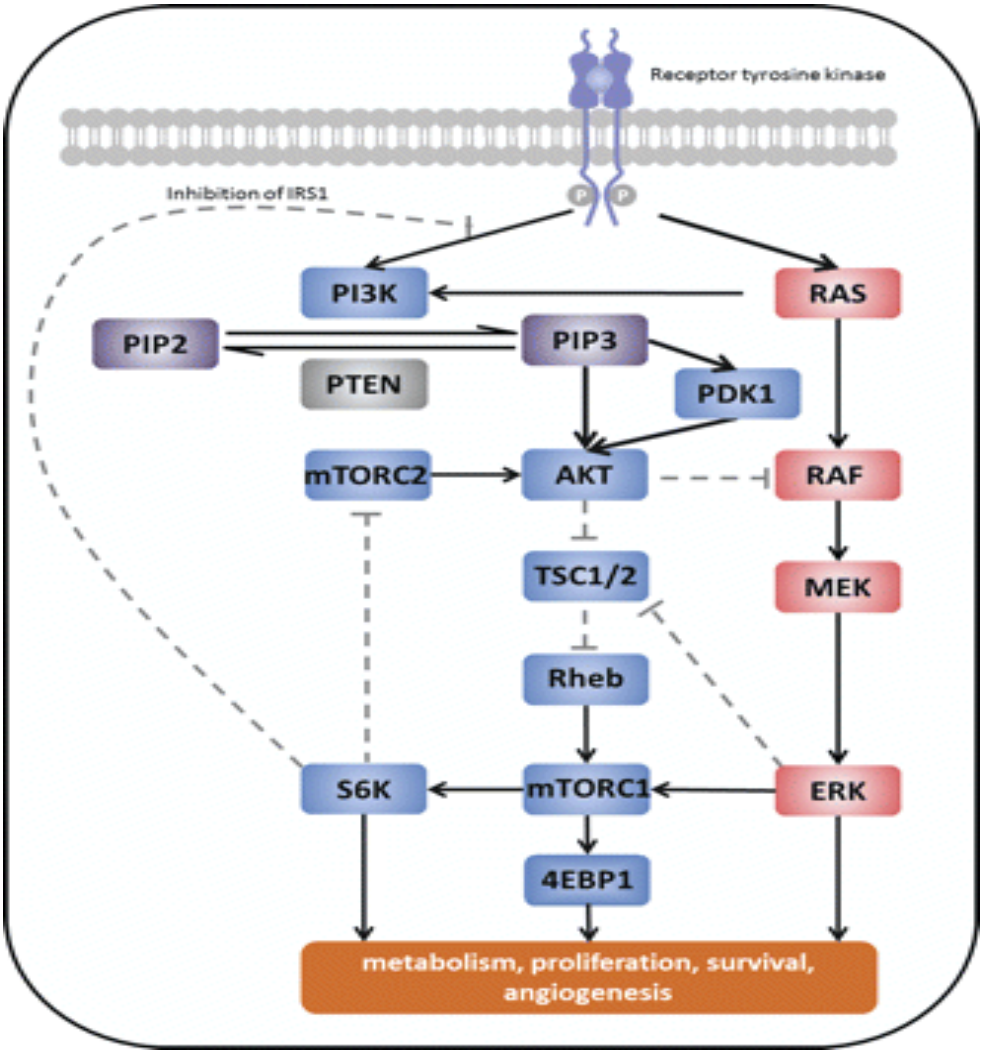

Figure 1: **Schematic representation of the PI3K pathway and its main components.** Solid lines represent activation; dashed lines represent inhibition. 4EBP1, eukaryotic initiation factor 4E binding protein 1; ERK, extracellular signal-related kinase; IRS1, insulin receptor substrate 1; MEK, mitogen-activated protein/ERK kinase; mTORC1/2, mammalian target of rapamycin complex 1/2; PI3K, phosphatidylinositol 3-kinase; PIP_2, phosphatidylinositol 4,5-bisphosphate; PIP_3, phosphatidylinositol 3,4,5-trisphosphate; PDK1, 3-phosphoinositide dependent protein kinase-1; PTEN, phosphatase and tensin homolog; RAS, rat sarcoma oncogene; Rheb, rat homolog enriched in the brain; S6K, S6 kinase; TSC, tuberous sclerosis protein.
Image from: Wen et al. Neuro-Oncology, 2012

PTEN is a phosphatase that negatively regulates the PI3K/Akt pathway, by converting PtdIns (3,4,5) P_3 in PtdIns (4,5) P_2, thus directly antagonizing PI3K activity. Akt is a key regulator of cell proliferation and survival pathways. It is a Serine/Threonine kinases able to

inhibit apoptosis, promote cell proliferation and regulate lipids and glucose metabolism, cell movements and vesicle trafficking.

High levels of phosphorylated/activated Akt and deletions or mutations in the PTEN gene are the most common alterations of the PI3K/Akt signalling in glioblastomas. These changes are crucial in determining the GBM malignant features, such as rapid tumour growth, invasiveness, resistance to cytotoxic treatments and massive angiogenesis [124, 133, 134].

p53 pathway

The p53 protein is one of the most important tumour suppressors. Its expression is up-regulated in response to conditions of cellular stress, such as γ and UV radiation, hypoxia, DNA damage and inappropriate oncogene activation. p53 acts as a transcription factor promoting the expression of genes that block the cell cycle and genes that repair DNA. If the amount of damage is beyond the cell's capacity for repair, p53 favours the expression of genes involved in apoptosis, promoting cell death.

p53 inactivating mutations are frequent in secondary GBM. Alterations of regulators of p53 levels and/or activity are common in primary GBM. For example, Mdm2 protein is a negative regulator of p53: Mdm2 binds to p53 promoting its ubiquitination and subsequent degradation via proteasome. Mdm2 is overexpressed in some GBM. Furthermore, the $p14^{ARF}$ protein, which negatively regulates the Mdm2 ability to bind p53, is often deleted in malignant gliomas or the corresponding gene is methylated so that its expression is inhibited. The abnormal p53 pathway functioning leads to a greater tolerance to DNA damages resulting in genomic instability [135, 136].

pRb pathway

The retinoblastoma protein (pRb) is a tumour suppressor involved in the regulation of the cell cycle, controlling cells transition from the G1 into the S phase. Cyclins/cyclin-dependent kinase (Cdk) complexes and Cdk inhibitors play a fundamental role in the regulation of cell proliferation. In particular, the cyclin D/Cdk4 complex catalyses the pRB phosphorylation resulting in the release of E2F transcription factors sequestered by the pRB binding, which are essential for the expression of the S-phase-genes, thus inducing DNA synthesis. Moreover, the $p16^{INK4a}$ protein inhibits cell cycle progression, negatively regulating the formation of the complex cyclin D/Cdk4. Inactivating mutations of pRB and $p16^{INK4a}$ or the amplification of genes coding for Cdk4 and cyclin D are typical features of

glioblastomas. All of these changes cause the pRB inability to bind E2F, resulting in an uncontrolled cell cycle progression from G1 to S phase [135, 136].

Ceramide in Glioblastoma

Cer is known to play an important role in the evolution of neoplastic tumours, being involved as a mediator in the signal transduction mechanisms that control growth arrest, differentiation, senescence and cell death [16]. Different studies have demonstrated that the generation of Cer in response to cytotoxic therapy is a key step leading to cell death. In gliomas, the involvement of an altered regulation of the Cer-mediated signalling pathways is strongly supported by the evidence for an inverse association between Cer intracellular levels and the progression of the tumour malignancy a lower content of Cer corresponds to a higher grade of malignancy. It was also demonstrated that Cer levels are directly related to patient survival: a low intracellular Cer content is a negative prognostic factor [137].

The metabolic pathways involved in the control of Cer levels in glial cells include enzymes of its metabolism (SMS, SPT, SMases) and its transport from the ER to the Golgi apparatus for the biosynthesis of complex sphingolipids.

It has been demonstrated that, in glioma cells, the administration of Δ9-tetrahydrocannabinol, the main active ingredient in marijuana, induces an accumulation of Cer in the ER through the stimulation of the "*de novo*" synthesis, resulting in apoptotic cell death [138]. Furthermore, the anti-proliferative effect of nitric oxide in glioma cells is associated to the inhibition of Cer vesicular transport from the ER to the Golgi apparatus [139]. Of interest, in glioma cells the PI3K/Akt signalling is able to regulate the sphingolipid metabolism promoting Cer vesicular transport, resulting in a reduction of the intracellular levels of this molecule and an increased synthesis of complex sphingolipids [140].

Moreover, Cer-mediated caspase activation has been implicated in the γ-radiation-induced apoptosis in U87MG glioma cells lacking functional p53 [141]. In the same cell line, TNF-α activates both neutral and acid SMases in a p53-mediated ROS-dependent or -independent pathway that results in Cer production, which, in turn, induces apoptotic cell death [142].

Interestingly, Cer induces not only apoptosis but also caspase-independent and/or non-apoptotic cell death in glioma cells. It has been demonstrated that administration of C2-Cer results in non-apoptotic cell death induction that can be inhibited by the constitutive active form of Akt [143]. It has been shown that C2-Cer induced cell death via autophagic mechanisms [144]; moreover, natural Cer has been recently implicated in cannabinoid-

induced and in Temozolomide-induced autophagic death in U87MG and T98G glioblastoma cells, respectively [145].

All this evidence suggests that the modulation of Cer intracellular levels can be crucial in determining the survival or death of glioma cells. Many anticancer drugs such as etoposide, doxorubicin, paclitaxel, cisplatin, cause an increase of the intracellular Cer levels [17]. Consequently, tumour cells that possess an aberrant Cer metabolism develop resistance to these cytotoxic treatments, thereby determining their clinical failure.

Sphingosine-1-phosphate in Gliobastoma

A growing body of evidence has implicated S1P and the genes involved in its synthesis, catabolism and signalling in various aspects of oncogenesis, cancer progression and drug- and radiation resistance [16]. S1P has emerged as an onco-promoter molecule in different tumours, including GBM [146-148]. Notably, it has been previously documented that S1P enhances proliferation [149], motility, invasiveness and malignant behavior of GBM cells [150]. As an indication of the importance of this molecule, different studies have reported that GBM cell lines and tissue specimens show an high SphK1 expression [151, 152] which correlates with a worst prognosis and a poor patient survival [153] and that silencing or pharmacological inhibition of both SphK1 and SphK2 decreases the proliferation rate in GBM cells, preventing their entry into the cell cycle [151, 153].

It has been reported that glioma cells are able not only to produce S1P, but also to release it in the extracellular milieu [152, 154]. This evidence suggests that S1P may play an important role as autocrine/paracrine messenger in GBM.

Furthermore, it has been extensively demonstrated that glioblastoma cells commonly express S1P receptors, $S1P_1$, $S1P_2$, and $S1P_3$ and very low levels of $S1P_5$ [149, 155, 156], all contributing to GBM cell growth and invasion through distinct, but overlapping mechanisms. For example, it has been demonstrated that, through activation of $S1P_1$, S1P up-regulates the expression of urokinase plasminogen activator (uPA), a potent stimulator involved in cancer cells invasion, in human glioblastoma multiforme cells [157].

AIM

S1P and Cer have emerged as bioeffector molecules, involved in the control of several fundamental biological processes such as cell growth, differentiation and survival [16]. Recent significant progress in understanding the role of these bioactive sphingolipids has identified crucial roles for these molecules in both cancer development and resistance [3, 14-17]. Emerging evidence suggest that S1P is an onco-promoter molecule enhancing proliferation, motility, invasiveness, and malignant behavior in different tumors, including glioblastomas [146-148, 158]. Moreover, S1P signaling have been implicated in the development of resistance to drug induced apoptosis, and escape from cell death [14].

On the other hand, different studies have suggested that Cer generally acts as a tumor suppressor lipid in many cancer types through the inhibition of cell growth or induction of cell death and interestingly, it has been previously demonstrated that in human gliomas Cer levels are inversely associated with their malignant progression and poor prognosis [137]. Intracellular Cer accumulation represents a common feature of the cytotoxic action of many chemotherapeutic drugs [16, 159, 160] and the escape from Cer-mediated apoptosis is a critical step in the development of drug resistance; thus raising Cer levels may help to overcome the chemotherapeutic treatment failure [159, 161, 162]. Several enzymes of Cer metabolism have been shown to be involved in regulating its levels [3, 14, 15], but recently the biosynthetic trafficking of Cer is emerged as an important pathway involved in the control of Cer metabolism.

Several lines of evidence indicate that, different anticancer drugs, including etoposide, exert cytotoxic effects also promoting accumulation of Cer in the ER. Thus, the transport of Cer from ER to Golgi apparatus can represent a key pathway for limiting Cer accumulation in the ER and escape from cell death. Moreover, we recently demonstrated that vesicular-mediated Cer transport is positively regulated by the pro-survival pathway phosphatidylinositol 3-phosphate kinase (PI3K)/Akt [18], a known mediator of extracellular S1P effects.

Based on these premises, the aim of this study was first to investigate in T98G glioma cells if S1P is involved in the regulation of Cer metabolism and traffic in the ER-Golgi compartment and, afterward, if S1P, by this way, can affect cell toxicity arising from Cer accumulation in the ER.

MATERIALS AND METHODS

Materials

All reagents were of analytical grade. Dulbecco's modified Eagle's medium (DMEM), Thiazolyl Blue Tetrazolium Bromide (MTT), fatty acid-free bovine serum albumin (BSA), Myriocin (MYR), Pertussis Toxin (PTX), Brefeldin A (BFA), fumonisin b1 (Fb1) and Etoposide were purchased from Sigma (St. Louis, MO, USA). Fetal calf serum (FCS) was from Cambrex (Walkersville, MD, USA). D-erythro- Sphingosine 1-Phosphate (S1P) e LY294002 were purchased from Enzo Life Sciences (Farmingdale, NY, USA). D-*erythro*-[3-^{3}H]sphingosine (Sph) (21.2 Ci/mmol) was from PerkinElmer Life Science (Boston, MA, USA). High performance thin layer chromatography (HPTLC) silica gel plates were from Merck (Darmstadt, Germany). N-(4,4,-difluoro-5-,7-dimethyl-bora-3a,4a-diaza-s-indacene-3-pentanoyl) sphingosine (BODIPY-C_5Cer) was from Invitrogen-Molecular Probes (Italy). LipofectAMINE 2000® and the Stealth RNAi were from Invitrogen (Carlsbad, CA, USA). The antibody recognizing Phospho-Akt (Ser473) was from Cell Signaling Technology, Inc. (Danvers, MA, USA). The antibody recognizing GAPDH was from Santa Cruz Biotecnology (Santa Cruz, CA, USA). The antibody recognizing Cert was from Bethyl Laboratories (Montgomery, TX, USA Secondary anti-rabbit Horse Radish Peroxidase (HRP)-conjugated antibody were from Santa Cruz Biotechnology (Santa Cruz, CA, USA). SuperSignal WestPico Chemioluminescent Substrate and SuperSignal WestFemto Maximum Sensitivity Substrate were from Thermo Scientific (Rockford, IL, USA).

Cell culture

We used the human glioma cell line T98G derived from a glioblastoma, which was purchased from the American Tissue Culture Collection (Rockville, MD) and cultured as recommended by the supplier. The cells were grown at 37°C in DMEM supplemented with 10% FCS, 1 mM Na-pyruvate, 2 mM L-glutamine, 100 U/ml penicillin, 100 μg/ml streptomycin and 0.25 μg/ml amphotericin B in a fully-humidified incubator containing 5% CO_2 and 95% air. The cells were starved of serum before the treatments, and thereafter kept under serum-free conditions.

Immunoblotting

In order to detect Akt phosphorylation, the cell extracts (40 μg proteins) were analysed by means of Western blotting. In brief, the T98G glioma cells were lysed with Akt buffer

(20mM Tris-HCl pH 7.4, 150 mM NaCl, 1% NP-40, 10 mM sodium fluoride, 1mM EDTA, 10mM $Na_4P_2O_7$, 1mM Na_3VO_4, 2 μg/ml pepstatin, 2 μg/ml leupeptin, 2 μg/ml aprotinin). Solubilized proteins were centrifuged at 14,000 x g at 4°C for 10 min. Supernatants were subjected to 10% SDS polyacrylamide gel electrophoresis and transferred to nitrocellulose membranes. Membranes were blocked for 1 hour at room temperature in Tris-buffered saline (10 mM Tris-HCl, pH 7.4, 140 mM NaCl) containing 0.1% Tween-20 (TBS-T) and 5% skim milk, and then incubated with primary antibodies against phospho-Akt overnight at 4°C. Membranes were washed in TBS-T, and bound antibodies visualized with horseradish peroxidase-coupled secondary antibodies (Immunopure) and chemiluminescent substrate. The relative intensities of bands were quantified by densitometry.

CERT immunoblotting was performed using si-control and si-CERT transfected cells lysed with CERT buffer (10mM Tris-HCl pH 7.4, 0.25M sucrose, 0.5mM phenylmethylsulfonyl fluoride, 1μg/ml aprotinin, 1μg/ml leupeptin, 1μg/ml pepstatin), processed and analyzed as previously described [11].

[^{3}H]Sphingosine metabolism

T98G cells plated at 1.5 x 10^4 cell/cm^2 were grown 24 h in DMEM plus 10% FCS, serum-starved for 24 hours and then pulsed with 0.15 μCi/ml [C3-^{3}H] Sph for 1 and then chased for the indicated times at 37°C in the presence or absence of 200 nM S1P. Otherwise, T98G cells were serum-starved for 24 hours and then incubated in serum-free medium in the absence or presence of 100 ng/ml PTX for 2 h. Then, cells were pulsed with 0.15 μCi/ml [C3-^{3}H] Sph for 30 min in the presence or absence of 1 μg/ml BFA and chased for 1 h in the presence or absence of 200 nM S1P and /or 100 ng/ml PTX and /or 1 μg/ml BFA. At the end, cells were washed twice with PBS, harvested and submitted to lipid extraction and partitioning as previously described [163]. The methanolized organic phase was analyzed by HPTLC using chloroform/methanol/water (110/40/6 by vol) as solvent system. Digital autoradiography of HPTLC plates was performed with Beta-Imager 2000 (Biospace, France) and the radioactivity associated with individual lipids was measured using the software provided with the instrument. The ^{3}H-labeled sphingolipids were recognized and identified as previously described [163].

RNA interference

Small interfering RNA (siRNA) duplexes for human CERT were obtained with the BLOCK-iT™ RNAi Designer from Invitrogen. The selected sequences were S87:

5’-CCUCAGUAAGUGGACAAACUACAUU-3’, S424:
5’-GGCUACUCUGCAACAUCCACCUCUU-3’ . The siRNA control is a nontargeting scrambled sequences of S87 and S424 oligonucleotide (NTS87; NTS424). The lack of targeting for other T98G genes by the designed siRNA duplexes was then checked by BLAST to avoid silencing of multiple genes other than CERT. T98G glioma cells plated at $1.5x10^4$ cell/cm^2 were maintained 24 h in DMEM plus 10% FCS and then transfected in the same medium with 100nM (final concentration) of S87 + S424 mix (1:1 by mol) and the non targeting corresponding sequences using Lipofectamine 2000 according to the manufacturer’s protocol. The experiments were performed 72 hours or, when indicated, 48 hours after transfection. Specific silencing achieved was evaluated by immunoblotting.

Analysis of the intracellular distribution of fluorescent ceramides

T98G cells plated at $1.5x10^4$ cell/cm^2 were grown on glass coverslips and transfected as described in the paragraph “RNA interference”. 24 h after transfection, cells were placed in DMEM without FCS for 24 h. First, cells were pretreated with 200nM S1P in the presence or absence of 10 μM LY294002 for 30min in DMEM without FCS at 37°C, then they were incubated with 2,5 μM BODIPY-C_5-Cer (as 1:1 complex with fatty acid free BSA) in DMEM at 4 °C for 30 min [11]. Then cells were washed with DMEM without FCS in the presence of 4 mg/ml fatty acid free BSA and treated with 200nM S1P in presence or not of 10 μM LY294002 for the indicated times at 37°C. Cells were then washed (three times with PBS) and fixed with 0.5% glutaraldehyde solution in PBS for 10 min at 4 °C. The specimens were immediately observed and analyzed with a fluorescence microscope (Olympus BX-50) equipped with a fast high-resolution CCD camera (Colorview 12) and an image analytical software (Analysis from Soft Imaging System GmbH).

Treatment of cultured T98G cells with etoposide and Sphingosine-1-phosphate

Serum-starved cells were incubated in the absence or presence of S1P and/or etoposide. Stock solutions of S1P and etoposide were prepared in PBS with fatty acid-free BSA (4 mg/ml) and in dimethyl sulfoxide (DMSO) respectively, then added to the medium to reach the final concentration. At the used concentrations, DMSO had no effect on cell growth and viability.

MTT assays

Cells were plated at 18000 cellls/cm^2 and mantained in DMEM plus 10% of FCS for 24h.Then, cells were placed in DMEM without FCS for 24h and incubated in serum-free medium in the absence or presence of 400 μM etoposide and/or 10 μM myriocin and/or 200 nM S1P for 24 hours at 37°C. At the end of treatments, cells were washed with PBS and incubated with 0.8 mg/ml of Thiazolyl Blue Tetrazolium Bromide (MTT) in DMEM without FCS at 37°C, 5%CO^2. After 4h cells were lysed in 2-propanol/formic acid (95:5) and absorbance was measured at 570 nm.

Other methods

Total protein amount was assayed with the Comassie Blue based Pierce reagent, using bovine serum albumin fraction V as standard. Radioactivity was measured by liquid scintillation counting.

Statistical analysis

Statistical significance of differences was determined by one-way ANOVA.

RESULTS

Role of S1P in the regulation of the PI3K/Akt pathway

We wanted to determine whether, in T98G glioma cell line, S1P was able to induce the activation of PI3K/Akt pathway. The data obtained demonstrated that in our cellular model, the PI3K/Akt pathway is not constitutively activated. Treatment with 200 nM S1P is able to stimulate the phosphorylation of Akt in a time-dependent manner in T98G cells (Fig. 3A): in particular, already after 15 minutes of treatment with S1P, phosphorylated Akt (p-Akt) levels are increased, and the maximum activation of Akt was observed 30 minutes after S1P administration, with an increase of approximately three times of p-Akt levels compared to control. At longer times of treatment a progressive reduction in the levels of p-Akt to return to the baseline levels after 1 hour was observed (Fig.1).

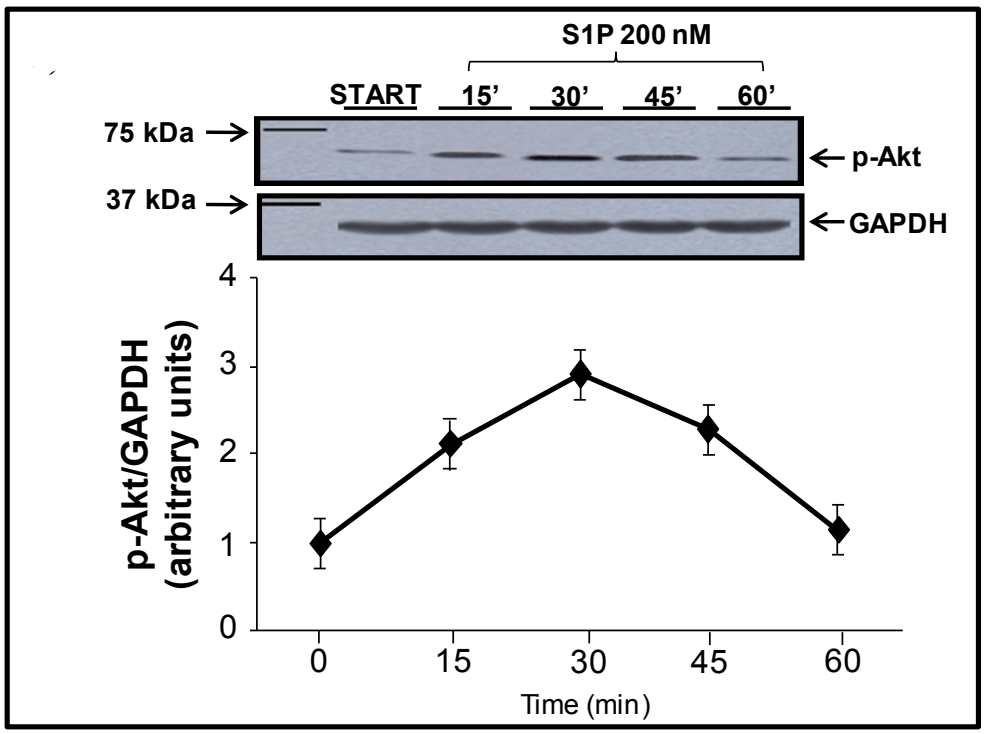

Figure 1: Effect of S1P on Akt phosphorylation in T98G glioma cells. T98G cells were serum-starved for 24 hours and then incubated in serum-free medium in the presence or absence of 200 nM S1P for 2h. At the end the cells were harvested for immunoblot analysis of p-AKT levels. GAPDH was used as loading control. All values are the mean ± S.D. of at least three individual experiments.

It is known that the PI3K/Akt pathway can be activated by S1P through $G_{0/i}$ protein-coupled receptors [64] which are expressed in glioma cells [164]. Thus, in order to verify if the S1P-dependent activation of PI3K/Akt pathway was promoted by S1P interaction through its $G_{0/i}$ coupled receptors, we determined by immunoblotting the level of p-Akt in T98G cells in the

presence of S1P and pertussis toxin (PTX). PTX catalyzes the ADP-ribosylation of α subunit of the heterotrimeric protein G_i and G_o preventing the release of GDP from the α subunit. Thus, PTX blocks the interaction of G protein with its receptor and downstream signal transduction.

The results obtained from the densitometric analysis of the immunoblotting (Fig. 2) show that in cells treated with PTX, S1P is no longer able to induce an increase in Akt phosphorylation. These results demonstrate that S1P acts as an extracellular mediator in the activation of PI3K/Akt pathway.

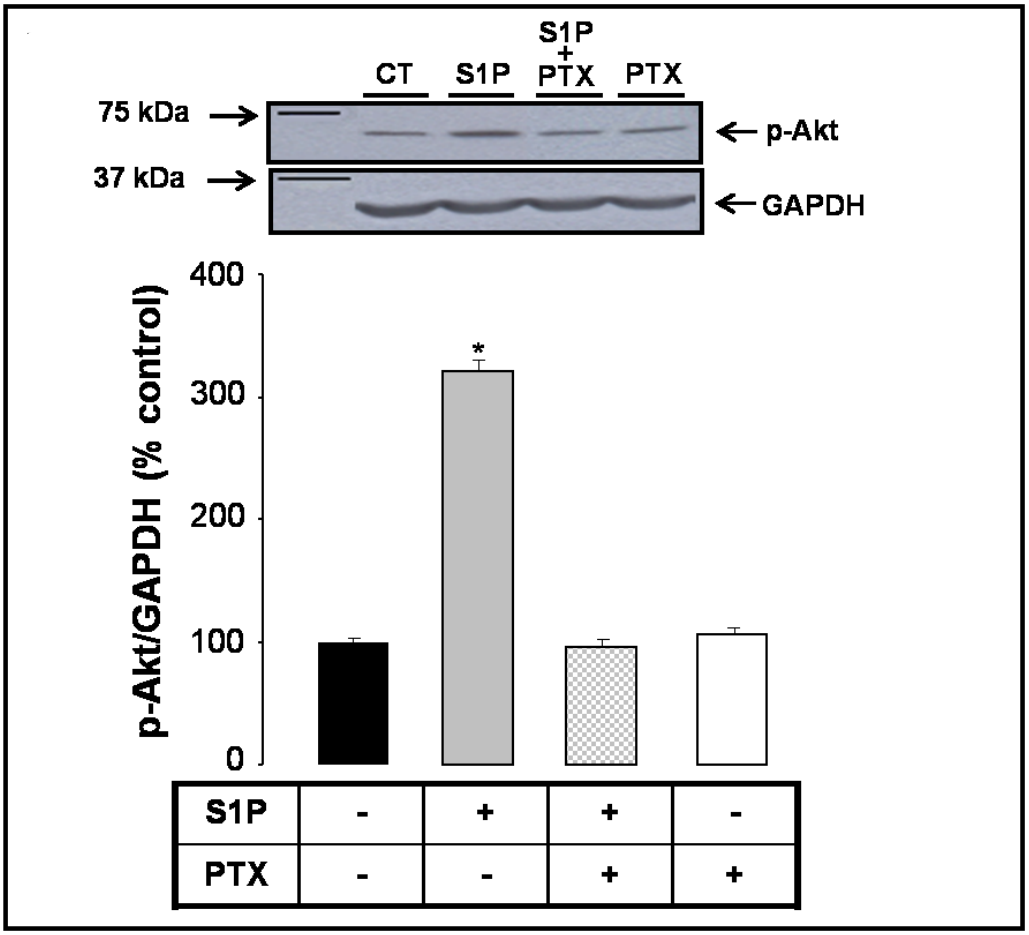

Figure 2: Effect of S1P and PTX on Akt phosphorylation in T98G glioma cells. T98G cells were pretreated in serum-free medium for 2 h with 100 ng/ml (100μM) PTX. At the end the cells were treated with 200 nM S1P for 30 min. Cells were harvested for immunoblot analysis of p-AKT levels. GAPDH was used as loading control. All values are the mean ± S.D. of at least three individual experiments. *p<0.05

Role of S1P on Cer utilization for complex sphingolipids synthesis

In order to investigate the effect of S1P on Cer metabolic use for the synthesis of complex sphingolipids, we performed a pulse chase metabolic study, using tritiated Sph ([C3-^{3} H]

Sph) as a precursor of sphingolipids; in fact, [^{3}H]Sph is efficiently internalized and rapidly incorporated first into Cer, and then, in SM and glycosphingolipids [102].

T98G cells were pulsed with [^{3}H]Sph for a pulse time of 1 hour and during different times of chase (15'-30'-45'-60') cells were treated with S1P.

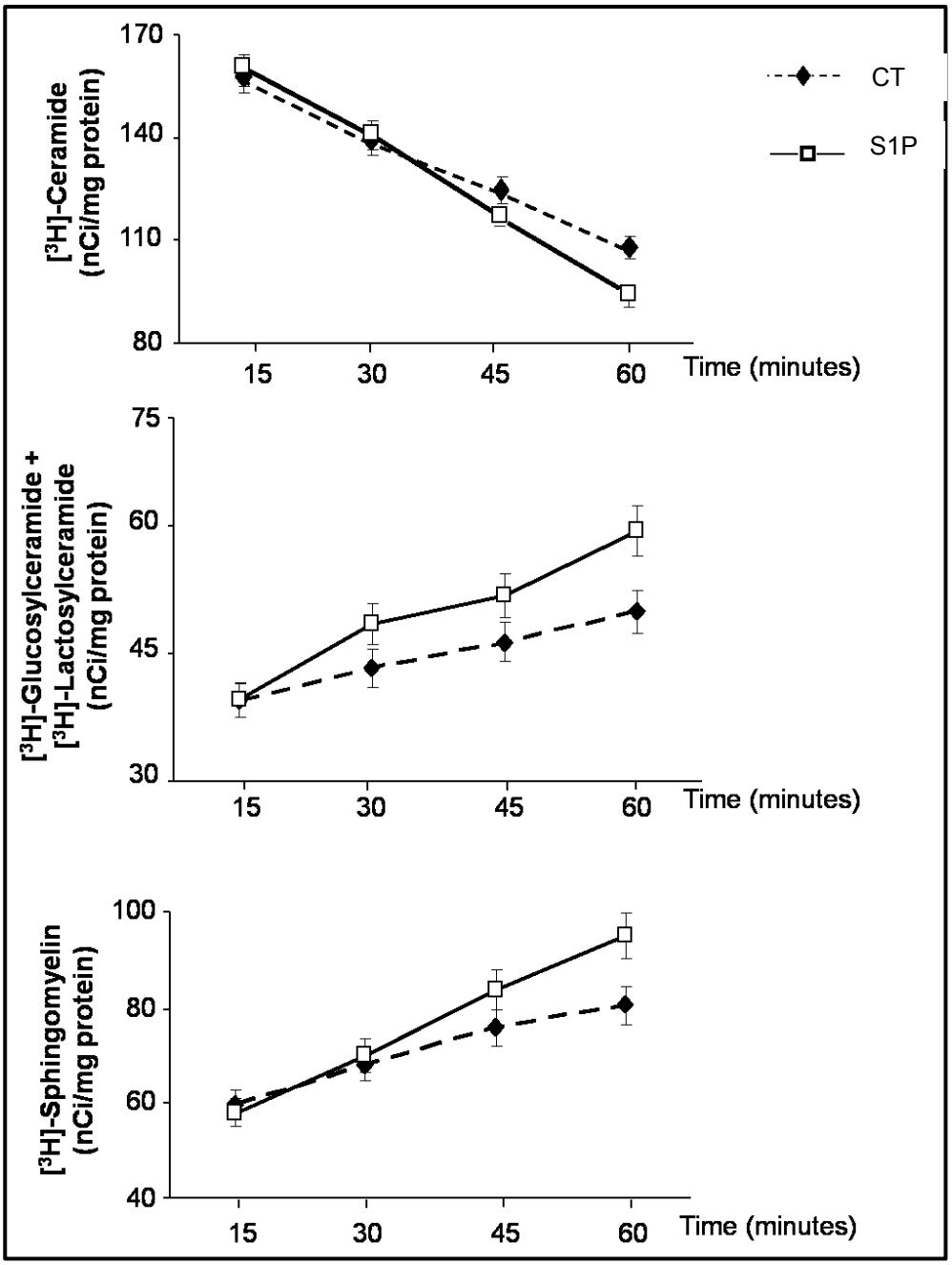

Figure 3: **S1P effect on [^{3}H]Sph metabolism in T98G glioma cells.** T98G cells were serum-starved for 24 hours and then pulsed with 0.15 μCi/ml [C3-^{3}H]Sph for 1 h. Then cells were chased for the indicated times at 37°C in the presence or absence of 200 nM S1P. Radioactivity associated with each lipid was determined. Values are expressed as nCi/mg protein. All values are the mean ± S.D. of at least three individual experiments done in triplicate.

The results obtained (Fig.3) show that in T98G cells treated with 200 nM S1P there was an increase in the radioactivity associated with [^{3}H]SM and [^{3}H]glycosphingolipids, and a concomitant decrease in the radioactivity associated with [^{3}H]Cer with respect to untreated cells.

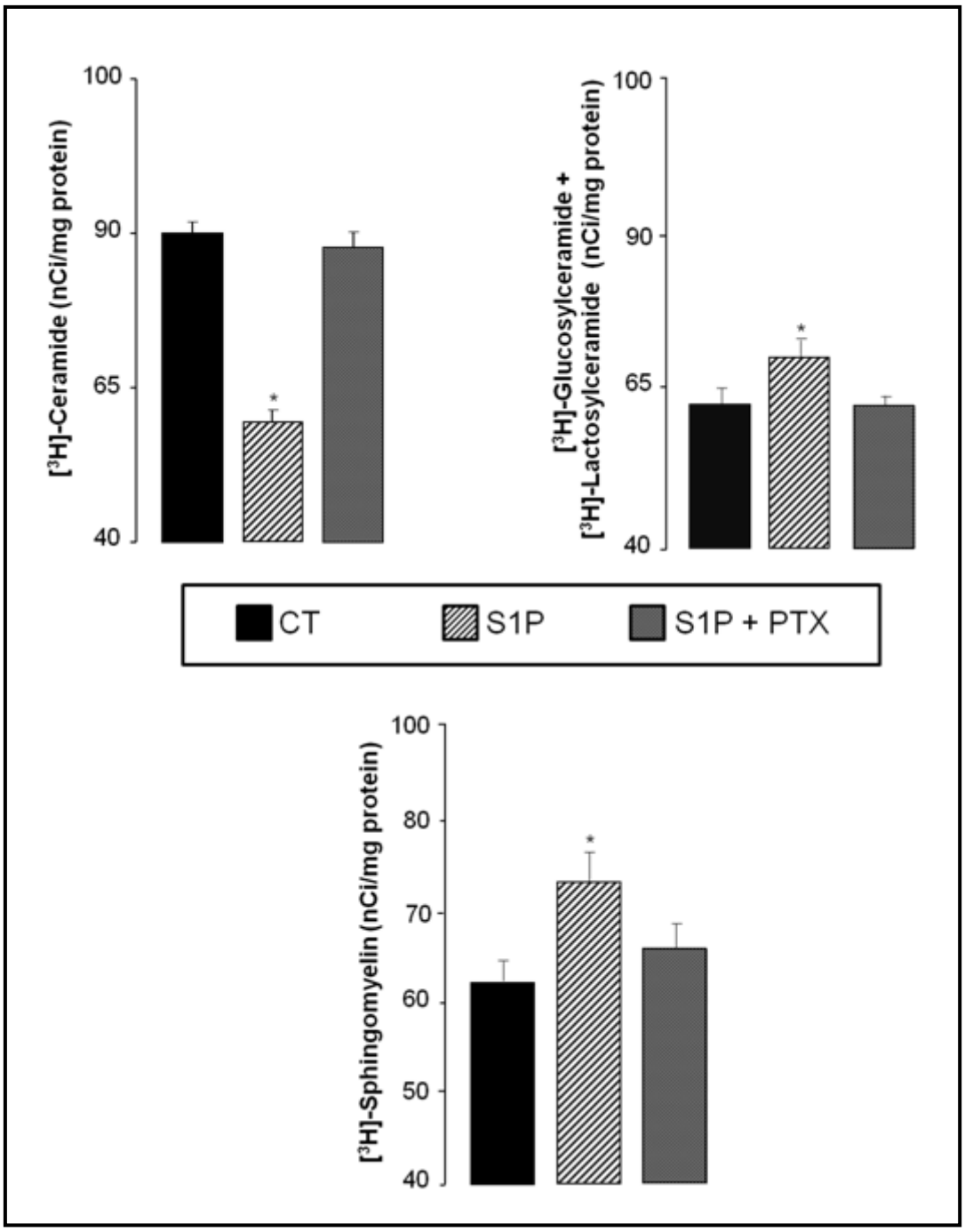

Fig.4: Effect of PTX on S1P-induced [^{3}H]Sph metabolism in T98G cells. T98G cells were serum-starved for 24 hours and then incubated in serum-free medium in the absence or presence of 100 ng/ml PTX. After 2 hours cells were pulsed with 0.15 μCi/ml [C3-^{3}H] Sph for 30 min and then chased for 1 h in the presence or absence of 200 nM S1P and /or 100 ng/ml PTX. Radioactivity associated with each lipid was determined. Values are expressed as nCi/mg protein. All values are the mean ± S.D. of at least three individual experiments done in triplicate.* $p<0.05$

In particular, the greatest increase in radioactivity associated with SM and glucosylceramide+lactosylceramide is observed after 60 minutes of chase in the presence of S1P. The treatment induced 18% and 19% increase respectively of [^{3}H]SM and [^{3}H]glucosylceramide+[^{3}H]lactosylceramide compared to control. In parallel, at the same time of chase, S1P leads to 14% decrease in the levels of radioactivity associated with [^{3}H]Cer. Treatment with 200 nM S1P does not cause significant changes in the levels of radioactivity associated with [^{3}H]Sph (data not shown).

Overall, the results suggest a role of S1P in the modulation of Cer metabolic use direct to the synthesis of complex sphingolipids.

To verify if the effect exerted by S1P was dependent on S1P binding to its receptors, we evaluated the effect of S1P on Cer metabolism in the presence of the Gi/Go protein coupled receptor inhibitor PTX. The results obtained (Fig.4) show that in the presence of PTX, S1P is no longer able to change the distribution of radioactivity associated with various sphingolipids, because the levels of radioactivity associated with [^{3}H]Cer, [^{3}H]SM and to [^{3}H]glucosylceramide+[^{3}H]lactosylceramide do not show significant differences compared to control.

These results indicate that the effect of S1P on the modulation of Cer metabolic use is due to the action of S1P as an extracellular mediator.

Role of S1P on Cer transport in the ER-Golgi district

To investigate how S1P stimulates the biosynthesis of SM and GSL, we evaluated the effect of S1P on Cer metabolism in T98G cells treated with Brefeldin A (BFA).

BFA is a fungal metabolite that causes persistent inactivation of Arf GTP-ase-1, which is crucial in mediating the formation of an intermediary compartment ER - Golgi (ERGIC) that give rise to the Golgi apparatus. It then determines a collapse of the Golgi apparatus that fuses its membrane with that of ER. Thus, in BFA treated cells, Cer synthesize in the ER is directly availablefor Golgi associated SMS and GCS.

As shown in fig.5, the results indicate that treatment with BFA, a condition in which Cer does not need any transport system to move from the ER to the Golgi, determines a 83% decrease of the radioactivity associated to [^{3}H]Cer and in an increase of 35% and 95% respectively of the radioactivity associated with [^{3}H]SM and [^{3}H]glucosylceramide+[^{3}H]lactosylceramide, compared to control.

In the presence of BFA, the treatment with S1P is not able to induce significant changes in the levels of radioactivity associated with the different tritiated sphingolipids compared to BFA treated cells.

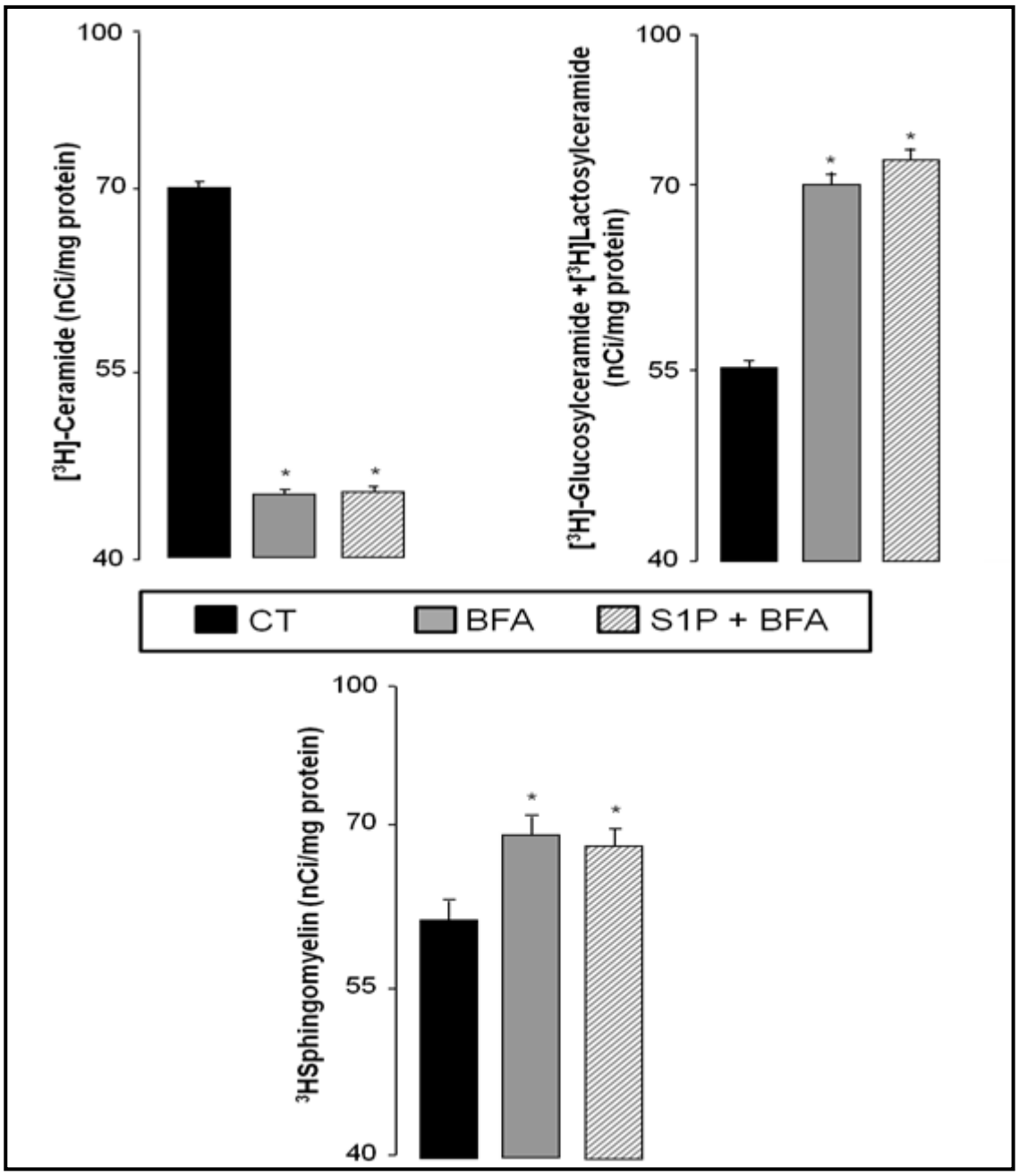

Figure 5: Effect of BFA on S1P-induced [^{3}H]Sph metabolism in T98G cells. Cells were serum-starved for 24 hours and then pulsed with 0.15 μCi/ml [C3-^{3}H] Sph for 30 min at 37°C in the absence or presence of 1 μg/ml BFA. Then cells were chased for 1 h in the presence or absence of 200 nM S1P and /or 1 μg/ml BFA. Radioactivity associated with each lipid was determined. Values are expressed as nCi/mg protein. All values are the mean ± S.D. of at least three individual experiments done in triplicate. *$p<0.05$

These data suggest that S1P effect on Cer metabolism is exerted through the regulation of Cer transport from the ER to the Golgi apparatus and does not involve a regulation of SMS and GCS. Moreover, we wanted to evaluate the effect of S1P specifically on Cer vesicular traffic. To this purpose we performed a microscopy fluorescence studies using the Cer analogue BODIPY-C_5Cer that mimics the behavior of natural Cer [106] , in CERT silenced cells. In these experiments the level of silencing of CERT in T98G cells evaluated by immunoblotting was >95% (Fig.6). In T98G silenced cells, we evaluated the kinetics of transport of the BODIPY-C_5-Cer, that mimics the behavior of natural ceramide [106], between the ER and the Golgi apparatus after treatment with 200 nM S1P (Fig.7).

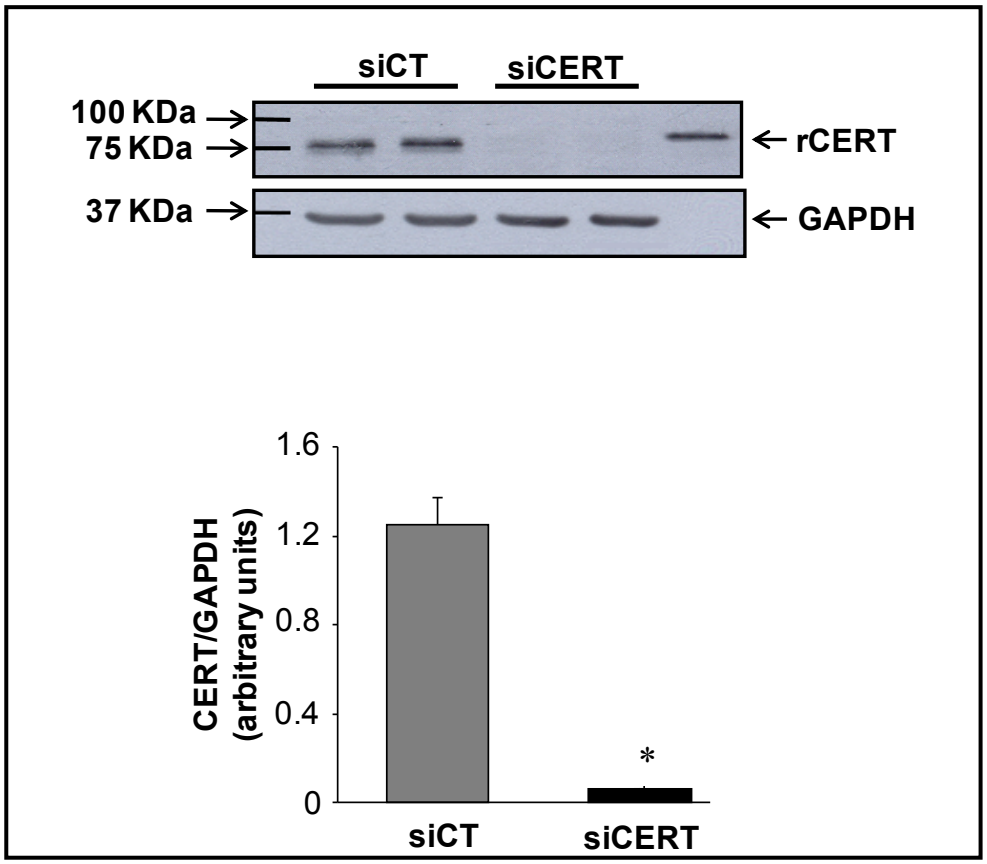

Figure 6: Effect of CERT down regulation in T98G glioma cells. Cells grown in DMEM supplemented with 10% FCS were transfected with a mix of H87 and H424 siRNA for CERT (siCERT) and the corresponding non targeting NT87 and NT424 as control (siNT) as described in Mat. and Meth. and analyzed for CERT levels. 72 hours after transfection cells were washed twice with PBS and harvested. Cell lysates (20 μg of protein) from two different preparations of siNT and siCERT transfected cells were analyzed by immunoblotting with a polyclonal anti-CERT antibody and polyclonal anti-GAPDH antibody. *$p<0.05$

This fluorescent Cer is internalized at the plasma membrane and it is distributed mainly in the ER. From this district, using the transport systems of natural Cer, it is transported to the Golgi apparatus and used for the synthesis of complex sphingolipids. The images acquired at time 0 'shows that the fluorescence is localized at the plasma membrane (data not shown). Images acquired after 5 minutes of incubation at 37°C, show that in control and S1P treated cells, fluorescence accumulated in the perinuclear region representative of the Golgi apparatus (Fig.8a). When T98G cells were treated 5 minutes without or with S1P, fluorescence accumulated mainly at the Golgi apparatus in 70 and 90% of the cells analysed respectively (Fig.8b). The results indicate that S1P modulates vesicular transport of Cer by increasing the speed of Cer traffic from the ER to the Golgi apparatus.

Next, we examined whether the effect of modulation of Cer vesicular transport by S1P was mediated by the PI3K/Akt signal transduction pathway. To this purpose we analyzed the distribution of BODIPY-C_5-Cer in T98G cells pretreated with the PI3K/ Akt inhibitor LY294002, in the presence or absence of S1P. In both cases, the accumulation of fluorescence at the Golgi is strongly reduced at all experimental times considered compared to control cells and S1P treated cells (Figure 5b and 5c).

In cells treated with LY294002 in the presence or absence of S1P fluorescence accumulated mainly at the Golgi apparatus respectively in 25 and 27% of the cells analysed (Fig. 5C upper panel). Altogether, the results obtained demonstrate that S1P, through PI3K/Akt activation, increases the rate of Cer vesicular transport from the ER to the Golgi apparatus promoting Cer removal from the ER direct to the synthesis of complex sphingolipids.

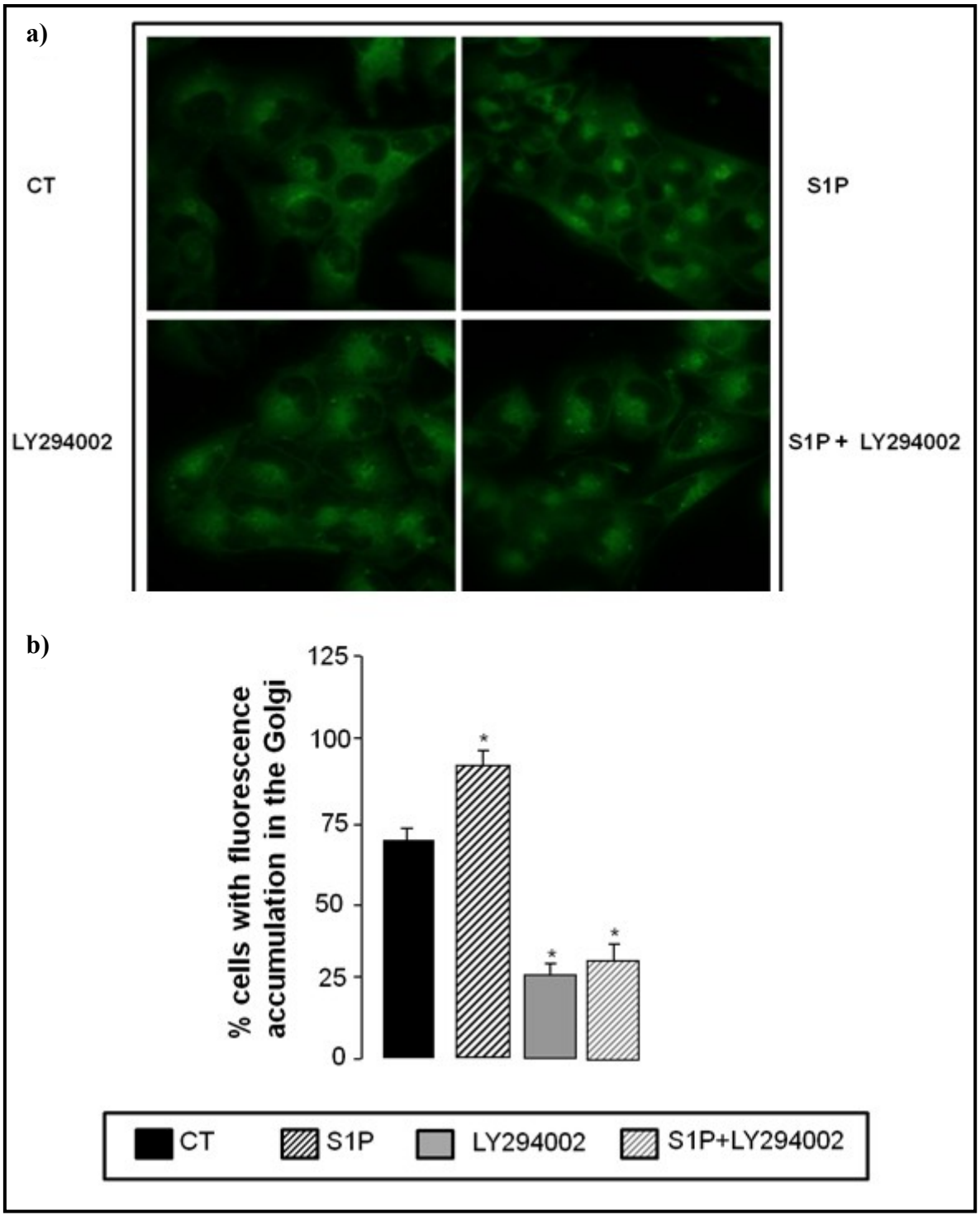

Figure 8: Effect of CERT down regulation on the intracellular distribution of BODIPY-C_5Cer in T98G glioma cells. a) T98G glioma cells grown on a coverslip were transfected for silencing as previously described and 48 hours after transfection, cells were pretreated in serum-free medium for 30 min with or without 200nM S1P and/or 10μM LY294002 and then, cells were incubated with 2.5 μM BODIPY-C_5Cer for 30 min at 4°C. Labeled cells were further incubated at 37 °C for 5' with or without 200nM S1P in the presence or absence of 10μM LY294002. Images are representative of at least 5 different experiments and were identically processed and printed. **b)** the percentage of cells with colocalization of BODIPY-C_5Cer and the Golgi apparatus in the presence or absence of S1P and/or LY294002 at the indicated times was determined. The data are means ± the SD. * $p<0.05$

Role of Cer in the etoposide-induced toxicity in T98G cells

Several lines of evidence indicate that also in glioma cells accumulation of Cer is functional to the cytotoxic effects of different anticancer treatments [16, 160, 161]. Among these drugs, etoposide has been reported to induce Cer accumulation in the ER due to the activation of Cer biosynthesis [165].

To study if Cer biosynthesis at the ER was implicated in the toxic effect of etoposide we evaluated cell viability of T98G cells after treatment with etoposide in the presence or absence of Cer biosynthesis inhibitors. We used two different enzyme inhibitors: myriocin (MYR), direct to serine palmitoyltransferase enzyme involved in *de novo* pathway, or Fumonisin b1 (Fb1), direct to Cer synthase enzyme, involved in both salvage and in *de novo* pathway. The results in fig.9 show that, 24 hours treatment with 400 μM etoposide determines a decrease in cell viability of 34% with respect to control cells. Treatment with sub-toxic dose of MYR together with 400 μM etoposide, caused a 15% decrease in cell survival indicating that MYR is able to significantly reduce the toxic effect of etoposide.

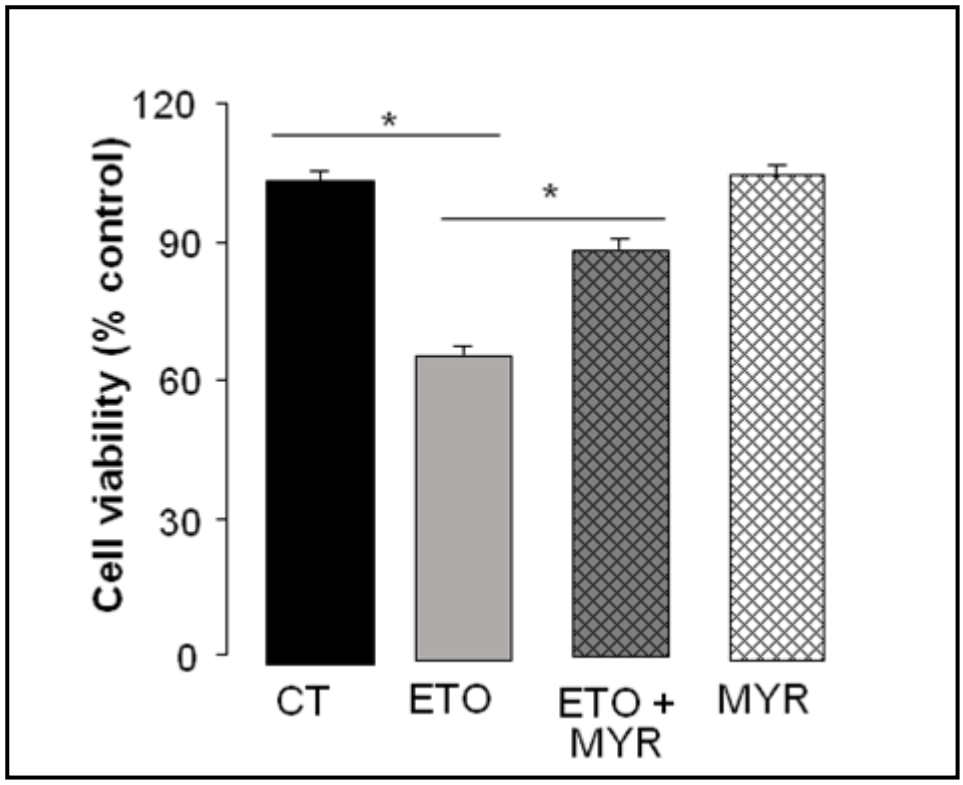

Fig. 9. Effect of etoposide and myriocin on T98G cells survival T98G cells were serum-starved for 24 hours and then incubated for 24 hours in serum-free medium with 400 μM etoposide (ETO) in the presence or absence of myriocin (MYR). Cell viability was evaluated by the MTT assay. The viability of untreated cells was regarded as 100%. Mean ± S.D. is shown. *$p<0.05$

Furthermore, cells treatment with a sub-toxic dose of Fb1 together with 400 μM etoposide (Fig.10) demonstrate that Fb1 is able to almost revert the toxic effect of etoposide when compared to cells treated with Fb1 alone which induces a cell viability reduction of 12%.

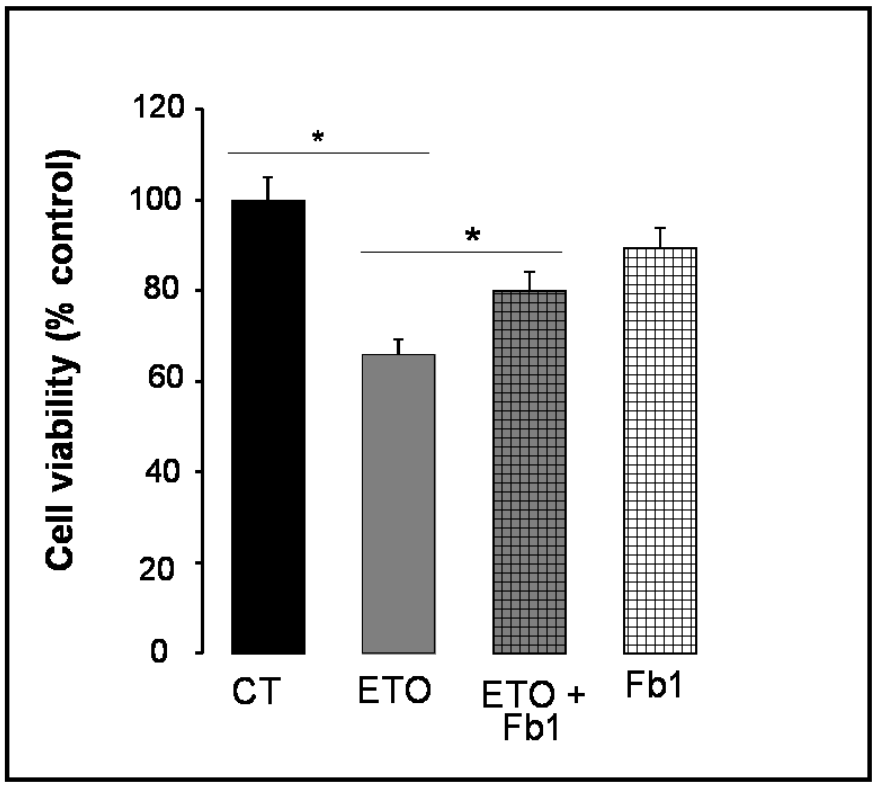

Figure 10: Effect of etoposide and Fumonisin b1 on T98G cells survival. b) T98G cells were serum-starved for 24 hours and then incubated for 24 hours in serum-free medium with or without 400 μM etoposide (ETO) in the presence or absence of 12.5μM Fumonisin b1 (Fb1). Cell viability was evaluated by the MTT assay.The viability of untreated cells was regarded as 100%. Mean ± S.D. is shown. *$p<0.05$

These results suggest that Cer accumulation in the ER is a relevant mechanisms involved in the toxicity of this molecule in glioma cells.

Role of sphingosine-1-phosphate and PI3K/Akt pathway in the etoposide-induced toxicity

We therefore evaluated if the activation of Cer traffic, promoted by S1P-dependent PI3K/Akt activation, could affect the viability of etoposide treated cells. To this purpose, cell survival was assessed after treatment with etoposide in the presence or absence of S1P and/or LY294002, a specific inhibitor of PI3K. The results show that, after 24 hours, treatment with LY294002 does not cause significant changes in cell survival and the concomitant treatment with etoposide, S1P and LY294002 almost completely abolish the protective effect of S1P on cell death induced by etoposide (Fig.11).

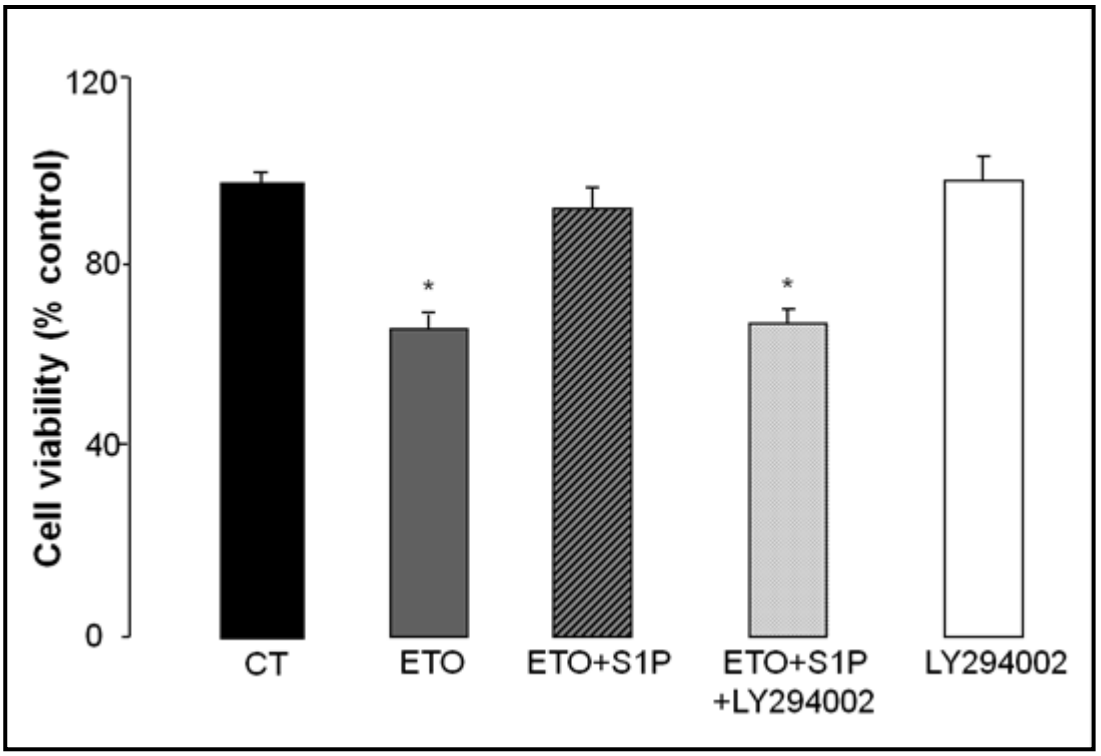

Figure 11: Effect of S1P and LY294002 on etoposide-induced toxicity in T98G cells. T98G cells were serum-starved for 24 hours and then pretreated, in serum-free medium, for 30 min with the inhibitor LY294002. Then 400 μM etoposide (ETO) in the presence or absence of 200 nM S1P was added for 24 hours. Cell survival was evaluated by the MTT assay. The viability of untreated cells was regarded as 100%. Mean ± S.D. is shown.*$p<0.05$

These results demonstrate that S1P, activating the PI3K/Akt signal, promotes Cer transport and metabolism, protecting cells from the toxicity induced by Cer accumulation at the ER.

DISCUSSION

This investigation demonstrates that, in T98G cells, extracellular S1P is able to increase vesicular Cer transport from the ER to the Golgi apparatus promoting Cer conversion to SM and GSL, by PI3K/Akt pathway activation. We then demonstrated that the S1P-mediated enhancement of Cer traffic is functional to the reduction of cellular toxicity induced by Cer accumulation in the ER. In fact, S1P significantly promotes viability of cells treated with the anticancer drug etoposide that stimulates Cer byosinthesis.

The first evidence provided by this study is that exogenous S1P exerts its effect through the binding of its receptors expressed in the plasma membrane, which in turn activate Akt. These results are in agreement with the literature that demonstrate that S1P can act as a potent onco-promoter molecule in glioblastomas [149, 150, 166] with an autocrine/paracrine effect; infact, glioma cells do express S1P receptors, and S1P administration promotes their proliferation, migration, and invasivity [149, 166]. Moreover, it is emerged that S1P acts in different cell types, including glioma cells, activating PI3K/Akt pathway [167]. Furthermore, we have shown in previous papers [18, 101] that the PI3K/Akt pathway is involved in the regulation of Cer vesicular transport from the ER to the Golgi apparatus. In this investigation, we first demonstrated that, in T98G glioma cells, S1P is able to increase the rate of Cer vesicular flow activating Cer metabolism direct to the biosynthesis of complex sphingolipids. The metabolic data obtained administering to the T98G cells the radioactive precursor [^{3}H]Sph indicate a role of S1P in the modulation of Cer metabolism, favouring Cer use direct to the synthesis of SM and glycosphingolipids. Moreover, S1P in the presence of PTX, is no longer able to modify Cer utilization indicating that the effect of S1P on the modulation of Cer metabolic use is due to the action of S1P as an extracellular mediator. Additionally, results obtained with BFA demonstrate that, in T98G glioma cells, the target of S1P action on Cer metabolism is the step of Cer transfer from ER to the Golgi apparatus. In fact, when cells were treated with BFA, which causes Golgi disassembly and redistribution to the ER [168], the conversion of Cer to both GlcCer and SM was strongly increased. The direct availability of Cer for SM and GlcCer synthases determined by BFA makes T98G glioma cells no more sensitive to S1P-dependent speeding of Cer utilization. This evidence further confirms that SM- and GlcCer-synthases are not the S1P target and strengthens the notion that the S1P-speeding Cer utilization is mainly due to an effect on its translocation from ER to *cis*-Golgi. Moreover, in cells down-regulated for CERT, which represent a good model to study the vesicular transport of Cer, we obtained additional evidence that S1P can positively influence the intracellular vesicular traffic of Cer from ER

to the Golgi apparatus, in agreement with previous data obtained in other cell types [115]. Infact, the analysis of BODIPY-C_5-Cer intracellular distribution, which mimics the intracellular movements of natural Cer in T98G cells knocked down for the Cer transport protein CERT, shows that the fluorescence accumulation to the Golgi apparatus induced by S1P is reduced when the PI3K/Akt pathway is inhibited. This observation let us to hypothesize that S1P can increase the rate of vesicular transport of Cer from the ER to the Golgi apparatus, in agreement with data demonstrating that S1P positively regulates vesicular-mediated protein transport [108],through the activation of PI3K/Akt.

Different lines of evidence indicate that both aberrant activation of the PI3K/Akt survival pathway [169, 170] and downregulation of the death mediator Cer [137] play a critical role in the aggressive behavior, apoptosis resistance, and adverse clinical outcome of glioblastomas. Cer accumulation at the ER represents a mechanism through which different antineoplasic drugs, including etoposide, promote cell death. Cer accumulation has been proposed to induce ER stress in different cellular types [171, 172], and in particular, in human glioma cells it is demonstrate that the induction of *de novo* Cer synthesis by cannabinoid promotes ER stress leading cells to apoptosis [145]. Our research demonstrates that S1P protect cells from the toxic effect of etoposide that acts stimulating Cer synthesis. In fact, in T98G cells, inhibition of Cer synthesis from both de novo and the recycling pathway significantly reduced the toxic effect of etoposide; furthermore, the PI3K inhibitor LY294002 completely abolished the protective effect of S1P on etoposide toxicity. These data demonstrate that the pro-survival action of S1P is mediated by the activation of the PI3K/Akt, which stimulates Cer movement from ER to the Golgi apparatus; through this mechanism, the toxic Cer accumulation in the ER was prevented, allowing escape from cell death.

The ability of the PI3K/Akt pathway to be regulated by/to regulate sphingolipid metabolism may be pathologically relevant in gliomas if we consider that the more malignant phenotypes of these tumors are associated with the up-regulation of the PI3K/Akt pathway [169, 170], increased amounts of SM [173] of glucosylceramide [174], and low Cer levels [137]. Thus, the S1P-dependent Cer removal from the ER could participate to the molecular mechanisms involved in the regulation of Cer levels. Interestingly, Spiegel and Milstien in their review of 2003 yet discussed for a role of S1P on Cer synthesis regulation. They, based on different studies, reported that the dephosphorylation of S1P is a relevant way to promote Cer synthesis from sphingosine in the salvage pathway. Our data demonstrate a new role of S1P in the regulation of Cer transport and metabolism. In agreement with Spiegel and

Milstien, we could speculate that the pro-survival activity of S1P controlling both Cer biosynthesis and traffic might be the mechanism for its ability to suppress Cer-mediated cell death. Furthermore, S1P, by stimulating Cer metabolism, favours the maintainance of low Cer levels and promotes the biosynthesis of new membranes needed for cell proliferation and growth, key elements in tumor progression. Moreover, it is also tempting to speculate that Cer removal from the ER, as a consequence of a S1P-hyper-activated PI3K/Akt pathway,could also be involved in refractoriness of glioma cells to Cer-based treatments in particular those treatments that, in ER, act through Cer biosynthesis stimulation [16, 175].

CONCLUSIONS

There is accumulating evidence that targeting sphingolipid metabolism may be useful in treatment of several pathologies, including cancer and diabetes. Considerable progress over the last few years in understanding the role and mechanism of Cer action in cancer and diabetes has been made. A growing amount of evidence indicate that Cer plays a relevant role in these pathologies and the control of Cer metabolism may hold promise over established methods to cancer and diabetes therapeutics. Over-production of Cer clearly has a decisive role in the induction of apoptosis, just as enhanced metabolic clearance of Cer has a vital role in preventing the induction of apoptosis. Thus it is important to develop strategies to modulate Cer metabolism and levels to prevent or induce cell death. Thus, it makes sense to increase Cer to trigger glioma cell death and, on the other hand, to lower Cer to avoid pancreatic β-cell failure. The Cer intracellular traffic from the ER to the Golgi apparatus represents a highly regulated step emerging in the control of Cer metabolism and levels. Furthermore, CERT dependent and independent pathways of Cer transport can be independently regulated, although the factors involved in the modulation of Cer traffic have to be investigated extensively.

Altogether, the results obtained during my Ph.D. course identify the Cer traffic as a possible target for new therapies against type 2 diabetes and glioblastoma. Notwhitstanding , a better understanding of the role of Cer traffic in cell survival and other key cell functions will open new perpectives to treat diseases in which alterations of Cer metabolism are involved.

REFERENCES

1. Bartke N, Hannun YA. Bioactive sphingolipids: metabolism and function. **J Lipid Res**. 2009;50 Suppl:S91-96.
2. Ohanian J, Ohanian V. Sphingolipids in mammalian cell signalling. **Cell Mol Life Sci**. 2001;58:2053-2068.
3. Hannun YA, Obeid LM. Principles of bioactive lipid signalling: lessons from sphingolipids. **Nat Rev Mol Cell Biol**. 2008;9:139-150.
4. Newton J, Lima S, Maceyka M et al. Revisiting the sphingolipid rheostat: Evolving concepts in cancer therapy. **Exp Cell Res**. 2015;333:195-200.
5. Galadari S, Rahman A, Pallichankandy S et al. Role of ceramide in diabetes mellitus: evidence and mechanisms. **Lipids Health Dis**. 2013;12:98.
6. Hanada K, Kumagai K, Yasuda S et al. Molecular machinery for non-vesicular trafficking of ceramide. **Nature**. 2003;426:803-809.
7. Yamaji T, Hanada K. Sphingolipid metabolism and interorganellar transport: localization of sphingolipid enzymes and lipid transfer proteins. **Traffic**. 2015;16:101-122.
8. Dufey E, Sepúlveda D, Rojas-Rivera D et al. Cellular mechanisms of endoplasmic reticulum stress signaling in health and disease. 1. An overview. **Am J Physiol Cell Physiol**. 2014;307:C582-594.
9. Urra H, Dufey E, Lisbona F et al. When ER stress reaches a dead end. **Biochim Biophys Acta**. 2013;1833:3507-3517.
10. Kloppel G, Lohr M, Habich K et al. Islet pathology and the pathogenesis of type 1 and type 2 diabetes mellitus revisited. **Surv Synth Pathol Res**. 1985;4:110-125.
11. Giussani P, Colleoni T, Brioschi L et al. Ceramide traffic in C6 glioma cells: evidence for CERT-dependent and independent transport from ER to the Golgi apparatus. **Biochim Biophys Acta**. 2008;1781:40-51.
12. Viani P, Giussani P, Brioschi L et al. Ceramide in nitric oxide inhibition of glioma cell growth. Evidence for the involvement of ceramide traffic. J Biol Chem. United States; 2003:9592-9601.
13. Polivka J, Rohan V, Topolcan O et al. New molecularly targeted therapies for glioblastoma multiforme. **Anticancer Res**. 2012;32:2935-2946.
14. Giussani P, Tringali C, Riboni L et al. Sphingolipids: key regulators of apoptosis and pivotal players in cancer drug resistance. **Int J Mol Sci**. 2014;15:4356-4392.

15. Gault CR, Obeid LM, Hannun YA. An overview of sphingolipid metabolism: from synthesis to breakdown. **Adv Exp Med Biol**. 2010;688:1-23.
16. Ogretmen B, Hannun YA. Biologically active sphingolipids in cancer pathogenesis and treatment. **Nat Rev Cancer**. 2004;4:604-616.
17. Truman JP, Garcia-Barros M, Obeid LM et al. Evolving concepts in cancer therapy through targeting sphingolipid metabolism. **Biochim Biophys Acta**. 2014;1841:1174-1188.
18. Giussani P, Brioschi L, Bassi R et al. Phosphatidylinositol 3-kinase/AKT pathway regulates the endoplasmic reticulum to golgi traffic of ceramide in glioma cells: a link between lipid signaling pathways involved in the control of cell survival. **J Biol Chem**. 2009;284:5088-5096.
19. Riboni L, Viani P, Bassi R et al. The role of sphingolipids in the process of signal transduction. **Prog Lipid Res**. 1997;36:153-195.
20. Huwiler A, Kolter T, Pfeilschifter J et al. Physiology and pathophysiology of sphingolipid metabolism and signaling. **Biochim Biophys Acta**. 2000;1485:63-99.
21. Futerman AH, Hannun YA. The complex life of simple sphingolipids. **EMBO Rep**. 2004;5:777-782.
22. Riboni L, Giussani P, Viani P. Sphingolipid transport. **Adv Exp Med Biol**. 2010;688:24-45.
23. Levy M, Futerman AH. Mammalian ceramide synthases. **IUBMB Life**. 2010;62:347-356.
24. Pewzner-Jung Y, Ben-Dor S, Futerman AH. When do Lasses (longevity assurance genes) become CerS (ceramide synthases)? Insights into the regulation of ceramide synthesis. **J Biol Chem**. 2006;281:25001-25005.
25. Michel C, van Echten-Deckert G. Conversion of dihydroceramide to ceramide occurs at the cytosolic face of the endoplasmic reticulum. **FEBS Lett**. 1997;416:153-155.
26. Baumann N, Pham-Dinh D. Biology of oligodendrocyte and myelin in the mammalian central nervous system. **Physiol Rev**. 2001;81:871-927.
27. Jeckel D, Karrenbauer A, Burger KN et al. Glucosylceramide is synthesized at the cytosolic surface of various Golgi subfraction. **J Cell Biol**. 1992;117:259-267.
28. Ichikawa S, Hirabayashi Y. Glucosylceramide synthase and glycosphingolipid synthesis. **Trends Cell Biol**. 1998;8:198-202.
29. Degroote S, Wolthoorn J, van Meer G. The cell biology of glycosphingolipids. **Semin Cell Dev Biol**. 2004;15:375-387.

30. Van Overloop H, Gijsbers S, Van Veldhoven PP. Further characterization of mammalian ceramide kinase: substrate delivery and stereo specificity, tissue distribution and subcellular localization studies. **J Lipid Res**. 2006;47:268-283.
31. Huitema K, van den Dikkenberg J, Brouwers JF et al. Identification of a family of animal sphingomyelin synthases. **Embo j**. 2004;23:33-44.
32. Tettamanti G. Ganglioside/glycosphingolipid turnover: new concepts. **Glycoconj J**. 2004;20:301-317.
33. Marchesini N, Hannun YA. Acid and neutral sphingomyelinases: roles and mechanisms of regulation. **Biochem Cell Biol**. 2004;82:27-44.
34. Duan RD. Alkaline sphingomyelinase: an old enzyme with novel implications. **Biochim Biophys Acta**. 2006;1761:281-291.
35. Mao C, Obeid LM. Ceramidases: regulators of cellular responses mediated by ceramide, sphingosine and sphingosine-1-phosphate. **Biochim Biophys Acta**. 2008;1781:424-434.
36. Sandhoff K, Kolter T. Topology of glycosphingolipid degradation. **Trends Cell Biol**. 1996;6:98-103.
37. Serra M, Saba JD. Sphingosine 1-phosphate lyase, a key regulator of sphingosine 1-phosphate signaling and function. Adv Enzyme Regul. England; 2010:349-362.
38. Le Stunff H, Peterson C, Thornton R et al. Characterization of murine sphingosine-1-phosphate phosphohydrolase. **J Biol Chem**. 2002;277:8920-8927.
39. Le Stunff H, Giussani P, Maceyka M et al. Recycling of sphingosine is regulated by the concerted actions of sphingosine-1-phosphate phosphohydrolase 1 and sphingosine kinase 2. **J Biol Chem**. 2007;282:34372-34380.
40. Pyne S, Lee SC, Long J et al. Role of sphingosine kinases and lipid phosphate phosphatases in regulating spatial sphingosine-1-phosphate signaling in health and disease. **Cell Signal**. 2009;21:14-21.
41. Tettamanti G, Bassi R, Viani P et al. Salvage pathways in glycosphingolipid metabolism. **Biochimie**. 2003;85:423-437.
42. Hanada K, Kumagai K, Tomishige N et al. CERT-mediated trafficking of ceramide. **Biochim Biophys Acta**. 2009;1791:684-691.
43. Ahn VE, Lo EI, Engel CK et al. A hydrocarbon ruler measures palmitate in the enzymatic acylation of endotoxin. **Embo j**. 2004;23:2931-2941.
44. Tidhar R, Futerman AH. The complexity of sphingolipid biosynthesis in the endoplasmic reticulum. **Biochim Biophys Acta**. 2013;1833:2511-2518.

45. Kawano M, Kumagai K, Nishijima M et al. Efficient trafficking of ceramide from the endoplasmic reticulum to the Golgi apparatus requires a VAMP-associated protein-interacting FFAT motif of CERT. **J Biol Chem**. 2006;281:30279-30288.
46. Perry RJ, Ridgway ND. Molecular mechanisms and regulation of ceramide transport. **Biochim Biophys Acta**. 2005;1734:220-234.
47. Bassi R, Viani P, Giussani P et al. GM3 ganglioside inhibits endothelin-1-mediated signal transduction in C6 glioma cells. **FEBS Lett**. 2001;507:101-104.
48. Dbaibo GS, Pushkareva MY, Jayadev S et al. Retinoblastoma gene product as a downstream target for a ceramide-dependent pathway of growth arrest. **Proc Natl Acad Sci U S A**. 1995;92:1347-1351.
49. Chalfant CE, Ogretmen B, Galadari S et al. FAS activation induces dephosphorylation of SR proteins; dependence on the de novo generation of ceramide and activation of proteine phosphatase. **J Biol Chem**. 2001;276:44848-44855.
50. Chalfant CE, Rathman K, Pinkerman RL et al. De novo ceramide regulates the alternative splicing of caspase 9 and Bcl-x in a549 lung adenocarcinoma cells. Dependence on protein phosphatase-1. **J Biol Chem**. 2002;277:12587-12595.
51. Ruvolo PP, Deng X, Ito T et al. Ceramide induces Bcl2 dephosphorylation via a mechanism involving mitochondrial PP2A. **J Biol Chem**. 1999;274:20296-20300.
52. Pettus BJ, Chalfant CE, Hannun YA. Ceramide in apoptosis: an overview and current perspectives. Biochim Biophys Acta. Netherlands; 2002:114-125.
53. Riboni L, Viani P, Bassi R et al. Biomodulatory role of ceramide in basic fibroblast growth factor-induced proliferation of cerebellar astrocytes in primary culture. **Glia**. 2000;32:137-145.
54. Meloche S, Pouyssegur J. The ERK1/2 mitogen-activated protein kinase pathway as a master regulator of the G1-to S-phase transition. **Oncogene**. 2007;26:3227-3239.
55. Mebratu Y, Tesfaigzi Y. How ERK1/2 activation controls cell proliferation and cell death. **Cell Cycle**. 2009;8:1168-1175.
56. Chalfant CE, Szulc Z, Roddy P et al. The structural requirements for ceramide activation of serine-threonine protein phosphatase. **J Lipid Res**. 2004;45:496-506.
57. Lee WJ, Kim DU, Lee MY et al. Identification of proteins interacting with the catalytic subunit of PP2A by proteomics. **Proteomics**. 2007;7:206-214.

58. Van Kanegan MJ, Adams DG, Wadzinski BE et al. Distinct protein phosphatase 2A heterotrimers modulate growth factor signaling to extracellular signal-regulated kinases and Akt. **J Biol Chem**. 2005;280:36029-36036.
59. Lahiri S, Futerman AH. The metabolism and function of sphingolipids and glycosphingolipids. **Cell Mol Life Sci**. 2007;64:2270-2284.
60. Bollinger CR, Teichgraber V, Gulbins E. Ceramide-enriched membrane domains. **Biochim Biophys Acta**. 2005;1746:284-294.
61. Siskind LJ, Kolesnick RN, Colombini M. Ceramide channels increase the permeability of the mitochondrial outer membrane to small proteins. **J Biol Chem**. 2002;277:26796-26803.
62. Liu H, Chakravarty D, Maceyka M et al. Sphingosine kinases: a novel family of lipid kinases. **Prog Nucleic Acid Res Mol Biol**. 2002;71:493-511.
63. Proia RL, Hla T. Emerging biology of sphingosine-1-phosphate: its role in pathogenesis and therapy. **J Clin Invest**. 2015;125:1379-1387.
64. Strub GM, Maceyka M, Hait NC et al. Extracellular and intracellular actions of sphingosine-1-phosphate. **Adv Exp Med Biol**. 2010;688:141-155.
65. Rosen H, Goetzl EJ. Sphingosine 1-phosphate and its receptors: an autocrine and paracrine network. **Nat Rev Immunol**. 2005;5:560-570.
66. Spiegel S, Milstien S. Sphingosine-1-phosphate: an enigmatic signalling lipid. **Nat Rev Mol Cell Biol**. 2003;4:397-407.
67. Takabe K, Paugh SW, Milstien S et al. "Inside-out" signaling of sphingosine-1-phosphate: therapeutic targets. **Pharmacol Rev**. 2008;60:181-195.
68. Biden TJ, Boslem E, Chu KY et al. Lipotoxic endoplasmic reticulum stress, beta cell failure, and type 2 diabetes mellitus. **Trends Endocrinol Metab**. 2014;25:389-398.
69. **Julien V**, **Lar**a **B**, **Paola G** et al. Roles of Sphingolipid Metabolism in Pancreatic β Cell Dysfunction Induced by Lipotoxicity. ***J Clin Med***. 2014;3:646-662.
70. Pietilainen KH, Ismail K, Jarvinen E et al. DNA methylation and gene expression patterns in adipose tissue differ significantly within young adult monozygotic BMI-discordant twin pairs. **Int J Obes (Lond)**. 2015.
71. Prause M, Christensen DP, Billestrup N et al. JNK1 protects against glucolipotoxicity-mediated beta-cell apoptosis. **PLoS One**. 2014;9:e87067.
72. Khodabandehloo H, Gorgani-Firuzjaee S, Panahi G et al. Molecular and cellular mechanisms linking inflammation to insulin resistance and beta-cell dysfunction. **Transl Res**. 2015.

73. Cunha DA, Igoillo-Esteve M, Gurzov EN et al. Death protein 5 and p53-upregulated modulator of apoptosis mediate the endoplasmic reticulum stress-mitochondrial dialog triggering lipotoxic rodent and human beta-cell apoptosis. **Diabetes**. 2012;61:2763-2775.
74. Guo B, Li Z. Endoplasmic reticulum stress in hepatic steatosis and inflammatory bowel diseases. **Front Genet**. 2014;5:242.
75. Boslem E, Meikle PJ, Biden TJ. Roles of ceramide and sphingolipids in pancreatic beta-cell function and dysfunction. **Islets**. 2012;4:177-187.
76. Lee MS, Kim KA, Kim HS. Role of pancreatic beta-cell death and cell death-associated inflammation in diabetes. **Curr Mol Med**. 2012;12:1297-1310.
77. Laybutt DR, Preston AM, Akerfeldt MC et al. Endoplasmic reticulum stress contributes to beta cell apoptosis in type 2 diabetes. **Diabetologia**. 2007;50:752-763.
78. Lei X, Barbour SE, Ramanadham S. Group VIA Ca2+-independent phospholipase A2 (iPLA2beta) and its role in beta-cell programmed cell death. **Biochimie**. 2010;92:627-637.
79. Taylor RC, Cullen SP, Martin SJ. Apoptosis: controlled demolition at the cellular level. **Nat Rev Mol Cell Biol**. 2008;9:231-241.
80. Thomas HE, McKenzie MD, Angstetra E et al. Beta cell apoptosis in diabetes. **Apoptosis**. 2009;14:1389-1404.
81. Liadis N, Murakami K, Eweida M et al. Caspase-3-dependent beta-cell apoptosis in the initiation of autoimmune diabetes mellitus. **Mol Cell Biol**. 2005;25:3620-3629.
82. Maestre I, Jordan J, Calvo S et al. Mitochondrial dysfunction is involved in apoptosis induced by serum withdrawal and fatty acids in the beta-cell line INS-1. **Endocrinology**. 2003;144:335-345.
83. Navarro P, Valverde AM, Rohn JL et al. Akt mediates insulin rescue from apoptosis in brown adipocytes: effect of ceramide. **Growth Horm IGF Res**. 2000;10:256-266.
84. Watson ML, Coghlan M, Hundal HS. Modulating serine palmitoyl transferase (SPT) expression and activity unveils a crucial role in lipid-induced insulin resistance in rat skeletal muscle cells. **Biochem J**. 2009;417:791-801.
85. Hu W, Ross J, Geng T et al. Differential regulation of dihydroceramide desaturase by palmitate versus monounsaturated fatty acids: implications for insulin resistance. **J Biol Chem**. 2011;286:16596-16605.

86. Chavez JA, Holland WL, Bar J et al. Acid ceramidase overexpression prevents the inhibitory effects of saturated fatty acids on insulin signaling. **J Biol Chem**. 2005;280:20148-20153.
87. Frangioudakis G, Garrard J, Raddatz K et al. Saturated- and n-6 polyunsaturated-fat diets each induce ceramide accumulation in mouse skeletal muscle: reversal and improvement of glucose tolerance by lipid metabolism inhibitors. **Endocrinology**. 2010;151:4187-4196.
88. Holland WL, Brozinick JT, Wang LP et al. Inhibition of ceramide synthesis ameliorates glucocorticoid-, saturated-fat-, and obesity-induced insulin resistance. **Cell Metab**. 2007;5:167-179.
89. Straczkowski M, Kowalska I, Nikolajuk A et al. Relationship between insulin sensitivity and sphingomyelin signaling pathway in human skeletal muscle. **Diabetes**. 2004;53:1215-1221.
90. Kelpe CL, Moore PC, Parazzoli SD et al. Palmitate inhibition of insulin gene expression is mediated at the transcriptional level via ceramide synthesis. **J Biol Chem**. 2003;278:30015-30021.
91. Guo J, Qian Y, Xi X et al. Blockage of ceramide metabolism exacerbates palmitate inhibition of pro-insulin gene expression in pancreatic beta-cells. **Mol Cell Biochem**. 2010;338:283-290.
92. Weir GC, Laybutt DR, Kaneto H et al. Beta-cell adaptation and decompensation during the progression of diabetes. **Diabetes**. 2001;50 Suppl 1:S154-159.
93. Prentki M, Joly E, El-Assaad W et al. Malonyl-CoA signaling, lipid partitioning, and glucolipotoxicity: role in beta-cell adaptation and failure in the etiology of diabetes. **Diabetes**. 2002;51 Suppl 3:S405-413.
94. Poitout V, Amyot J, Semache M et al. Glucolipotoxicity of the pancreatic beta cell. **Biochim Biophys Acta**. 2010;1801:289-298.
95. Karaskov E, Scott C, Zhang L et al. Chronic palmitate but not oleate exposure induces endoplasmic reticulum stress, which may contribute to INS-1 pancreatic beta-cell apoptosis. **Endocrinology**. 2006;147:3398-3407.
96. Cunha DA, Hekerman P, Ladriere L et al. Initiation and execution of lipotoxic ER stress in pancreatic beta-cells. **J Cell Sci**. 2008;121:2308-2318.
97. Eizirik DL, Cardozo AK, Cnop M. The role for endoplasmic reticulum stress in diabetes mellitus. **Endocr Rev**. 2008;29:42-61.

98. Lang F, Ullrich S, Gulbins E. Ceramide formation as a target in beta-cell survival and function. **Expert Opin Ther Targets**. 2011;15:1061-1071.
99. Back SH, Kaufman RJ. Endoplasmic reticulum stress and type 2 diabetes. **Annu Rev Biochem**. 2012;81:767-793.
100. Kumagai K, Yasuda S, Okemoto K et al. CERT mediates intermembrane transfer of various molecular species of ceramides. **J Biol Chem**. 2005;280:6488-6495.
101. Gjoni E, Brioschi L, Cinque A et al. Glucolipotoxicity impairs ceramide flow from the endoplasmic reticulum to the Golgi apparatus in INS-1 beta-cells. **PLoS One**. 2014;9:e110875.
102. Riboni L, Viani P, Bassi R et al. Cultured granule cells and astrocytes from cerebellum differ in metabolizing sphingosine. **J Neurochem**. 2000;75:503-510.
103. Shaner RL, Allegood JC, Park H et al. Quantitative analysis of sphingolipids for lipidomics using triple quadrupole and quadrupole linear ion trap mass spectrometers. **J Lipid Res**. 2009;50:1692-1707.
104. Van Veldhoven PP, Mannaerts GP. Inorganic and organic phosphate measurements in the nanomolar range. **Anal Biochem**. 1987;161:45-48.
105. Livak KJ, Schmittgen TD. Analysis of relative gene expression data using real-time quantitative PCR and the 2(-Delta Delta C(T)) Method. **Methods**. 2001;25:402-408.
106. Pagano RE, Martin OC, Kang HC et al. A novel fluorescent ceramide analogue for studying membrane traffic in animal cells: accumulation at the Golgi apparatus results in altered spectral properties of the sphingolipid precursor. **J Cell Biol**. 1991;113:1267-1279.
107. Veret J, Coant N, Berdyshev EV et al. Ceramide synthase 4 and de novo production of ceramides with specific N-acyl chain lengths are involved in glucolipotoxicity-induced apoptosis of INS-1 beta-cells. **Biochem J**. 2011;438:177-189.
108. Veret J, Coant N, Gorshkova IA et al. Role of palmitate-induced sphingoid base-1-phosphate biosynthesis in INS-1 beta-cell survival. **Biochim Biophys Acta**. 2013;1831:251-262.
109. Guo J, Zhu JX, Deng XH et al. Palmitate-induced inhibition of insulin gene expression in rat islet beta-cells involves the ceramide transport protein. **Cell Physiol Biochem**. 2010;26:717-728.
110. Kumagai K, Kawano M, Shinkai-Ouchi F et al. Interorganelle trafficking of ceramide is regulated by phosphorylation-dependent cooperativity between the PH and START domains of CERT. **J Biol Chem**. 2007;282:17758-17766.

111. El-Assaad W, Buteau J, Peyot ML et al. Saturated fatty acids synergize with elevated glucose to cause pancreatic beta-cell death. **Endocrinology**. 2003;144:4154-4163.

112. Fukasawa M, Nishijima M, Hanada K. Genetic evidence for ATP-dependent endoplasmic reticulum-to-Golgi apparatus trafficking of ceramide for sphingomyelin synthesis in Chinese hamster ovary cells. **J Cell Biol**. 1999;144:673-685.

113. Lei X, Zhang S, Emani B et al. A link between endoplasmic reticulum stress-induced beta-cell apoptosis and the group VIA Ca2+-independent phospholipase A2 (iPLA2beta). **Diabetes Obes Metab**. 2010;12 Suppl 2:93-98.

114. Boslem E, MacIntosh G, Preston AM et al. A lipidomic screen of palmitate-treated MIN6 beta-cells links sphingolipid metabolites with endoplasmic reticulum (ER) stress and impaired protein trafficking. **Biochem J**. 2011;435:267-276.

115. Giussani P, Maceyka M, Le Stunff H et al. Sphingosine-1-phosphate phosphohydrolase regulates endoplasmic reticulum-to-golgi trafficking of ceramide. **Mol Cell Biol**. 2006;26:5055-5069.

116. Granero F, Revert F, Revert-Ros F et al. A human-specific TNF-responsive promoter for Goodpasture antigen-binding protein. **FEBS J**. 2005;272:5291-5305.

117. Kim SJ, Winter K, Nian C et al. Glucose-dependent insulinotropic polypeptide (GIP) stimulation of pancreatic beta-cell survival is dependent upon phosphatidylinositol 3-kinase (PI3K)/protein kinase B (PKB) signaling, inactivation of the forkhead transcription factor Foxo1, and down-regulation of bax expression. **J Biol Chem**. 2005;280:22297-22307.

118. Martinez SC, Tanabe K, Cras-Meneur C et al. Inhibition of Foxo1 protects pancreatic islet beta-cells against fatty acid and endoplasmic reticulum stress-induced apoptosis. **Diabetes**. 2008;57:846-859.

119. Wrede CE, Dickson LM, Lingohr MK et al. Protein kinase B/Akt prevents fatty acid-induced apoptosis in pancreatic beta-cells (INS-1). **J Biol Chem**. 2002;277:49676-49684.

120. Lei X, Zhang S, Bohrer A et al. Role of calcium-independent phospholipase A(2)beta in human pancreatic islet beta-cell apoptosis. **Am J Physiol Endocrinol Metab**. 2012;303:E1386-1395.

121. Shimabukuro M, Higa M, Zhou YT et al. Lipoapoptosis in beta-cells of obese prediabetic fa/fa rats. Role of serine palmitoyltransferase overexpression. **J Biol Chem**. 1998;273:32487-32490.

122. Elghazi L, Bernal-Mizrachi E. Akt and PTEN: beta-cell mass and pancreas plasticity. **Trends Endocrinol Metab**. 2009;20:243-251.
123. Davis FG, McCarthy BJ. Current epidemiological trends and surveillance issues in brain tumors. **Expert Rev Anticancer Ther**. 2001;1:395-401.
124. Rich JN, Bigner DD. Development of novel targeted therapies in the treatment of malignant glioma. **Nat Rev Drug Discov**. 2004;3:430-446.
125. Wen PY, Kesari S. Malignant gliomas in adults. **N Engl J Med**. 2008;359:492-507.
126. Guha A, Mukherjee J. Advances in the biology of astrocytomas. **Curr Opin Neurol**. 2004;17:655-662.
127. Rao RD, James CD. Altered molecular pathways in gliomas: an overview of clinically relevant issues. **Semin Oncol**. 2004;31:595-604.
128. Dolecek TA, Propp JM, Stroup NE et al. CBTRUS Statistical Report: Primary Brain and Central Nervous System Tumors diagnosed in the United States in 2005-2009. **Neuro Oncol**. 2012;14 Suppl 5:v1-v49.
129. Behin A, Hoang-Xuan K, Carpentier AF et al. Primary brain tumours in adults. **Lancet**. 2003;361:323-331.
130. Miller CR, Perry A. Glioblastoma, morphologic and molecular genetic diversity. **Arch Pathol Lab Med**. 2007;131:397-406.
131. Comprehensive genomic characterization defines human glioblastoma genes and core pathways. **Nature**. 2008;455:1061-1068.
132. Cloughesy TF, Cavenee WK, Mischel PS. Glioblastoma: from molecular pathology to targeted treatment. **Annu Rev Pathol**. 2014;9:1-25.
133. Furnari FB, Fenton T, Bachoo RM et al. Malignant astrocytic glioma: genetics, biology, and paths to treatment. **Genes Dev**. 2007;21:2683-2710.
134. Chakravarti A, Zhai G, Suzuki Y et al. The prognostic significance of phosphatidylinositol 3-kinase pathway activation. **J Clin Oncol**. 2004;22:1926-1933.
135. Ichimura K, Ohgaki H, Kleihues P et al. Molecular pathogenesis of astrocytic tumours. **J Neurooncol**. 2004;70:137-160.
136. Merlo A. Genes and pathways driving glioblastomas in humans and murine disease models. **Neurosurg Rev**. 2003;26:145-158.
137. Riboni L, Campanella R, Bassi R et al. Ceramide levels are inversely associated with malignant progression of human glial tumors. **Glia**. 2002;39:105-113.
138. Velasco G, Galve-Roperh I, Sanchez C et al. Cannabinoids and ceramide: two lipids acting hand-by-hand. **Life Sci**. 2005;77:1723-1731.

139. Viani P, Giussani P, Brioschi L et al. Ceramide in nitric oxide inhibition of glioma cell growth. **J Biol Chem**. 2003;278:9592-9601.

140. Giussani P, Brioschi L, Bassi R et al. Phosphatidylinositol 3-kinase/AKT pathway regulates the endoplasmic reticulum to Golgi traffic of ceramide in glioma cells. **J Biol Chem**. 2009;284:5088-5096.

141. Hara S, Nakashima S, Kiyono T et al. Ceramide triggers caspase activation during gamma-radiation-induced apoptosis of human glioma cell lacking functional p53. **Oncol Rep**. 2004;12:119-123.

142. Sawada M, Kiyono T, Nakashima S et al. Molecular mechanisms of TNF-alpha-induced ceramide formation in human glioma cells: p53 mediated oxidant stress-dependent and -independent pathways. **Cell Death Differ**. 2004;11:997-1008.

143. Mochizuki T, Asai A, Saito N et al. Akt protein kinase inhibits non-apoptotic programmed cell death induced by ceramide. **J Biol Chem**. 2002;277:2790-2797.

144. Daido S, Kanzawa T, Yamamoto A et al. Pivotal role of the cell death factor BNIP3 in ceramide-induced autophagic cell death in malignant glioma cells. **Cancer Res**. 2004;64:4286-4293.

145. Salazar M, Carracedo A, Salanueva IJ et al. Cannabinoid action induces autophagy-mediated cell death through stimulation of ER stress in human glioma cells. **J Clin Invest**. 2009;119:1359-1372.

146. Pyne NJ, Pyne S. Sphingosine 1-phosphate and cancer. **Nat Rev Cancer**. 2010;10:489-503.

147. Kim RH, Takabe K, Milstien S et al. Export and functions of sphingosine-1-phosphate. **Biochim Biophys Acta**. 2009;1791:692-696.

148. Yester JW, Tizazu E, Harikumar KB et al. Extracellular and intracellular sphingosine-1-phosphate in cancer. **Cancer Metastasis Rev**. 2011;30:577-597.

149. Van Brocklyn J, Letterle C, Snyder P et al. Sphingosine-1-phosphate stimulates human glioma cell proliferation through Gi-coupled receptors: role of ERK MAP kinase and phosphatidylinositol 3-kinase beta. **Cancer Lett**. 2002;181:195-204.

150. Van Brocklyn JR, Young N, Roof R. Sphingosine-1-phosphate stimulates motility and invasiveness of human glioblastoma multiforme cells. **Cancer Lett**. 2003;199:53-60.

151. Zhang H, Li W, Sun S et al. Inhibition of sphingosine kinase 1 suppresses proliferation of glioma cells under hypoxia by attenuating activity of extracellular signal-regulated kinase. **Cell Prolif**. 2012;45:167-175.

152. Edsall LC, Cuvillier O, Twitty S et al. Sphingosine kinase expression regulates apoptosis and caspase activation in PC12 cells. **J Neurochem**. 2001;76:1573-1584.
153. Van Brocklyn JR, Jackson CA, Pearl DK et al. Sphingosine kinase-1 expression correlates with poor survival of patients with glioblastoma multiforme: roles of sphingosine kinase isoforms in growth of glioblastoma cell lines. **J Neuropathol Exp Neurol**. 2005;64:695-705.
154. Anelli V, Gault CR, Cheng AB et al. Sphingosine kinase 1 is up-regulated during hypoxia in U87MG glioma cells. Role of hypoxia-inducible factors 1 and 2. **J Biol Chem**. 2008;283:3365-3375.
155. Young N, Van Brocklyn JR. Roles of sphingosine-1-phosphate (S1P) receptors in malignant behavior of glioma cells. **Exp Cell Res**. 2007;313:1615-1627.
156. Kim K, Kim YL, Sacket SJ et al. Sphingosine 1-phosphate (S1P) induces shape change in rat C6 glioma cells through S1P2 receptor: development of an agonist for S1P receptors. **J Pharm Pharmacol**. 2007;59:1035-1041.
157. Young N, Pearl DK, Van Brocklyn JR. Sphingosine-1-phosphate regulates glioblastoma cell invasiveness through the urokinase plasminogen activator system and CCN1/Cyr61. **Mol Cancer Res**. 2009;7:23-32.
158. Riccitelli E, Giussani P, Di Vito C et al. Extracellular sphingosine-1-phosphate: a novel actor in human glioblastoma stem cell survival. **PLoS One**. 2013;8:e68229.
159. Gouaze-Andersson V, Cabot MC. Glycosphingolipids and drug resistance. **Biochim Biophys Acta**. 2006;1758:2096-2103.
160. Maurer BJ, Metelitsa LS, Seeger RC et al. Increase of ceramide and induction of mixed apoptosis/necrosis by N-(4-hydroxyphenyl)- retinamide in neuroblastoma cell lines. **J Natl Cancer Inst**. 1999;91:1138-1146.
161. Oskouian B, Saba JD. Cancer treatment strategies targeting sphingolipid metabolism. **Adv Exp Med Biol**. 2010;688:185-205.
162. Ponnusamy S, Meyers-Needham M, Senkal CE et al. Sphingolipids and cancer: ceramide and sphingosine-1-phosphate in the regulation of cell death and drug resistance. **Future Oncol**. 2010;6:1603-1624.
163. Riboni L, Viani P, Tettamanti G. Estimating sphingolipid metabolism and trafficking in cultured cells using radiolabeled compounds. **Methods Enzymol**. 2000;311:656-682.

164. Quint K, Stiel N, Neureiter D et al. The role of sphingosine kinase isoforms and receptors S1P1, S1P2, S1P3, and S1P5 in primary, secondary, and recurrent glioblastomas. **Tumour Biol**. 2014;35:8979-8989.

165. Cuvillier O, Pirianov G, Kleuser B et al. Suppression of ceramide-mediated programmed cell death by sphingosine-1-phosphate. **Nature**. 1996;381:800-803.

166. Young N, Van Brocklyn JR. Roles of sphingosine-1-phosphate (S1P) receptors in malignant behavior of glioma cells. Differential effects of S1P2 on cell migration and invasiveness. **Exp Cell Res**. 2007;313:1615-1627.

167. Guan H, Song L, Cai J et al. Sphingosine kinase 1 regulates the Akt/FOXO3a/Bim pathway and contributes to apoptosis resistance in glioma cells. **PLoS One**. 2011;6:e19946.

168. Klausner RD, Donaldson JG, Lippincott-Schwartz J. Brefeldin A: insights into the control of membrane traffic and organelle structure. **J Cell Biol**. 1992;116:1071-1080.

169. Ermoian RP, Furniss CS, Lamborn KR et al. Dysregulation of PTEN and protein kinase B is associated with glioma histology and patient survival. **Clin Cancer Res**. 2002;8:1100-1106.

170. Chakravarti A, Zhai G, Suzuki Y et al. The prognostic significance of phosphatidylinositol 3-kinase pathway activation in human gliomas. **J Clin Oncol**. 2004;22:1926-1933.

171. Swanton C, Marani M, Pardo O et al. Regulators of mitotic arrest and ceramide metabolism are determinants of sensitivity to paclitaxel and other chemotherapeutic drugs. **Cancer Cell**. 2007;11:498-512.

172. Kolesnick R, Altieri D, Fuks Z. A CERTain role for ceramide in taxane-induced cell death. **Cancer Cell**. 2007;11:473-475.

173. Lou HO, Clausen J, Bierring F. Phospholipids and glycolipids of tumours in the central nervous system. **J Neurochem**. 1965;12:619-627.

174. Giussani P, Bassi R, Anelli V et al. Glucosylceramide synthase protects glioblastoma cells against autophagic and apoptotic death induced by temozolomide and Paclitaxel. **Cancer Invest**. 2012;30:27-37.

175. Morales A, Lee H, Goni FM et al. Sphingolipids and cell death. **Apoptosis**. 2007;12:923-939.